

Investigating the Genetic Influence on the Pathological Burden of
Multiple Sclerosis

By

Kelsey Allen

Medical Biochemistry BSc

Submitted to

Swansea University

In Fulfilment of the Requirements of the Degree of

Master of Science by Research in Medical and Healthcare Studies
(MSc Res)

Swansea University

2024



Abstract

Introduction: Permanent disability in multiple sclerosis (MS) is primarily driven by neuronal and axonal loss. While genome-wide association (GWAS) studies have begun identifying genetic variants associated with the clinical course of MS, the variants underpinning pathological severity have not been described. Understanding these novel variants and their influence on the clinical course of MS can be used to further develop our knowledge of this heterogeneous disease.

Aims: To uncover genetic variants and describe the expression of mapped genes that associate with the pathological severity of MS.

Methods: Using data from an integrated GWAS expression quantitative trait loci COLOCation (eQTL COLOC) analysis of progressive MS ($n = 310$), we investigated the association between gene variant status and neuron density, extent of demyelination and retrospectively determined clinical milestones. In situ hybridisation (ISH) revealed gene expression and localisation in a subset of MS and controls ($n = 20$).

Results: Previously described variant rs7289446 (SEZ6L) was not associated with quantitative measures of neuron density, demyelination or clinical outcomes. A 2nd variant mapping to DYSF:CYP26B1 (rs7564433), which represents the first GWAS validated mapped gene (rs10191329), was associated with higher neuron density, lower demyelination, slower disease progression and an older age at death in heterozygote allele carriers ($p < 0.05$). Independent single nucleotide polymorphisms (SNPs), mapping to PCSK5 and COMMD10, genes not previously linked to MS, were associated with increased neuron density in the thalamus, pons ($p < 0.05$; PCSK5) and frontal cortex ($p < 0.05$; COMMD10), specifically among heterozygous carriers. The average age of onset was 4.6 yrs lower in COMMD10 major allele carriers compared to heterozygotes. COMMD10 and PCSK5 neuronal and glial expression was elevated in normal MS grey matter (GM) compared to control and lesion GM.

Summary: We describe gene variants that associate with neuron density and show the altered expression of mapped genes in MS. Our findings provide insights into biological mechanisms underlying MS severity, offering potential opportunities for targeted therapies and personalised MS care.

Declaration and Statements

DECLARATION

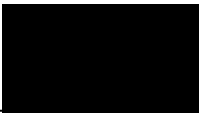
This work has not previously been accepted in substance for any degree and is not being concurrently submitted in candidature for any degree.

Signed:  (candidate)

Date: 22/09/2024

STATEMENT 1

This thesis is the result of my own investigations, except where otherwise stated. Where correction services have been used, the extent and nature of the correction is clearly marked in a footnote(s). Other sources are acknowledged by footnotes giving explicit references. A bibliography is appended.

Signed:  (candidate)

Date: 22/09/2024

STATEMENT 2

I hereby give consent for my thesis, if accepted, to be available for electronic sharing after expiry of a bar on access approved by the Swansea University.

Signed:  (candidate)

Date: 22/09/2024

Table of Contents

Abstract	2
Declaration and Statements	3
Acknowledgements	8
List of Figures.....	9
Abbreviations	11
1.1 Multiple Sclerosis	14
1.2 Epidemiology of Multiple Sclerosis.....	15
1.3 Subtypes of Multiple Sclerosis	16
1.3.1 Classifying the Multiple Sclerosis Lesion	20
1.4 Pathophysiology of Multiple Sclerosis: Neurodegeneration is the Main Pathological Component of MS Progression.	21
1.5 Current Treatment Therapies and Clinical Trials	23
1.6 The Genetics of Multiple Sclerosis Risk and Progression	25
1.7 Genome Wide Association Studies and their Importance in MS Research	26
1.7.1 GWAS Studies to Understand the Genetic Drivers of Progression.....	26
1.7.2 The Role of Dystrophy-Associated Fer-1-Like Gene	28
1.7.3 The Role of the Seizure 6-Like Gene.....	28
1.7.4 The Role of the Proprotein Convertase Subtilisin/Kexin Type 5 Gene	29
1.7.5 The Role of the COMM Domain Containing 10 Gene	30
1.7.6 The Polygenic Risk of Genetic Influences in Multiple Sclerosis	31
1.8 Aims and Objectives	31
1.8.1 Project Impact	33
2.0 Methods	34
2.1 A Literature Review to Summarise the Known Expression and Function of Novel Target Genes PCSK5 and COMMD10 in the Human Brain	34
2.2 UK MS Tissue Bank MS Cohort for Gene Pathological Comparisons	35
2.2.1 Summary Tables of Human MS and Control Post-Mortem Cases.....	36
2.2.2 Data Retrieval of MS Cases Carrying SNPs of Gene Variants of Interest	40

2.2.3 Assessing the Association Between Carrying Two or More Gene Variants of Interest and the Clinical and Pathological Severity of MS	40
2.3 Tissue Characterisation	41
2.4 Primary Antibodies Used for Immunostaining and In Situ Hybridisation	42
2.5 Immunohistochemistry	43
2.5.1 Immunostaining Non-Neurological Disease Control Cases for the Quantification of HuC ⁺ Neurons	44
2.5.2 Staining for PCSK5 Protein Expression in MS and Control Cohort.....	45
2.6 In-Situ Hybridisation	46
2.6.1 RNAScope Singleplex Assay for SEZ6L, PCSK5 and COMMD10	47
2.6.2 ISH Combined with Immunostaining to Identify Transcript Positive Cells	48
2.6.3 RNAScope With Duplex Red and Green Detection for the Combined Detection of PCSK5 and COMMD10.....	49
2.7 Digital Pathology: Quantification Using QuPath	50
2.7.1 Quantification of HuC ⁺ Neurons	51
2.7.2 Quantifying the Density of HuC ⁺ Neurons Expressing SEZ6L.....	55
2.7.3 Quantifying PCSK5 ⁺ Cells.....	57
2.7.4 Quantifying the PCSK5 and COMMD10 Gene Expression in Control and MS Brain	58
2.8 Statistical Analysis	59
3.0 Results.....	60
3.1 MS is a Neurodegenerative Disease	60
3.2 DYSF is Highly Expressed at Protein Level in the Brain	63
3.2.1 SEZ6L is Enriched to the Brain.....	66
3.2.2 The PCSK5 Gene Has Varying Levels of Expression in Different Organs	68
3.2.3 COMMD10 Expression is Not Exclusive to the Brain	70
3.2.4 An Insight into Gender Differences, Cellular Expression Profiles and Gene Expression Levels in MS and Control Cohort using Cellxgene Analysis.....	72
3.3 DYSF:CYP26B1 rs7565433 SNP Heterozygous Alleles Are Associated with Higher Neuron Density in the Thalamus and Pons, Reduced Demyelination in the Cerebellum and a Later Onset to Progression and Age Died	75

3.3.1 SEZ6L rs7289446 SNP Shows No Protective Features in Neuropathology and Clinical Outcomes in Our MS Cohort.....	77
3.3.2 PCSK5 rs10869757 SNP Heterozygous Alleles are Associated with a Higher Neuron Density in the Thalamus and Pons	78
3.3.3 Heterozygous and Minor Alleles of COMMD10 SNPs rs185263 and rs1567335 are Associated with Increased Neuron Density in the SFG	81
3.4 The SEZ6L Gene Expression is Significantly Reduced in the MS Grey Matter Lesion	81
3.5 The PCSK5 and COMMD10 Genes are Co-Expressed in Neuronal Cells.....	83
3.5.1 PCSK5 has Elevated Expression in NGM Compared to GML of MS Cohort	84
3.5.2 COMMD10 has Elevated Expression in NGM of MS Cohort Compared to MS GML Areas and Control Cohort	85
3.5.3 PCSK5 Protein Expression is Elevated in MS NGM	87
3.6 Polygenic Effect of PCSK5 and COMMD10.....	87
Discussion	91
Uncovering Neurodegeneration: Exploring its Impact on Clinical Measures in MS Patients	92
Heterozygous rs7565433 SNP Mapping to DYSF:CYP26B1 is Suggested to be Linked to Neuroprotective Traits and Delayed Onset and Progression of MS	94
The SEZ6L Gene is Suggested to Have a Neuroprotective Effect in the MS Brain but Carrying the rs7289446 SNP Mapping to SEZ6L Suggests No Neuropathological or Clinical Differences	97
Carriers of Heterozygous rs10869757 Alleles are Suggested to Have Neuroprotective Mechanisms to Delay the Onset of Neurodegeneration and Disease Progression.....	99
Elevated PCSK5 Expression in MS NGM Suggests Neuroprotective Mechanisms.....	100
Carriers of Major rs185263 and rs1567335 SNPs Mapping to COMMD10 are Suggested to Have Less Neuroprotective Mechanisms to Delay Neurodegeneration in the SFG Compared to Minor and Heterozygous Carriers	101
MS Carriers of Heterozygous rs1567335 SNPs are Suggested to have a Delayed Age of Onset Which Provides Opportunity for Improved Treatment Management	102
Elevated COMMD10 Gene Expression in MS NGM Suggests Neuroprotective Mechanisms via Neuroinflammatory Mediation.....	103

The Co-Expression of PCSK5 and COMMD10 in the MS Brain: Insights into Inflammation and Neurodegeneration	104
The Presence of Grey Matter Lesions May Alter the PCSK5 Protein Availability in Multiple Sclerosis	105
Finding Evidence for a Polygenic Effect on the Neuropathological and Clinical Severity of MS	107
Limitations of the Project	109
Future Work	111
Summary	113
Supplementary Tables.....	137

Acknowledgements

Firstly, I would like to thank Dr Owain Howell for his continuous support and guidance throughout my research. Working at the Howell group has been an enriching experience, and their expertise has proven invaluable. A special thanks to Dr Lauren Griffiths and Ben Cooze for their insightful feedback and encouragement, which has played a crucial role in shaping this work. I am extremely thankful to all for their mentorship.

On a personal note, I am immensely grateful to both my parents for their constant support and belief in my academic journey. I would also like to express my appreciation to my partner, Jack, for his encouragement throughout the duration of my research project. I also wish to honour my grandparents whose wisdom has greatly influenced the path I have taken. I am very grateful to them for always believing in me.

Finally, I want to thank my colleagues in the ILS 1 floor 3 office. Their encouragement and insightful discussions have inspired me to continue my journey in research. I am excited to see where this path leads and remain grateful for the support and friendships that have made this experience truly rewarding.

List of Figures

Introduction

Figure 1. Patients with relapsing MS tend to transition to progressive MS over time....	17
Figure 2. The five major pathological processes underlying neuronal and axon loss in PMS.....	23

Methods

Figure 3. Identification of post-mortem human brain tissue regions used in the project.	42
Figure 4. Single antigen labelling in IHC protocol.	44
Figure 5. The AMP steps for the RNAscope protocol	48
Figure 6. Simultaneous detection of PCSK5 and COMMD10 gene expression using RNAscope Duplex Assay	50
Figure 7. The annotations of regions of interest in selected brain regions to retrieve positive cell counts from control cohort.....	52
Figure 8. Default parameters for positive cell detection on QuPath	54
Figure 9. Comparison of QuPath approaches for SEZ6L expression analysis	56
Figure 10. Quantification of PCSK5 IHC positively stained cells in MS and control cases	57

Results

Figure 11. Immunohistochemically stained human brain tissue sections at SFG, CG and thalamic regions of MS and control	61
Figure 12. Neuron density in the SFG, CG and thalamus is significantly reduced in MS in comparison to controls and associated with a worse clinical outcome	63
Figure 13. The DYSF protein expression is extremely high in the brain, but gene expression is considerably lower.....	65
Figure 14. Differential expression and cellular location of the SEZ6L gene.....	67
Figure 15. PCSK5 expression at RNA and protein level in various organs and cells.....	69
Figure 16. The COMMD10 is expressed in various organs and cell types.....	71
Figure 17. Gene expression patterns of DYSF, SEZ6L, PCSK5 and COMMD10 across MS and control cohorts, gender and cell types	74
Figure 18. The heterozygous genotype A/G of rs7565433 is associated with a higher neuron density count, a lower demyelination area, a later onset to progression and a later age died.....	76

Figure 19. Individuals carrying the major rs10869757 variant exhibit lower neuron density in the thalamus and pons compared to individuals carrying the heterozygous genotype.....	78
Figure 20. Comparing neuron density in the pons between the rs11144848 SNP genotypes	80
Figure 21. The neuron density in major allele carriers of the rs185263 and rs1567335 COMMD10 SNP are lowest in the SFG.....	81
Figure 22. SEZ6L gene expression in control and MS revealed a reduced expression in MS cortical grey matter lesions	83
Figure 23. The co-expression of PCSK5 and COMMD10 genes were detected in and around neuronal-like cells in control and MS cohort	84
Figure 24. The highest PCSK5 and COMMD10 percentage puncta positive area was found in the MS NGM tissue	86
Figure 25. PCSK5 ⁺ cells are found widespread through normal-appearing and damaged tissue.....	87
Figure 26. Neuron density is elevated in those carrying two or more variants of interest at heterozygous level	89

Abbreviations

ABC – avidin-biotin complex

AKT – protein kinase B

AP – alkaline phosphatase

BACE1 – beta-site APP cleaving enzyme 1

BBB – blood brain barrier

CASP – caspase

Cb DN – cerebellum and dentate nucleus

CG – cingulate gyrus

CIS – clinically isolated syndrome

CNS – central nervous system

COMMD – COMM domain containing

CRISPR – clustered regularly interspaced short palindromic repeats

CSF – cerebrospinal fluid

CYP – cytochrome P450

DAB – diaminobenzidine

DAPB – dihydrodipicolinate reductase

DMT – disease modifying therapy

DYSF – dysferlin/dystrophy-associated fer-1-like

EBV – Epstein-Barr virus

EDSS – Expanded Disability Status Scale

ELAV – embryonic lethal abnormal visual system

EN – excitatory neuron

ER – endoplasmic reticulum

eQTL COLOC – expression quantitative trait loci COLOCation

ERK – extracellular signal-regulated kinase

FDA – Food and Drug Administration

FFPE – formalin-fixed paraffin embedded

FOS – FBJ osteosarcoma oncogene
GM – grey matter
GML – grey matter lesion
GWAS – genome wide association studies
HLA – human leukocyte antigen
HRP – horseradish peroxidase
IFN- γ – interferon-gamma
IHC – immunohistochemistry
ISH – in situ hybridisation
LFB - luxol fast blue
LOMS – late onset multiple sclerosis
MEOX – mesenchyme homebox
MOG – anti-myelin oligodendrocyte glycoprotein
MRI – magnetic resonance imaging
MS – multiple sclerosis
NCBI – National Center for Biotechnology Information
NF – κ B – nuclear factor κ -light chain-enhancer of activated B cells
NGM – normal-appearing grey matter
NICE – National Institute of Health and Care Excellence
NK – natural killer
NOTCH2NLA – notch 2 N-terminal like A
nTPM – normalised transcripts per million
OL – oligodendrocyte
OPC – oligodendrocyte precursor cell
OPTN – optineurin
PBS – phosphate-buffered saline
PBST – phosphate-buffered saline with triton
PCSK5 – proprotein convertase subtilisin/kexin type 5

PFA – paraformaldehyde
PIRA – progression independent of disease activity
PMI – post-mortem interval
PMS – progressive multiple sclerosis
PIIB – peptidylprolyl isomerase B
PPMS – primary progressive multiple sclerosis
Pro-MMP – pro-matrix metalloproteinase
PRS – polygenic risk score
RALDH2 – retinaldehyde dehydrogenase 2
ROI – region of interest
RRMS – relapsing-remitting multiple sclerosis
RT – room temperature
SCC – saline sodium citrate
SEZ6L – seizure related 6 homolog like
SF – snap frozen
SFG – superior frontal gyrus
SNAPIN – SNAP associated protein
SNARE – soluble N-ethylmaleimide-sensitive factor attachment protein receptor
SNP – single nucleotide polymorphism
SPMS – secondary progressive multiple sclerosis
TNF- α – tumour necrosis factor-alpha
UPR – unfolded protein response
WC – wheelchair
WM – white matter
WML – white matter lesion
ZNF – zinc-finger protein

1.0 Introduction

1.1 Multiple Sclerosis

Multiple sclerosis (MS) is a chronic disease of the central nervous system (CNS) (Ghasemi et al., 2017). The pathological manifestations of this autoimmune disease are inflammation, the demyelination of axons and neurodegeneration (Correale et al., 2019). This can give rise to complications such as cognitive decline and reduced sensory or motor function, partly due to impaired nerve impulse transmission within the CNS (Mey et al., 2023). Symptoms of MS include blurry or double vision, dizziness, slurred speech and problems with co-ordination or mobility, which vary in severity depending on lesion location, lesion activity, inflammation and the degree of neuro-axonal injury (Tafti et al., 2024). The immune dysregulation in patients with MS is related to the influx of immune cells, including T cells, B cells and macrophages entering the CNS, which is associated with damage to the blood brain barrier (BBB) and activation of resident microglia and astrocytes. Neuroinflammation, including a local activated glial response (microglial and astrocytes), in MS is associated with both acute and chronic inflammation (Rodríguez et al., 2022; Yamout & Alroughani., 2018).

Inflammation in MS is associated with damage to oligodendrocytes and their myelin sheaths, leading to reduced axonal insulation, axonal degeneration and neuron loss (Kalafatakis & Karagogeos., 2021). The damage caused by infiltrating immune cells target tissue in the brain and spinal cord, resulting in inflammation, tissue loss and lesion formation, which reflects the involvement of various cell types and biological pathways in the symptoms and progression of MS (Adiele & Adiele., 2019). These demyelinated lesions can form in both the grey and white matter (WM) of the CNS (Prins et al., 2015). Inflammation and oxidative stress are key molecular drivers of MS disease onset and progression (Zeydan & Kantarci, 2020). Inflammation can lead to axonal damage and demyelination and contributes towards patient disability (Simkins et al., 2021). So far, it is not known what causes MS and whether the initiating immune

triggers arise in the CNS or peripherally. However, advances in neuropathology using large cohorts, genetics and other 'omic' approaches and magnetic resonance imaging (MRI), are providing a deeper understanding of this complex neurological disease (Baecher-Allan et al., 2018; Reich et al., 2018). Advancing our understanding of the pathological mechanisms contributing to MS progression is key for an earlier diagnosis and the development of targeted therapeutic interventions (Faissner & Gold, 2019; Huang et al., 2017).

1.2 Epidemiology of Multiple Sclerosis

More than 2 million people worldwide have been diagnosed with MS (Reich et al., 2018; Walton et al., 2020). The incidence of MS continues to rise annually, with an estimated 7000 new diagnoses occurring in the United Kingdom each year (MS Society., 2020.). The rise in MS diagnoses over the past three decades may reflect greater awareness of the disease, driven by the introduction of MRI imaging and the availability of new treatment therapies (Hawkes et al., 2020). Whilst MS can occur at any age, it most commonly presents between 18 to 40 years, with a higher prevalence in women than in men (3:1 ratio; Ford, 2020). MS is the greatest cause of disability in young adults (Walton et al., 2020). Both genetic and environmental factors, including lifestyle habits like smoking, can contribute to the risk of developing MS (Jakimovski et al., 2019). MS has different incidence rates geographically, with higher rates observed in regions such as North America and Europe and lower rates reported in African and Western Pacific regions, which suggests genetic predisposition influences (Jakimovski et al., 2024; Walton et al., 2020). Exposure to higher levels of Vitamin D has been shown to reduce the risk of developing MS and is associated with decreased disease activity and a reduced relapse rate, demonstrating a role for Vitamin D in the geographic incidence of this disease (Sintzel et al., 2018). Worse disability progression in males compared to females has been identified through greater cortical grey matter (GM) atrophy and a poorer performance on the 9-hole peg test, indicating greater neurodegeneration

(Voskuhl et al., 2020). However, current evidence is insufficient to confirm sex-based differences in the extent of the underlying pathobiological mechanisms.

Viral infections, such as Epstein-Barr virus (EBV), have been identified as potential triggers for MS, with prior EBV infection linked to an increased risk of developing the disease (Bjornevik et al., 2022). Comorbidities are common in patients with MS and include depression, anxiety, cardiovascular diseases and autoimmune conditions such as diabetes (Magyari & Sorensen, 2020). Smoking is a major lifestyle factor associated with MS development, as it affects the immune response by reducing the number of B cells and natural killer (NK) cells, as well as cytokine production and immunoglobulins in the blood (Nishanth et al., 2020; O’Gorman et al., 2012). Smoking is associated with an increased risk of worsening disability and conversion from relapsing-remitting MS (RRMS) to secondary progressive MS (SPMS), although no direct causal link has been established (Rodgers et al., 2022; Wingerchuk, 2012). Patients with MS are said to have a shortened lifespan of 7-14 years but the life expectancy of patients with MS has significantly improved due to the medical advancements, symptomatic management and changes in lifestyle habits (Lunde et al., 2017).

1.3 Subtypes of Multiple Sclerosis

There are four main clinical types of MS; clinically isolated syndrome (CIS), RRMS, SPMS and primary progressive MS (PPMS) (Klineova & Lublin, 2018). RRMS is the most common subtype of MS that affects approximately 85% of MS patients (Huisman et al., 2017). It is presented as clear clinical relapses – most often a temporary increase in disability with recovery. Disability in MS is measured using the Expanded Disability Status Scale (EDSS) (Filippi & Rocca, 2019; Krieger et al., 2022). Relapses in MS are partly due to acute focal inflammation and demyelination (Kalincik, 2015; Steinman, 2014; Wang et al., 2018). These relapses are often followed by remission periods that can cause a reduction in symptoms, which can happen spontaneously or in response to treatment (Cree et al., 2021). It is common for relapse frequency to decline with age,

but for their severity to increase and recovery to decrease. Cerebellar relapses are more prevalent in older males, whereas females show signs of visual or sensory symptoms (Kalincik et al., 2014). RRMS can progress to SPMS, which involves the slow transition to a phase with fewer relapses and an accumulation in neurological dysfunction (see Figure 1) (Saleem et al., 2019). It is important to note that relapses can happen at any stage of the disease and that progression (the accumulating neurological dysfunction) can be present from disease onset (Cree et al., 2021).

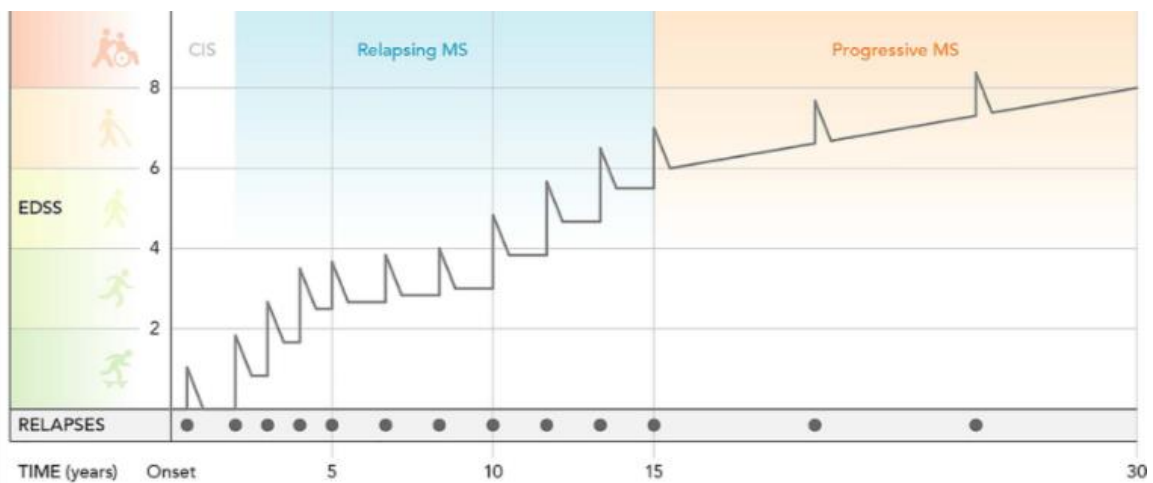


Figure 1. Patients with relapsing MS tend to transition to progressive MS over time. Patients who experience their first neurological symptoms lasting at least 24 hours are classified as having CIS, which can progress to MS. During the relapse phase, disability (measured using the EDSS score) accumulates with the number of relapses with incomplete recovery. Most patients transition to progressive MS (PMS), characterised by fewer relapses but ongoing neurodegeneration and gradual worsening of neurological function. Higher EDSS scores during relapses are linked to increased risk of progression. Adapted from Hauser & Cree, (2020), DOI: [10.1016/j.amjmed.2020.05.049](https://doi.org/10.1016/j.amjmed.2020.05.049)

Distinguishing between progressive phenotypes has proven to be challenging for clinicians (Correale et al., 2016). SPMS is more commonly diagnosed with this subtype being the second most common form of MS (Inojosa et al., 2021). The gradual worsening of disability in progressive MS (PMS) (both SPMS and PPMS) is caused by complex immune mechanisms and further neurodegeneration, with evidence of active inflammation and focal demyelination, which is less common than in the relapse remitting-stage (Macaron & Ontaneda, 2019). Although it is the changing balance in the

extent of these pathologies that underlines the different subtypes, rather than them being fundamentally different forms of the disease (Kuhlmann et al., 2023).

People with PPMS do not experience an initial relapse-remitting phase and instead present with steadily worsening symptoms from diagnosis. While relapses are not typical, some individuals may show inflammatory activity or MRI changes suggestive of disease activity (Antel et al., 2012; Macaron & Ontaneda, 2019). The primary pathological hallmark of SPMS and PPMS is slowly expanding lesions (also termed chronic active lesions), extensive cortical and deep GM demyelination, neuron and axon loss, widespread glial activation and inflammation of the perivascular and leptomeningeal spaces (Abdelhak et al., 2017; Kee et al., 2022; Kutzelnigg et al., 2005; Lassman, 2014).

Alongside clinically recognised subtypes, radiologically isolated syndrome (RIS) is used to describe a patient who has abnormal radiological findings in the CNS, particularly in the WM, that is reminiscent of MS (Lebrun-Frénay et al., 2023). The presence of demyelinating white matter lesions (WML) can be an indicator of MS development, thus RIS classified patients should be monitored more closely for a prompt diagnosis (Yamout & Khawajah, 2017). Recent evidence suggests that early treatment with disease modifying therapies (DMTs) is beneficial in both CIS and RIS patients and delays the onset of clinically definitive MS (Cobo-Calvo et al., 2023; Okuda et al., 2023).

As well as classifying the main clinical types of MS, the disease can also be additionally described as active or non-active and with or without progression, as stated by Lublin et al., (2014). MS with disease activity is defined as a patient experiencing a clinical relapse or having new or enlarging inflammatory lesions on MRI. The term ‘with progression’, refers to a steady worsening of disability over time, which can occur with or without relapses or new MRI activity. The purpose of phenotype classification is to enhance effective communication within the healthcare setting and can assist with treatment decision making, as, for example, the DMT Ocrelizumab can only be prescribed to

progressive MS patients with evidence of disease activity (National Institute for Health and Care Excellence, 2019).

Progression Independent of Relapse Activity (PIRA) is a primary mechanism contributing to the disability accumulation in MS (Tur & Rocca, 2024). It refers to the level of neurological disability that accumulates independently of relapse episodes, a defining aspect of MS that is associated with neurodegeneration and chronic, diffuse inflammatory processes (Dimitriou et al., 2023), although the pathological basis for PIRA has not yet been demonstrated. PIRA is an increase in EDSS scores during periods of no relapses (Tur et al., 2023). This is important because it suggests that MS can progress independent of inflammatory responses and indicates that there is a neurodegenerative component independent of new lesions and new inflammatory attacks.

In addition to the main subtypes of MS classified by the Lublin classification (RRMS, PPMS, SPMS and CIS), there are other less common descriptors, which help to further describe disease variability (Lublin et al., 2014). Late-onset MS (LOMS) refers to MS diagnosed in older patients (typically ≥ 50 years) and is often associated with a more progressive phenotype, as age and the comorbidities associated with older people are significant factors influencing disability (Knowles et al., 2024). Paediatric MS is defined as the clinical manifestation of MS in patients under 18 years of age, which is almost exclusively RRMS and usually presents as a milder disease course, but can lead to severe disability at a young age (Brola & Steinborn, 2020). Patients who experience little disability over a sustained time are often classified as having benign MS (Reynders et al., 2017). Recent studies have shown that a low EDSS score (≤ 3) 15 years after diagnosis may be a more reliable indicator of MS, as the term 'benign' is often viewed as controversial for not considering the full impact of the disease (Sartori et al., 2017; Tallantyre et al., 2019). These definitions help to provide a framework for understanding and managing MS (Klineova & Lublin, 2018).

1.3.1 Classifying the Multiple Sclerosis Lesion

Demyelinated lesions are a pathological hallmark, representing inflammation and myelin loss in the CNS (Popescu et al., 2013). Demyelinated lesions can be formed in both the WM and GM of the brain or spinal cord (Lassman, 2018). Lesions are important biomarkers in MS diagnosis and can be visualised using MRI imaging to monitor disease worsening, as lesions can increase in size or quantity over the disease course (Basaran et al., 2022). Lesions directly cause symptoms such as muscle weakness, sensory loss and vision impairment, which can have a negative effect on patient disability and quality of life (Huang et al., 2017).

MS lesions can be classified at autopsy as pre-active, active, chronic active (smouldering or slowly expanding), or chronic inactive, and the type of lesion is characterised by the extent of demyelination and microglia activation within the affected area (Jonkman et al., 2015). In a study of 182 post-mortem MS cases (mean disease duration = 28.6 years) conducted by Luchetti et al., (2018), 7562 brain lesions were analysed and 57% of these lesions were deemed to be chronic active lesions. The study also found that patients with a more severe disease progression had a greater number of chronic active lesions and a higher total lesion count at the time of death. Additionally, patients with a progressive disease course (both SPMS and PPMS) had a higher proportion of lesions compared to those with RRMS. The study concluded that chronic active lesions are more prevalent in PMS than in RRMS, suggesting that lesion count can serve as a prognostic tool for MS patients. Moreover, their work showed that, pathologically, SPMS and PPMS are indistinguishable.

Lesions in the cortical GM differ in immunological and histopathological features compared to WML, which indicates a location-specific manifestation of MS disease mechanisms (Calabrese et al., 2013). Grey matter lesions (GML) are important hallmarks to study in PMS as recent evidence suggests that GM pathology is associated with early disease onset, occurs with disease progression and is related to clinical consequences of MS such as cognitive and motor impairments (Kalver et al., 2013). GML can be found in

the early stages of MS and in patients who died within months of diagnosis (Bevan et al., 2018; Lucchinetti et al., 2011). However, imaging of these cortical lesions can be challenging as they predominantly affect the superficial areas of the cortex, where myelin density is low and immune cell infiltration is sparse (Fillipi et al., 2019). The lesions in the cortical GM are classified as: type I GML, or leukocortical lesions, which refers to lesions that occur between the WM and GM regions; type II lesions (or intra-cortical), which are localised in the GM areas of the cerebral cortex and are often found around blood vessels; and type III, or subpial lesions, which are widespread within the cortical GM and are located under the pial surface (Griffiths et al., 2020; Magliozzi et al., 2018).

1.4 Pathophysiology of Multiple Sclerosis: Neurodegeneration is the Main Pathological Component of MS Progression.

Hauser & Cree (2020) stated that there are five main pathologies underlying the pathogenesis of PMS; the presence of acute MS lesions, meningeal B cell rich follicles, slowly expanding lesions, diffuse WM gliosis and age-related atrophy that reflects neuronal and axonal loss (see Figure 2). Signs of neurodegeneration are observed early in disease, with neuronal loss and injury, which results in brain atrophy, seen in RIS and CIS, together with raised neurofilament protein (released by damaged and dying neurons) in cerebrospinal fluid (CSF) and blood (Andravizou et al., 2019).

Neurodegeneration is a major component for disease progression and underpins cognitive, neuropsychiatric and sensory dysfunction and sustains irreversible motor disability (Mey et al., 2023). Neurodegeneration is notably in areas of GM demyelination but can occur partly independent of both grey and WM demyelination (Magliozzi et al., 2023).

Carassiti et al., (2018) investigated the relationship between brain volume and neuron count estimation, demonstrating a 9.5 billion lower neuron count compared to controls. The neuron density and cortical volume in the MS brain were reduced by 28% and 26%

respectively, suggesting that there is a strong relationship between neuronal loss and cortical volume. It is evident that meninges have an important role in influencing the neurogenerative processes underlying PMS pathology (Magliozzi et al., 2023), which correlates with disability worsening and an earlier death. An increase in inflammation in the leptomeninges is associated with more extensive cortical (subpial) demyelination and lower neuron density, which correlates with a shorter time to progression, greater disability and earlier death (Magliozzi et al., 2010; Magliozzi et al., 2023). This emphasises the need to further investigate the contribution of neurodegeneration to progression and to determine the factors which associate with neuron loss in the MS brain (Mahad et al., 2015).

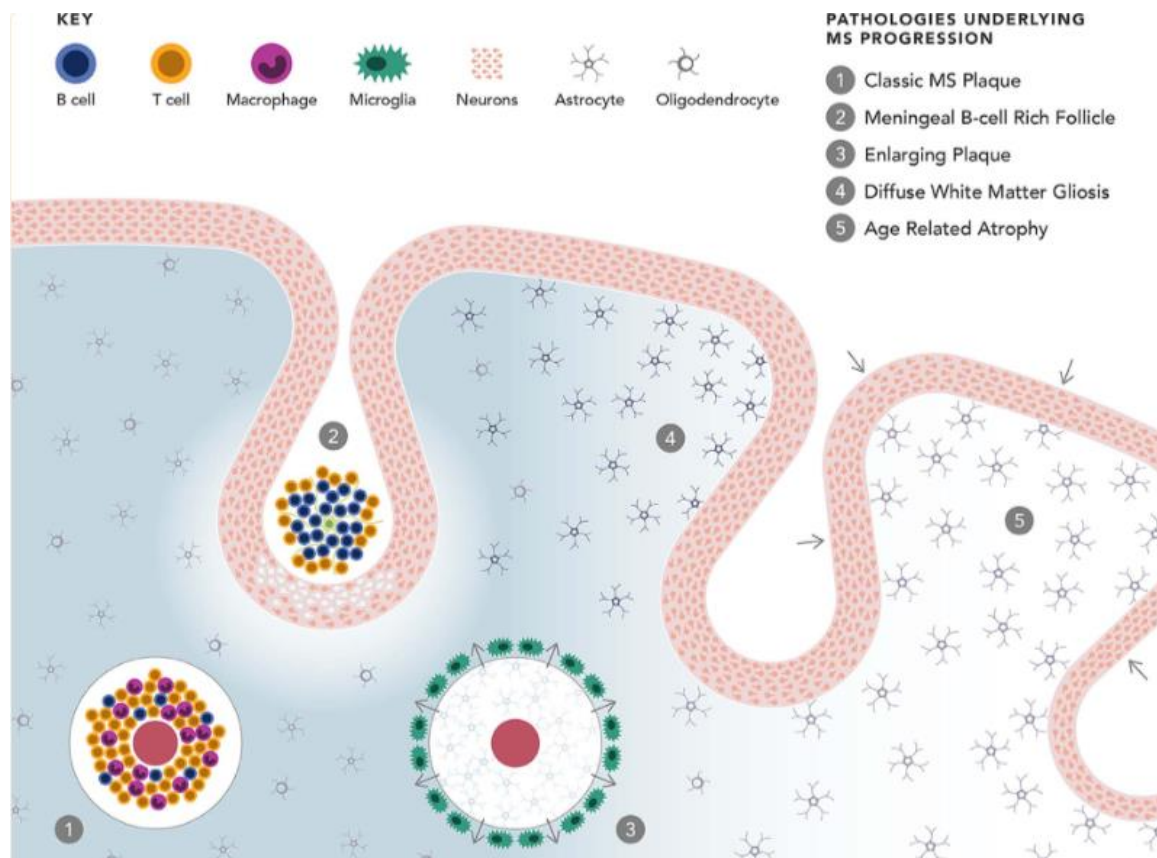


Figure 2. The five major pathological processes underlying neuronal and axon loss in PMS. 1) The presence of acute MS lesions is associated with continuous inflammatory activity and demyelination, often observed in patients with frequent relapses, but also in those who experience progression without relapse activity. 2) Meningeal B cell rich follicles are linked to increase inflammation, cortical demyelination and substantial neuronal and axonal loss. 3) Slowly expanding lesions result from enlarging plaques and are formed due to activated microglia, proliferation of astrocytes and stressed oligodendrocytes causing axonal injury. 4) Widespread diffuse microglial inflammation is present throughout the WM of the CNS and is associated with decreased myelin density and ongoing axonal and neuronal damage. 5) Age-related neurodegeneration involves a natural decline in neuron count and brain volume, which is accelerated in people with MS. This atrophy may interact with MS-specific pathologies and lead to more severe clinical outcomes in older patients. This figure was taken from Hauser & Cree (2020) with the appropriate DOI link: [10.1016/j.amjmed.2020.05.049](https://doi.org/10.1016/j.amjmed.2020.05.049).

1.5 Current Treatment Therapies and Clinical Trials

Treatment options in MS help manage acute relapses, reduce relapse frequency and severity and modify the disease course to varying degrees (Doshi & Chataway, 2016).

There are approximately 20 Food and Drug Administration (FDA) approved treatments for patients with MS that can be taken orally, administered by injection (either subcutaneous or intramuscular), or delivered intravenously via infusion, depending on

the specific therapy (Amin & Hersh, 2022; MS Society, 2022). The National Institute of Health and Care Excellence (NICE) has provided specific guidelines on what treatment options should be considered first for different MS subtypes, based on both cost-effectiveness and clinical benefit and access to certain medications may be restricted in the United Kingdom (National Institute of Health and Care Excellence, 2022).

Early treatment intervention is used to control disease activity, slow disease progression, and preserve neurological function (Brown et al., 2019; Ziemssen et al., 2016). The most frequent DMTs administered to patients with PMS are siponimod and ocrelizumab (Sorensen et al., 2020; Pozzilli et al., 2023). Clinical trials of patients with SPMS have shown that siponimod treatment is associated with less thalamic and cortical GM atrophy, a lower disability and a less severe disease course, when compared with a placebo (Cohan et al., 2022; Kappos et al., 2018). Ocrelizumab is the only approved treatment for patients with PPMS and is associated with a reduction in disease activity and progression over 24-months (Hauser & Cree, 2020). However, evidence for the long-term effectiveness of these DMTs in altering the clinical course is limited (Gozzo et al., 2023). Current DMT options primarily target the immune system, which emphasises the need for further development of DMTs that aim to address other drivers of MS worsening beyond inflammation, such as neurodegeneration (Bierhansl et al., 2022). The use of DMTs in older patients has been carefully considered due to a greater risk of developing comorbidities, which can influence the therapeutic mechanism, but evidence investigating the effects of DMT discontinuation in older generation remains inconclusive (Buscarinu et al., 2022; Zhu & Xia, 2024). The use of clinical trials has been instrumental for the development of new DMTs and ongoing advancements continue to drive further therapeutic innovation (Manouchehri et al., 2022). The most recent trial, known as the Octopus trial, is the first multi-arm, multi-stage study aiming to develop new treatments for PMS that slow disability progression by providing neuroprotection (Gray et al., 2023).

1.6 The Genetics of Multiple Sclerosis Risk and Progression

Although the mechanism of MS is not fully understood, it is said to be a combination of genetic, immunologic and environmental factors that contribute to disease progression (Olsson et al., 2017; Tafti et al., 2024). Advancements in research and collaborations has advanced our understanding of non-human leukocyte antigen (HLA) genetic risk factors, with current studies focusing on the identification of causal alleles of SNPs (Gourrad et al., 2012; Waubant et al., 2019).

Research into the genetic contributors to MS risk has revealed over 200 gene variants (Goris et al., 2022; Jokubaitis & Butzkueven, 2023). However, the genetic contribution to MS severity remains an ongoing area of research. So far, studies using small cohorts have failed to identify validated variants associated with MS severity (Fitzgerald et al., 2019; Harroud et al., 2023; Jokubaitis et al., 2023; Kreft et al., 2024). The HLA-DRB1*15:01 allele is strongly associated with an increased risk of developing MS and individuals carrying this allele are more likely to be diagnosed with MS (at a three-fold increase) compared to those without it (Barrie et al., 2024). Moreover, studies suggest that the HLA-DRB1*15 gene influences clinical outcomes in MS patients by modulating the amount of demyelination and inflammation in the spinal cord and causes a worsening in patient disability (Brownlee et al., 2023; DeLuca et al., 2013).

Most MS-associated variants identified by GWAS studies are mapped to the non-coding regions of the genome, with the associated genes mainly located in regulatory regions (Ma et al., 2023; Madireddy et al., 2019). Recent findings from DNA sequencing technologies have identified non-coding RNA as important regulators of cellular processes in MS and they need to be investigated further, as coding regions account for only 2% of the genetic information in the genomic DNA (Mycko & Baranzini, 2020). The suggested functions of many of these genetic variants imply the involvement of cells from both the adaptive and innate immune responses in the pathogenesis of MS (Goris et al., 2022), supporting the concept of MS as an autoimmune disease that can be modified by immune-targeting therapeutics.

1.7 Genome Wide Association Studies and their Importance in MS Research

Genome wide association studies (GWAS) are conducted on a large-scale to identify genetic variations that are associated with a particular disease (Favorova et al., 2014). GWAS has identified SNPs that occur more frequently in the MS population (Cotsapas & Mitrovic, 2018). As well as being able to identify MS-associated genetic variants, GWAS can aid the development of polygenic risk scores which is a predictive tool capable of estimating a person's susceptibility to MS. Genes linked to MS risk and influencing clinical phenotypes are likely to have modest effects individually, but in combination with other variants can represent a polygenic impact on the patients' clinical outcomes (Ma et al., 2023). As of yet, polygenic risk scoring is not used clinically for MS but does hold a huge promise for improving patient care (Lennon et al., 2024). GWAS has more recently been beneficial to further understanding the genetic and environmental interactions in MS by identifying that the coding region for the transient transcriptome is enhanced in genetic variants associated with MS. These genomic regions for the transient transcriptome show an increased presence of DNA binding sites associated with molecule transducers that are implicated in non-genetic contributors of MS, such as EBV and Vitamin D levels (Umeton et al., 2022). This emphasises the importance of GWAS studies in complex diseases such as MS, as they can provide insight into disease mechanisms and highlight therapeutic targets that may aid drug discovery and the development of new treatment strategies (Reay & Cairns, 2021).

1.7.1 GWAS Studies to Understand the Genetic Drivers of Progression

A cohort analysis conducted by Pan et al., (2016) revealed that gene susceptibility variants could provide insights into the clinical course of MS. This study investigated 116 SNPs associated with MS risk and identified 2 non-HLA SNPs and 1 HLA SNP that was associated with predicting MS and relapse risk, and other non-HLA and HLA SNPs that

were involved with predicting relapse or the EDSS score. This shows that there are genetic underpinnings which can alter the course of MS.

A notable link involving rs10191329 located in the dysferlin-zinc finger protein 638 (DYSF-ZNF638) region was discovered (Harroud et al., 2023). The risk allele has been reported to correlate with a 3.7-year reduction in the median time until a walking aid is required at the homozygous minor level. Additionally, this SNP was associated with increased brainstem and cortical abnormalities observed in brain tissue. This rs10191329 SNP was then analysed in another cohort of MS patients and results showed that those carrying the minor allele had higher rates of brain atrophy (Gasperi et al., 2023). However, these findings were not replicated in a relapse-onset MS cohort (n = 1813) studied by Campagna et al., (2024) or in an independent MS patient cohort (n = 1455) investigated by Kreft et al., (2024), as both studies concluded that the SNP did not influence the clinical outcomes of their cohort. They did however find that the rs7289446 SNP intronic to seizure related 6 homolog like (SEZ6L) had a strong association that nearly met the GWAS threshold, and this gene was associated with dendritic spine density and arborization (Jokubaitis et al., 2023). The investigation into genetic SNPs and their association with severity highlighted in these studies emphasises the dynamic and evolving nature of research in this field. These findings also highlight the innovative pathways researchers are exploring to further understand these genetic variants, demonstrating the ongoing advancements to increase our understanding of genetics and its implications.

To understand the genetic basis of progression (and to uncover variants that map to the principal pathological features that drive MS worsening) it would be necessary to combine genetic (or GWAS) analysis with quantitative neuropathology. Ongoing work in our group, in collaboration with Professor Richard Reynolds and the UK MS Society Tissue Bank (unpublished), using GWAS of a large neuropathological cohort, has shown candidate gene variants of proprotein convertase subtilisin/kexin type 5 (PCSK5) and COMM domain containing 10 (COMMD10) to be associated with a differential neuron density. Therefore, as few genes have been linked to MS severity, GWAS studies can be

used to identify genes of interest that are correlated with neuropathology to determine whether carriers of these gene variants have altered neuroprotective traits, resulting in less neuron loss and a less severe MS disease course.

1.7.2 The Role of Dystrophy-Associated Fer-1-Like Gene

Dysferlin, or dystrophy-associated fer-1-like (DYSF), is a gene that encodes the DYSF protein which is expressed in muscle tissues and is important in cell membrane maintenance (Ivanova et al., 2022). Mutations in the DYSF gene (known as dysferlinopathies) can cause complications such as progressive muscle weakness and degeneration (Anwar & Yokota, 2024; Spadafora et al., 2022). Research using DYSF-deficient mouse models has revealed alterations in immune cell function and cytokine production, increasing susceptibility to autoimmune diseases (Hornsey et al., 2013). rs10191329, located in the DYSF-ZNF638 locus, is the first described genetic variant linked to MS severity that passes rigorous GWAS statistical thresholds (Harroud et al, 2023).

1.7.3 The Role of the Seizure 6-Like Gene

The SEZ6L gene encodes the SEZ6L protein that is responsible for neural connectivity, synaptic plasticity and dendritic spine formation (Jokubaitis et al., 2023; Nash et al., 2020). SEZ6L is widely expressed in the brain including the cortex, hippocampus, striatum and cerebellum (Nash et al., 2020). There have been few studies that have explored the role of SEZ6L in motor and cognitive functions, but these have utilised mouse models and not human brain tissue from individuals with MS, which is the focus of our study (Nash et al., 2020; Ong-Pålsson et al., 2022). SEZ6L can act as a substrate for beta-site APP cleaving enzyme 1 (BACE1), which is involved in the production of beta-amyloid peptides implicated in Alzheimer's disease and Niemann-Pick type C disease, thereby influencing SEZ6L function (Causevic et al., 2018; Pigoni et al., 2016; Müller et al., 2023). The role of SEZ6L and its implication in neurodegenerative diseases

highlights the importance of further research into this gene in MS. rs7289446, which is intronic to the SEZ6L gene, had the strongest signal in the study conducted by Jokubaitis et al., (2023), indicating a potential role in influencing disease severity in individuals with MS.

1.7.4 The Role of the Proprotein Convertase Subtilisin/Kexin Type 5 Gene

PCSK5 is a member of the proprotein convertase family and plays an important role in processing immature proteins into their functional forms, as well as being crucial for cell migration and transformation (Gong et al., 2024). PCSK5 is also important for lipid, glucose and bile metabolism (Parvaz & Jalali, 2021). The minor allele of a SNP mapping to PCSK5 (rs10521467) has been shown to be associated with an increased risk of cognitive impairment and hypotension in a GWAS study using hypotensive cases in Taiwan (Chen et al., 2019). Knockout of PCSK5 in mice resulted in complications such as cardiac malformations, tracheoesophageal defects and early embryonic death, but did not affect the neural crest, which is responsible for normal embryonic development (Szumska et al., 2017). Recent studies have also elucidated the pivotal role of PCSK5 within the CNS, particularly in facilitating the motility of microglia and monocytes, by converting the inactive pro-matrix metalloproteinase 14 (pro-MMP14) and pro-matrix metalloproteinase 2 (pro-MMP2) enzymes into their active forms. The suppression of PCSK5 has been shown to reduce the pathological mobilisation of monocytes and increase the presentation of depressive-like behaviours in mice (Ito et al., 2021). Further study of PCSK5 in the MS brain is crucial for improving our understanding of disease pathogenesis and for identifying additional therapeutic targets to manage the condition. Variants rs10869757 and rs11144848, both predicted to map to PCSK5, were identified by our collaborators as part of our large scale GWAS neuropathology analysis (unpublished).

1.7.5 The Role of the COMM Domain Containing 10 Gene

The COMMD10 gene is a member of the COMMD family and has been linked to copper homeostasis. It has also been shown to inhibit the nuclear factor κ -light-chain-enhancer of activated B cells (NF- κ B) signalling pathway, demonstrating beneficial effects in suppressing colorectal cancer metastasis and inducing apoptosis by upregulating genes such as caspase 3 (CASP3) and caspase 9 (CASP9), thereby inhibiting tumour growth in hepatocellular carcinoma (Fan et al., 2020; Yang et al., 2021). COMMD10 mRNA has been previously detected in the brain, but at low levels (Fan et al., 2020). NF- κ B transcription elements play a vital role in cell signalling pathways in response to inflammation. They are universally expressed in neurons and regulate the transcription of genes and proinflammatory modulators linked to neuronal survival. The specific subunit composition of NF- κ B dimers determines functional outcomes, influencing neuronal protection by modulating the expression of genes involved in cell survival and inflammatory responses (Shih et al., 2015). This makes the COMMD10 gene an important target for studying neuronal survival in the GM of the brain. In a study conducted by Phan et al. (2023), it was shown that COMMD10 plays a crucial role in early embryogenesis. Knockout of the COMMD10 gene in mice resulted in embryonic death before day 8.5, halting further development. The study concluded that COMMD10 is essential, particularly for neural crest development. This emphasises the importance of COMMD10 in the regulation of neural development and neuronal survival, and further investigation of this gene within the MS brain is crucial to uncover its role in neuroinflammation, neuroprotection and potential therapeutic strategies. Variants rs185263, rs1567335, rs200645460 and rs784480, predicted to map to COMMD10, were identified by our collaborators in our large scale GWAS neuropathology analysis, but only the top two SNPs (rs185263 and rs1567335) were further investigated in our study herein.

1.7.6 The Polygenic Risk of Genetic Influences in Multiple Sclerosis

MS is a polygenic condition meaning that an individual who has been diagnosed with MS has multiple genetic variants contributing to disease risk (Shams et al., 2023). It is evident that a single gene variant cannot have a strong influence on the manifestation of MS and therefore the genetic contribution is via several variants, each having a small effect, but together make a telling contribution to risk or severity (Goris et al., 2022). The combined influence of gene variants that contribute to the risk of MS is important for how healthcare professionals personalise their support to MS patients regarding the risk and predicted outcome of the disease (Goris et al., 2022). Polygenic risk scores (PRS) have a vital role in understanding both the risk of developing MS and the severity of the disease (Lewis & Vassos, 2020). PRS are computed by assessing the collective impact of various genetic risk alleles, with each allele's contribution weighted by its known effect size (Breedon et al., 2023). It is evident that polygenic risk profiling can aid in prioritising patients with lower PRS scores, as individuals with these scores may carry rare or uncommon genetic variants, highlighting the need for more frequent sequencing studies to identify such variants (Lu et al., 2021).

1.8 Aims and Objectives

Ongoing research in the group, which has combined GWAS with quantitative neuropathology, has already identified various genes of interest that might be linked with a more severe neurodegenerative disease phenotype. My project will focus on better understanding the relative contribution of PCSK5 and COMMD10, alongside DYSF and SEZ6L, which represent the first published gene variants linked to MS severity. The focus will be on GM tissue and neuron density, given their key association with progression.

We hypothesise that genetic variants mapping to PCSK5 and COMMD10, identified using a large scale GWAS neuropathology study, correlate with increased neurodegeneration and a worsening in clinical outcomes. In addition, we hypothesise that PCSK5 and COMMD10 will be localised to neurons and will be differentially expressed in the MS brain.

We will test this hypothesis by using a cohort of post-mortem MS and non-neurological disease human brain sections with linked quantitative pathological data, immunohistochemistry, in situ hybridisation and new digital pathology analysis.

The overall aim of the project is to further investigate the genetic and pathological influence on PMS severity.

The project aims are as follows:

- To compare neuron density in a large cohort of PMS cases in comparison to matched controls to determine the relative extent of neurodegeneration in MS.
- To compare neuron density, lesion size and diffuse microglial activation in representative cohorts of major allele homozygotes, heterozygotes and minor allele homozygotes for gene variants of interest, including those mapping to PCSK5 and COMMD10.
- To use *in situ* hybridisation and immunohistochemistry to identify cellular sources and expression patterns of genes of interest, including PCSK5 and COMMD10, and to describe their association with lesion pathology.

1.8.1 Project Impact

The project investigates the stated aims using post-mortem human brain tissue from individuals with PMS and from those without neurological complications, serving as non-neurological disease control (control). The project utilises individuals with PMS because this stage marks the disease endpoint, providing insight into how the condition has evolved since diagnosis. Control cases included in the study had died from causes unrelated to neurological disease, such as drug overdose and heart failure, whereas the MS cases had died due to MS and its associated complications, characterised by accumulating disability and complex care needs typical of MS patients approaching end of life, as reported by Martin et al., (2016). There is an urgent need to identify the genetic factors underlying more severe forms of MS. The project has the potential to further understand the key molecular drivers of MS contributing to disease worsening. There is little to no evidence consolidating knowledge of MS progression and the mechanisms driving increased severity. Although significant strides have been made in identifying genetic risk factors for MS, a gap remains in understanding the genetic predispositions associated with disease progression and worsening. This emphasises the importance of further investigation, as certain genetic SNPs may influence neuropathological and clinical outcome in patients. Any new findings from the project could eventually allow us to create better treatment plans and devise new biomarker tests to monitor patients with the disease. The identification of novel gene variants and associated pathological traits of MS can be used to answer significant research questions regarding MS progression and severity. It is evident that severe cases of MS can lead to disability, thus identifying genes that impact disease severity can support healthcare professionals in selecting appropriate treatment plans and drug targets to slow down MS progression (Lublin et al., 2022).

2.0 Methods

The primary aim is to explore the genetic influence of a select number of target genes on the clinical and pathological expression of MS. We firstly used a literature and resource review to summarise key information regarding the genes and proteins of interest and what is currently known regarding the function of the first published variants linked to MS severity (rs72894266 mapping to SEZ6L and rs10191329 mapping to DYSF-ZNF) and our two novel variants (rs10869757 and rs11144848 mapping to PCSK5 and rs185263 and rs1567335 mapping to COMMD10). We established a workflow to firstly; using the linked data available, explore the inter-relationship between the genetic variants and important pathological and clinical measures of disease severity. As the SNP rs10191329 mapping to DYSF-ZNF was not found in our GWAS study but another SNP rs7565433 mapping to DYSF:CYP26B1 was, we utilised this workflow for this variant to further explore the impact of MS patients carrying this SNP. We then, described the expression of our target genes of interest (PCSK5, COMMD10) in control and MS brain, by immunohistochemistry (IHC) and in situ hybridisation (ISH), to finally quantify the relative gene and/or protein expression in MS versus control and between normal-appearing and demyelinating tissue. This project represents the first report of the localisation and expression of novel gene variants and their mapped genes discovered by combined MS GWAS and neuropathology.

2.1 A Literature Review to Summarise the Known Expression and Function of Novel Target Genes PCSK5 and COMMD10 in the Human Brain

A literature review was conducted to gather further genetic and cell biological information on the genes mapped to variants of interest from the accompanying GWAS study and those described in the recent literature. The genes COMMD10 and PCSK5 represent those identified in the ongoing GWAS analysis of the UK MS Tissue Bank, whilst variants mapping to SEZ6L (rs72894266) and DYSF-ZNF638 (rs10191329), associated with disease progression (Harroud et al, 2023; Jokubaitis et al., 2023). The

search strategy involved Google and querying the databases: National Center for Biotechnology Information (NCBI) (Sayers et al., 2022) and Human Protein Atlas (<https://www.proteinatlas.org/>) to access the latest information concerning function and expression at RNA and protein level (Karlsson et al., 2021; Uhlén et al., 2015; Sjöstedt et al., 2020; Thul et al., 2017). The protein-protein interaction for each gene is based on data from the IntAct and BioGRID databases, as well as the BioPlex and OpenCell experimental datasets, showing interactions for 15038 genes (Cho et al., 2022; Huttlin et al., 2021; Oughtred et al., 2021; Tu et al., 2021). The visualisation and analysis of single-nucleus gene expression of our imputed genes of interest (SEZ6L, DYSF, PCSK5 and COMMD10), were carried out using the publicly available resource cellxgene VIP (<https://cellxgenevip-ms.bxgenomics.com/>). This information is based on brain tissue from 12 MS patients consisting of cortical and subcortical WM samples first described by Schirmer et al., (2019).

2.2 UK MS Tissue Bank MS Cohort for Gene Pathological Comparisons

As part of our wider collaborative studies with the UK MS Tissue bank, we have access to tissue sections and immunostained slides from $n = 310$ cases (199 female, 31 years of age at onset, 59 years of age at death, 227 with a relapse-onset) that have also been genotyped (Illumina Infinium Omni 2.5 Exome BeadChip array). A detailed overview of the cohort is presented in Table 9 of supplementary. Each case is coupled with detailed lifetime clinical history summarised by the Tissue bank. The post-mortem tissue sections were provided by the UK MS Tissue Bank, Imperial College London with ethical approval (#19/WA/0238). The post-mortem brain sections used in the project were both formalin-fixed paraffin embedded (FFPE) and snap frozen (SF) sections of brains from different regions of MS cases and non-neurological disease controls (UK MS Tissue Bank and Thomas Willis Brain Bank, Oxford). The FFPE tissue sections were provided at a thickness of $6\mu\text{m}$. The SF sections were prepared from frozen tissue blocks at the same thickness and stored in the -80°C freezer. The sampled regions for quantitative analysis were 1. superior frontal gyrus (SFG), 2. cingulate gyrus (CG), 3. thalamus; 4. occipital

lobe, 5. cerebellum and dentate nucleus (Cb DN) and 6. pons. We (Howell group) have collected new data on the extent of demyelination, neuron density, perivascular and leptomeningeal inflammation and measures of microglia/macrophage activation, from systematically sampled blocks using a digital pathology approach (which is outlined below) (Cooze et al., 2024). This thesis utilises a selection of cases and sections from this large neuropathological cohort and makes use of some of the quantitative data captured by the Howell group and UK MS Tissue bank researchers from the entire cohort.

2.2.1 Summary Tables of Human MS and Control Post-Mortem Cases

To fulfil the project aims, a range of different cases was required for the various protocols employed. Table 1 shows the MS cohort used to compare neuron density in the SFG, CG and thalamus and Table 2 provides information on the non-neurological disease control cohort used for comparison. Tissue sections were selected to include various MS phenotypes, with both male and female MS cases of different ages, to ensure the findings are more representative. Table 3 shows the MS cohorts that were used to investigate the relative gene expression of SEZ6L, PCSK5 and COMMD10 and its localisation in neurons, as well as the presence of the PCSK5 and COMMD10 genes together using RNAscope Duplex protocol. It is important to note that the MS cases in this project were not receiving any DMTs that could have influenced disease progression.

Overview of the MS Cases Used for Neuropathological and Genetic Analyses:

Number of MS cases	Sex	Age of onset (years)	Age of progression (years)	Age at WC (years)	Age died (years)	Onset to death (years)	Onset to progression (years)	Onset to WC (years)	Progression to death (years)
310	199 F, 100 M, 11 unknown	31 (7-69)	31 (15-85)	34 (18-86)	59 (34-98)	28 (3-66)	11 (0-49)	16 (0-47)	12 (0-54)

Table 1. A summary of the MS cases used for quantitative neuropathology and genotyping. Data includes the number of MS cases, a breakdown of sex, age of onset, age at progression, age at wheelchair (WC) use, age at death, duration from onset to death, onset to progression, onset to WC and progression to death. All age-related variables and time intervals are reported in years.

Human Non-Neurological Disease Control Cases:

Case	Age	Sex	Cause of death	PMI (hrs)	Protocol(s) used
C026	78	F	Myeloid leukaemia	33	HuC ⁺ IHC
C032	88	M	Prostate cancer	22	HuC ⁺ IHC
C045	77	M	Prostate cancer	22	HuC ⁺ IHC
C036	68	M	Heart failure and alveolitis	24	HuC ⁺ IHC
C037	84	M	Bladder cancer, pneumonia	5	HuC ⁺ IHC
C039	82	M	Rheumatoid arthritis	24	HuC ⁺ IHC
C048	68	M	Metastatic colon cancer, microvascular pathology	10	HuC ⁺ IHC
NP013/011	62	F	Metastatic colorectal cancer	24	HuC ⁺ IHC, SEZ6L + HuC, Duplex, PCSK5 IHC
NP013/012	60	F	Metastatic breast cancer	48	HuC ⁺ IHC, PCSK5 IHC
NP012/023	69	M	-	24	HuC ⁺ IHC
NP013/039	41	M	Myocardial infarction	24	HuC ⁺ IHC, SEZ6L + HuC, Duplex, PCSK5 IHC
NP012/046	72	M	-	24	HuC ⁺ IHC
NP012/052	42	F	Metastatic pancreatic carcinoma	48	HuC ⁺ IHC
NP011/073	64	M	Gastrointestinal bleed, sepsis	48	HuC ⁺ IHC
NP013/073	59	M	Infective exacerbation of chronic obstructive pulmonary disease	24	HuC ⁺ IHC, SEZ6L + HuC, Duplex, PCSK5 IHC
NP012/088	51	M	Cardiac arrest	24	HuC ⁺ IHC
NP011/093	52	F	Chronic liver disease	48	HuC ⁺ IHC
NP013/103	48	F	End-stage interstitial lung disease	56	HuC ⁺ IHC
NP013/109	69	M	Myocardial infarction	34	HuC ⁺ IHC
NP122/011	65	F	Infective exacerbation of chronic obstructive pulmonary disease	<24	HuC ⁺ IHC
NP013/126	56	M	Cardiac arrest	40	HuC ⁺ IHC, PCSK5 + HuC, COMMD10 + HuC, Duplex, PCSK5 IHC
NP013/127	60	M	Cardiac arrest	30	HuC ⁺ IHC, Duplex, PCSK5 IHC
NP013/128	68	M	Cardiac arrest	48	HuC ⁺ IHC, Duplex, PCSK5 IHC
NP012/132	67	F	-	48	HuC ⁺ IHC
NP013/141	56	M	intra-operative death during coronary artery bypass graft	48	HuC ⁺ IHC
NP013/161	73	M	Metastatic colorectal cancer	52	HuC ⁺ IHC, SEZ6L + HuC, PCSK5 + HuC, COMMD10 + HuC, Duplex, PCSK5 IHC
NP013/172	69	M	Drug overdose	36	HuC ⁺ IHC, SEZ6L + HuC, Duplex, PCSK5 IHC
R1 1231 93	58	M	-	48	HuC ⁺ IHC,

Table 2. Donor information for non-neurological disease controls utilised in this study. A combination of FFPE and SF blocks were available to perform various ISH and IHC techniques, as well as a combined approach for SEZ6L + HuC and PCSK5 + HuC protocols. All cases were region-matched across the SFG, CG and thalamus. Details of the cases such as sex, age and cause of death and post-mortem interval (PMI; hours) are shown above.

MS Cases Used:

Case	Age	Sex	Cause of death	MS Classification	Disease Duration (years)	PMI (hrs)	Protocol(s) Used
MS402	46	M	MS, Bronchopneumonia	SPMS	20	12	PCSK5 IHC
MS407	44	F	Septicaemia, Pneumonia	SPMS	19	22	PCSK5 IHC
MS408	39	M	Pneumonia, Sepsis	SPMS	10	21	PCSK5 + HuC, COMMD10 + HuC, Duplex
MS422	58	M	Chest infection due to MS	SPMS	-	25	PCSK5 IHC
MS423	54	F	Pneumonia	SPMS	30	11	PCSK5 + HuC, COMMD10 + HuC, Duplex, PCSK5 IHC
MS425	46	F	Pneumonia, MS	SPMS	21	25	SEZ6L + HuC, Duplex, PCSK5 IHC
MS438	53	F	MS	SPMS	18	17	SEZ6L + HuC, Duplex, PCSK5 IHC
MS461	43	M	Bronchopneumonia	SPMS	21	13	PCSK5 IHC
MS473	39	F	Bronchopneumonia, MS	PPMS	13	9	SEZ6L + HuC, Duplex, PCSK5 IHC
MS485	57	F	Bronchopneumonia, Advanced MS	PPMS	13	24	Duplex, PCSK5 IHC
MS491	64	F	Anaphylactic reaction	SPMS	26	9	PCSK5 IHC
MS492	66	F	Sigmoid cancer	PPMS	31	15	Duplex, PCSK5 IHC
MS497	60	F	Aspiration pneumonia, MS	SPMS	29	26	SEZ6L + HuC, Duplex, PCSK5 IHC
MS510	38	F	Pneumonia, MS	SPMS	22	19	Duplex, PCSK5 IHC
MS513	51	M	MS, respiratory failure	SPMS	18	17	SEZ6L + HuC, PCSK5 IHC
MS523	63	F	Bronchopneumonia, MS	SPMS	32	20	SEZ6L + HuC, Duplex, PCSK5 IHC
MS527	47	M	Pneumonia, MS	SPMS	24	10	Duplex, PCSK5 IHC
MS528	45	F	MS	SPMS	25	17	PCSK5 IHC
MS530	42	M	MS	SPMS	24	15	SEZ6L + HuC, PCSK5 IHC
MS538	62	M	Pneumonia	SPMS	39	12	Duplex, PCSK5 IHC
MS543	66	F	Ischaemic bowel (inoperable), MS	SPMS	40	24	PCSK5 IHC

Table 3. Post-mortem MS cases used in this study. These tissue samples were taken from the frontal region of the brain to perform ISH to detect the presence of SEZ6L, PCSK5 and COMMD10 gene expression in NGM and GML regions (Singleplex or Duplex detection), IHC to detect the presence of PCSK5 at protein level and a combined ISH/IHC approach to identify gene expression in immunostained HuC⁺ neurons (SEZ6L + HuC). The clinical information such as the age died, sex, cause of death, type of MS (PPMS = primary progressive MS, SPMS = secondary progressive MS, RRMS = relapse remitting MS), the disease duration and PMI are reported.

2.2.2 Data Retrieval of MS Cases Carrying SNPs of Gene Variants of Interest

The gene variants associated with MS neuropathology were selected for this project by our collaborative team. I compared the burden of neuronal, myelin and inflammatory pathology between cases defined by their variant status (homozygous major, heterozygous, homozygous minor) for the rs7565433 mapping to DYSF:CYP26B1, rs72894266 mapping to SEZ6L, rs10869757 and rs11144848 SNPs mapping to PCSK5, rs185263 and rs1567335 mapping to COMMD10. The number of cases in our cohort for each genotype of the SNPs of interest can be found in Table 10 of supplementary. The mean HuC⁺ neuron density per brain region (frontal gyrus, cingulate, thalamus, occipital lobe, basal pons and the cerebellar dentate nucleus) for homozygous major, heterozygous and homozygous minor genotypes was plotted as a scattergram with mean and standard deviation. Groups were compared by Kruskal-Wallis and Dunn's multiple comparison post-tests. The same analysis was conducted for measures of demyelination (% demyelination) and was calculated using the methodology outlined in protocol 2.7.1. I further investigated the effects of carrying both the PCSK5 and COMMD10 gene variants, specifically exploring the differences between the associated genotypes. Additionally, I expanded the investigation by examining whether specific genotypes of both gene variants of PCSK5 and COMMD10 were correlated with clinical differences, particularly in terms of outcomes such as age at death, age at wheelchair dependence and disease duration from symptom onset to death (method 2.2.3).

2.2.3 Assessing the Association Between Carrying Two or More Gene Variants of Interest and the Clinical and Pathological Severity of MS

We wanted to investigate whether carrying both SNPs mapping to PCSK5, or both SNPs mapping to COMMD10, influences measures of neuropathological or clinical severity in MS. The gene variants with the highest hits for the PCSK5 gene were rs10869757 and rs11144848 respectively and the top hits for the COMMD10 gene were rs185263, which was the top hit on the gene versus neuropath list and rs1567335 which was the 2nd most frequent hit. To investigate whether carrying more than one SNP of interest had an

impact on neuron density, demyelination and clinical outcomes, we performed a Dunn's multiple comparison between cases that carried all 4 SNPs of interest and cases that did not.

2.3 Tissue Characterisation

A subset of human brain tissue sections from a small number of MS and non-neurological disease controls were available for further analysis at Swansea (see Table 2 and Table 3). Tissue sections were stained with luxol fast blue (LFB)/haematoxylin to visualise patterns of myelin and to identify cell nuclei. Tissue sections were immunohistochemically stained with anti-HLA-DR (Human Leukocyte Antigen) to identify immune cell infiltration and activation, which is found in areas of damage and neuroinflammation; anti-myelin oligodendrocyte glycoprotein (MOG) to visualise myelin and demyelinated lesions; and anti-HuC (Hu proteins are mammalian embryonic lethal abnormal visual system (ELAV)-like neuronal RNA-binding proteins) for the staining of mature neurons. The GM of the frontal sections of MS brain tissue was characterised into normal grey matter (NGM) and GM lesion (GML) using the MOG-stained tissue sections. The previously stained MOG tissue sections aided the confirmation of lesion and NGM areas in cases that were also stained separately to confirm protein expression of PCSK5 and gene expression patterns of SEZ6L, PCSK5 and COMMD10 in control, normal and lesion tissue (protocols 2.5.2 and 2.6.1 respectively).

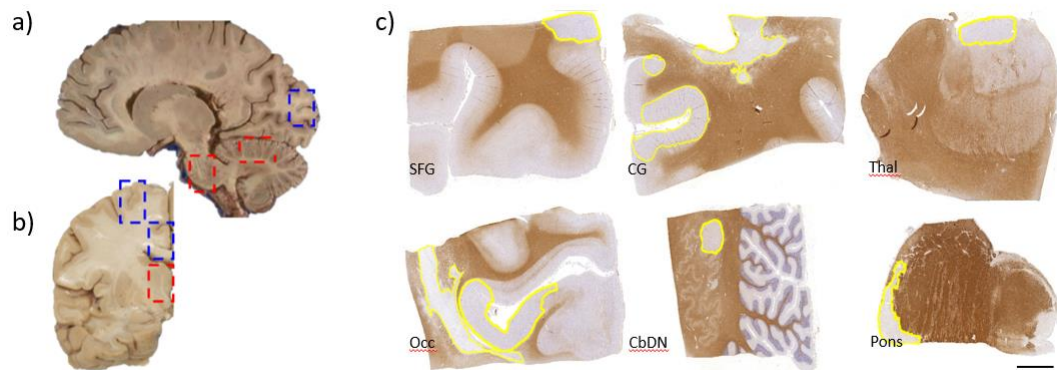


Figure 3. Identification of post-mortem human brain tissue regions used in the project. The a) sagittal plane shows the pons, cerebellum and occipital lobe from left to right and the b) coronal plane shows the SFG, CG and thalamus from top to bottom, as highlighted by the boxed regions annotated on the images. MOG immuno-staining confirmed the presence of c) NGM and GML regions and confirmed the type of lesion that is present based on its location. The areas of demyelination from the MOG sections are highlighted in yellow using the QuPath annotation tool. Stained HuC and HLA paired sections (seen later) were also used to quantify neuron density and diffuse microglia/macrophage activation, respectively. Scale bar: c = 1cm.

2.4 Primary Antibodies Used for Immunostaining and In Situ Hybridisation

Post-mortem brain sections were used for IHC, ISH and a combination of both protocols to assess SEZ6L, PCSK5 and COMMD10 gene expression using specific RNA probes and HuC/D for the staining of mature neurons. PCSK5 protein expression was also analysed using IHC. Scanned images were imported into QuPath digital pathology software for quantitative analysis (Bankhead et al., 2017; Cooze et al., 2024).

Antibody (Species)	Target	Secondary detection antibody	Dilution	Company & Product Details
Anti-HuC/D (Mouse)	Post-mitotic Neurons	Goat anti-mouse	1:1000	Clone: 15A7.1 Merck
Anti-MOG (Mouse)	Myelin oligodendrocyte glycoprotein	Goat anti-mouse	1:50	Clone: Z12 Prof Reynolds/Imperial College London
Anti-HLA (Mouse)	HLA-DR positive microglia/macrophage	Goat anti-mouse	1:150	Clone: cr3/43 Dako/Agilent
PCSK5 (Rabbit)	PCSK5 protein	Goat anti-rabbit	1:200	Polyclonal antibody: Invitrogen (product code 15734541)
COMMD10 (Rabbit)	COMMD10 cells	Goat anti-rabbit	1:800	Polyclonal antibody: Invitrogen (product code 13466387)

Table 4. A list of primary antibodies used in the project. Information includes the appropriate dilutions and manufacturer details.

2.5 Immunohistochemistry

IHC is an important method for determining the expression and localisation of a protein of interest by identifying the specific binding between an antibody and antigen that is presented on the tissue section (Bruan et al., 2013; Crowe & Yue, 2019; Magaki et al., 2019). I used IHC for the identification and quantification of HuC⁺ neurons in the SFG, CG and thalamus of the control cohort (Table 2), for the identification of myelin and demyelinated lesions (anti-MOG IHC) and for the immuno-staining of PCSK5 in our control and MS cohort (Table 2 and Table 3 respectively).

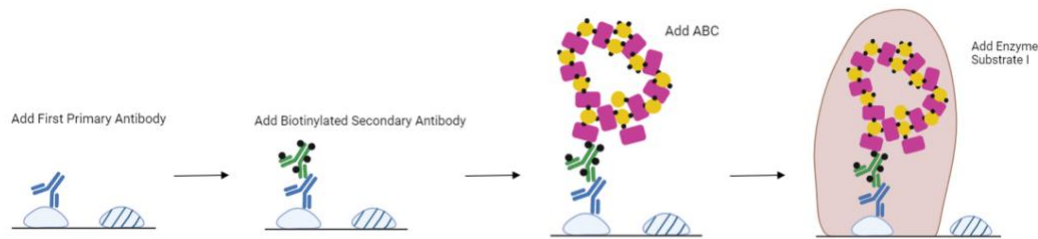


Figure 4. Single antigen labelling in IHC protocol. This diagram shows the important steps of IHC to visualise specific proteins within a tissue section. The primary antibody that is designed to target a specific antigen on the tissue (e.g. HuC) is bound by a biotinylated-conjugated secondary antibody and a tertiary enzyme-linked complex (peroxidase). This complex is visualised by adding a substrate (typically hydrogen peroxide with the chromogen diaminobenzidine) to allow detection through the generation of a coloured and insoluble reaction product that forms at the target protein within the tissue. This figure was created using Biorender.com.

2.5.1 Immunostaining Non-Neurological Disease Control Cases for the Quantification of HuC⁺ Neurons

Human control brain tissue was histologically stained to detect the presence of mature neurons using anti-HuC/D. There were 28 non-neurological disease control cases in this study (see Table 2 for clinical information on the cohort), comprising of 59 brain tissue sections from the SFG, CG and thalamus regions. The FFPE sections were first baked in the oven at 60°C for 30 minutes and placed in xylene (Fischer Scientific) for 20 minutes to remove the paraffin wax, which is a process known as de-paraffinization. The sections were rehydrated by submerging in a series of alcohol concentrations from 100% alcohol to water at 2-minute intervals (100%, 75%, 50%, 25%, 0%). The sections were placed in a solution of hot 0.05% v/v citraconic anhydride (Sigma) in a household steamer for 60 minutes. The citraconic anhydride was used as the antigen retrieval buffer. When removed from the steamer, the sections were placed in water to cool for 10 minutes, and the edges of the slides were dried and marked with a hydrophobic barrier prior to phosphate-buffered saline (PBS) washes (Sigma). The peroxidase enzymes in the brain tissue were blocked using a solution of 0.6% hydrogen peroxide (Fischer Scientific) in 0.1% of PBS-Triton (PBST) for 8 minutes. This was followed by two PBS washes and a

pre-immune incubation using 10% normal goat serum for 30 minutes to block the non-specific antibody binding prior to the addition of the primary antibody. The primary antibody used was mouse anti-HuC/D (see Table 4), which was diluted in PBST, at a 1:200 dilution and pipetted over sections for an overnight incubation. The following day, the sections were PBS washed and the biotinylated secondary antibody (goat anti-mouse; Vector Labs Ltd.) was added to the sections for 60 minutes. Avidin-biotin complex (ABC)-peroxide linked (supplier Vector; catalogue # PK6100) was applied to the sections and incubated for a further 60 minutes. The sections were washed and left in PBS whilst the solution for the diaminobenzidine (DAB) detections was prepared (immPACT DAB; Vector Labs; SK-4103). The stopwatch was started when the immPACT DAB was added to the sections to time the colour development. Sections were observed using the Olympus BH2 microscope until a clear positive reaction product was observed and background staining was minimal. To ensure that the sections were not stained too intense one section was trialled independently before batch processing the rest of the cases. The average development time was applied for the remaining sections in the experiment. Stained sections were placed in water to quench the reaction and prevent overstaining. Sections were counter stained in haematoxylin (Vector). To mount the samples, they were dehydrated back through increasing alcohol concentrations (0%,25%,50%,75%,100% to 100%) at 2-minute intervals, followed by immersion in fresh 100% alcohol. These were placed back in a fresh solution of xylene for clearing and mounted using a coverslip and xylene based DPX mountant (Sigma). When dried these sections were scanned and digitalised using ZEISS Axio scanner so the resulting .czi files could be viewed, annotated and measured as a QuPath project.

2.5.2 Staining for PCSK5 Protein Expression in MS and Control Cohort

The IHC protocol was applied to a selected MS and control cohort to detect PCSK5 protein expression in the NGM and GML of MS tissue and in the GM of the control tissue. The sections were cut from SF tissue and fixed with 4% paraformaldehyde (PFA) (Sigma) for 30 minutes at room temperature. Sections were rinsed in PBS, marked with

the hydrophobic pap pen and endogenous enzyme activity in the tissue was quenched (0.6% H₂O₂). Pre-immuno blocking to reduce non-specific antibody binding was performed using 10% normal goat serum (Sigma) for 30 minutes. The PCSK5 antibody was diluted in PBST at a 1:200 dilution and was left on the tissues overnight. Following three PBS washes, the sections were incubated with a secondary biotinylated goat anti-mouse antibody (Vector) at a 1:500 dilution for 60 minutes. The ABC kit (supplier Vector AK500) was applied to the sections and incubated at room temperature for a further 60 minutes, followed by three PBS washes before the DAB substrate (Immpact DAB) was applied. Staining intensity was monitored under the microscope. The reaction was quenched using water and counterstained using haemoxylin before being dehydrated through graded ethanol and placed in xylene for mounting. The sections were mounted using a coverslip and DPX mountant. These sections were then scanned to be digitally analysed using QuPath software to count the cells expressing PCSK5 in lesion and non-lesion tissue of MS cases and in the NGM of the control cases.

2.6 In-Situ Hybridisation

ISH is a molecular technique used to detect specific nucleic acid sequences within the tissue and to allow visualisation of target transcripts of interest, providing information about the localisation and pattern of the gene expression (Wang et al., 2012). In this study, ISH was used to detect and quantify SEZ6L, PCSK5 and COMMD10 expression in MS and non-neurological disease controls. To ensure assay reliability, control slides were included: a positive control using *Homo sapiens* peptidylprolyl isomerase B (PPIB), a negative control using *Escherichia coli* dihydrodipicolinate reductase (DAPB) and a no-probe (blank) control.

The workflow of ISH firstly involved the post-fixing in 4% PFA of the SF section for 30 minutes at room temperature, followed by rinsing in tap water and dehydration through a graded series of alcohols at 5-minute intervals (50%,70%,100% to fresh 100%). Sections were air-dried for 15 minutes and incubated with hydrogen peroxide solution

(1:50 dilution in deionised water for 8 minutes). The solution was removed from the slides, and 3-4 drops of protease IV were added to the sections for 15 minutes to uncover target RNA (RNAscope Protease IV; AcDBio), followed by two washes with PBS solution. The RNAscope target probes of choice (in the instance of this project, either SEZ6L, PCSK5 and/or COMMD10) were hybridised to specifically bind target RNA molecules and the hybridisation signals were amplified prior to chromogenic detection. Tissue sections were visualised using an Olympus BH2 microscope, with each punctum representing a single target RNA molecule. Quantification was performed using QuPath. ISH was used to localise one gene of interest, either with a simple haematoxylin counterstain (Singleplex approach, 2.6.1), in combination with immunostaining (IHC, 2.6.2) or as a dual ISH to identify two genes of interest simultaneously (Duplex ISH, 2.6.3).

2.6.1 RNAscope Singleplex Assay for SEZ6L, PCSK5 and COMMD10

The RNAscope Fast Red development protocol was used to detect and quantify SEZ6L, PCSK5 and COMMD10 expression in MS and non-neurological disease control brain tissue. Singleplex RNAscope assay followed the general protocol described above (ISH, 2.6). The probe (either SEZ6L: RNAscope™ Probe- Hs-SEZ6L, Cat No. 480051; PCSK5: RNAscope™ Probe- Hs-PCSK5-C2, Cat No. 803981-C2; or COMMD10: RNAscope™ Probe- Hs-COMMD10-C1, Cat No. 1241261-C1; ACD Bio.com, Biotechnique) was added to the sections and hybridised for 2 hours at 40°C. Slides were washed with wash buffer before being stored in 5 x saline sodium citrate (SSC) buffer at room temperature overnight. The following day the sections were washed 4 times with wash buffer, and the AMP process began (see Figure 5, RNAscope® 2.5 HD Detection Reagents-RED, Catalog No. 322360 according to the manufacturer's instructions). Final chromogenic detection involved diluting fast B into fast A at a 1:60 dilution which was made up and used immediately due to its sensitivity to light. These were added to the slides incrementally and the development time was monitored under the Olympus microscope. The sections were counterstained with haematoxylin for 1 minute and were placed in two changes of

tap water. The sections were air dried for 15 minutes at room temperature and dried further at 37°C for 15 minutes before being mounted with Vectamount (Vector Labs, Inc.). Images of the cases at NGM and GML areas, at 4 images per region, were captured using the Zeiss Axio Scope 1 fitted with a Zeiss MRm 503 colour camera at 100-630x magnification.

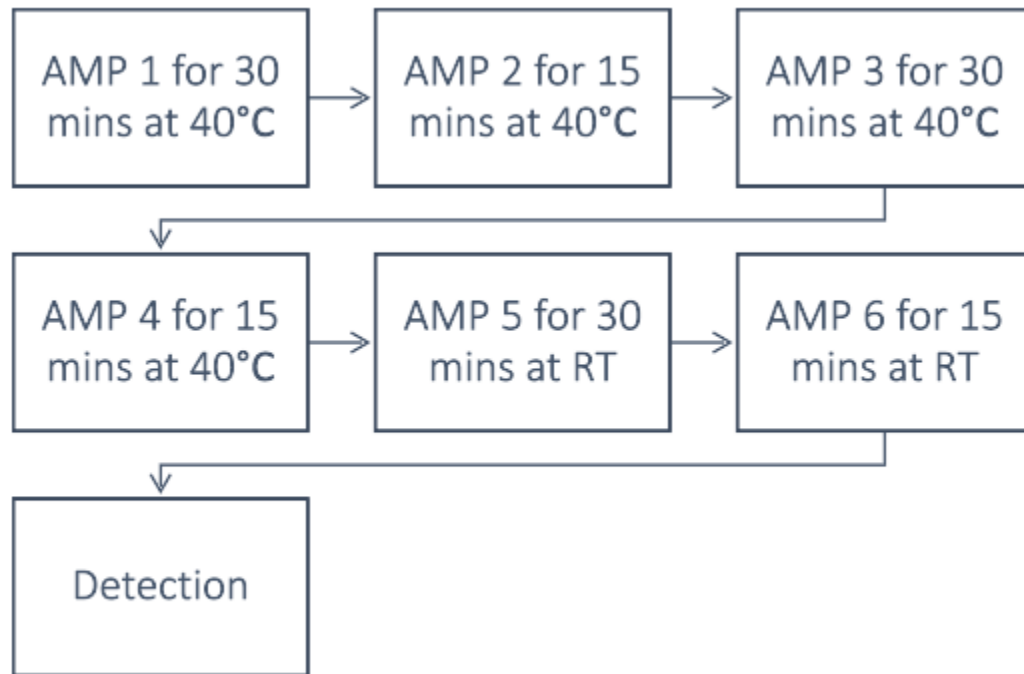


Figure 5. The AMP steps for the RNAscope protocol. The AMP 1-4 application required the use of a 40°C oven whereas AMP 5 and AMP 6 were applied to the sections at room temperature (RT). Each AMP application was followed by 3 series of wash buffer rinses to remove the previous AMP from the tissue section. The puncta for the RNAscope protocol were pink in colour.

2.6.2 ISH Combined with Immunostaining to Identify Transcript Positive Cells

A combined approach of methods 2.6 ISH followed by 2.5 IHC was used to identify the presence of PCSK5, COMMD10 and SEZ6L gene expression in neuronal-like cells. The ISH protocol was performed as standard but following the detection stage, sections were quenched with water and washed with PBS solution. Bloxall endogenous blocking

solution was subsequently applied to the sections for 10 minutes to minimise non-specific binding by blocking exposed tissue binding sites. The sections were washed again with PBS solution to remove the blocking solution, and 10% normal goat serum was added to the sections for 20 minutes. Anti-HuC/D was added for an overnight incubation. Sections were washed and then goat anti-mouse biotinylated secondary antibody was added for 60 minutes prior to incubation with an Avidin-linked alkaline phosphatase tertiary complex (cat #AK5000). Vector blue (cat #SK-5300) was prepared in a 100mM Tris-HCl solution and colour development was observed under the microscope. The reaction was quenched when the desired intensity was achieved, after which the sections were air dried and mounted with Vectamount (Vector Labs, Inc.).

2.6.3 RNAScope With Duplex Red and Green Detection for the Combined Detection of PCSK5 and COMMD10

The Duplex RNAScope 2.5 Detection Kit (#322500) allows the visualisation of two RNA species simultaneously. The protocol followed the initial stages of the Singleplex RNAScope assay (2.6.1), with the simultaneous hybridisation of two probes (PCSK5 and COMMD10), requiring additional detection steps to visualise both the red signal (PCSK5 expression) and the green signal (COMMD10 expression). Therefore, AMP treatments were applied to the sections as normal up to AMP 6, followed by the red detection stage. Steps AMP 7 to AMP 10 were applied to detect the green signal, achieved by diluting green-B into green-A at a 1:50 dilution, as shown in Figure 6. The sections were counterstained with haematoxylin for 1 minute, rinsed twice with tap water, air dried and subsequently placed at 37°C before being mounted with a coverslip using Vectamount (Vector Labs, Inc.).

Once the sections were dry, we used previous MOG staining of the MS cases to identify NGM and GML areas which we could map to our PCSK5 and COMMD10 gene expression brain section slides. Images were captured on the Zeiss Axio Scope 1 at 100-630x

magnification fitted with the Zeiss MRm 503 colour camera and 4 images were taken per NGM region for MS and control cases and 4 images per GML area for MS cases.

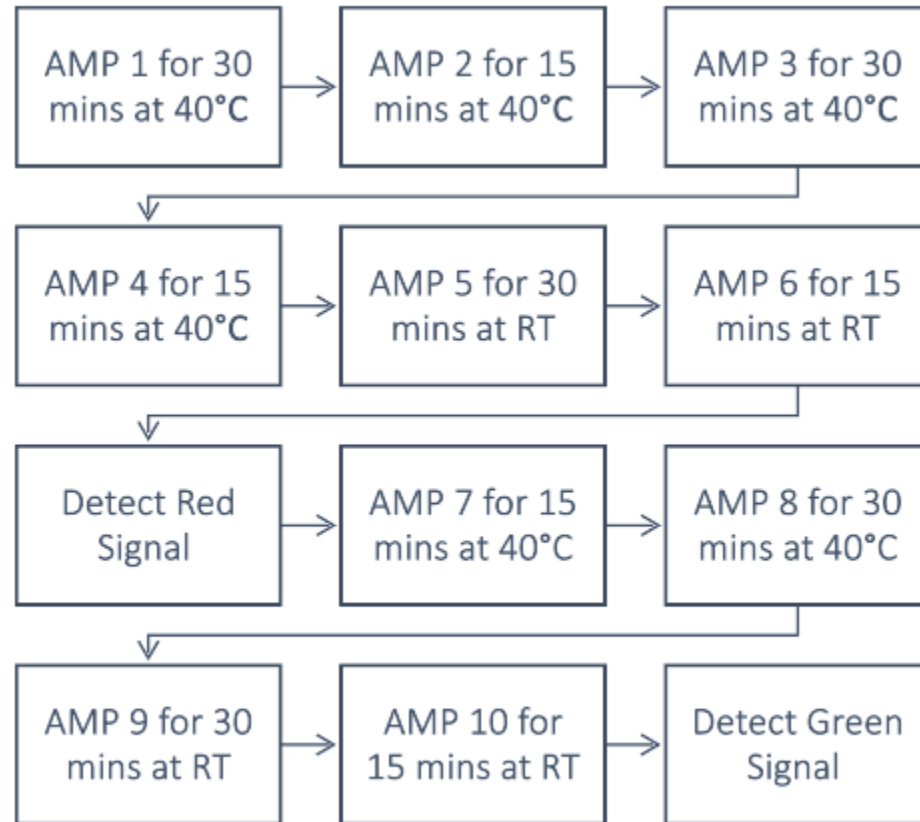


Figure 6. Simultaneous detection of PCSK5 and COMMD10 gene expression using RNAscope Duplex Assay. The protocol was employed for the simultaneous detection of the C2 probe, an alkaline phosphatase (AP)-linked probe targeting PCSK5, which revealed pink puncta when hybridised to the target RNA and the C1 probe, a horseradish peroxidase (HRP)-linked probe targeting COMMD10, which produced green puncta when bound to the target RNA. The linking of these enzyme systems is important for converting the substrate molecules into detectable signals, thus allowing the visualisation of the gene targets.

2.7 Digital Pathology: Quantification Using QuPath

QuPath is an open-source software which can be utilised to generate quantitative data to measure pathology. The software allows the visualisation and measurement of features in a much quicker and more convenient way compared to traditional manual microscopy (Bankhead et al., 2017). The software can be used for interpretation by

annotating regions of interest and image analysis to detect cells in that given area. Each project can custom a workflow script to adjust the cell detection parameters for images that may have intense staining or have artefacts present on the tissue. Additionally, scanned images and annotated image files can be easily shared between investigators or re-opened and inspected at a later point.

This technique of digital pathology was used in my project for the immunohistochemically stained control cohort to calculate the number of mature neurons, to count the number of HuC⁺ cells expressing the SEZ6L gene in MS lesion and non-lesion tissue and control, to count the number of cells expressing PCSK5 at protein level and the number of PCSK5 and COMMD10 transcript positive cells detected by the Duplex assay.

2.7.1 Quantification of HuC⁺ Neurons

The 6-layered neocortex consists of the outermost layer (layer 1) to the innermost layer (layer 6). Layer 1 typically contains few neurons and was not included in the counts. For the SFG and CG two regions of interest with a combined area between 5.5µm - 11µm were annotated between the cortical layers 2-6 where an identifiable sulcus could be found.

Rather than sampling a region of interest we annotated the entire thalamus for those blocks. It was important to keep the borders of the thalamus consistent between cases as regions outside this are highly variable between sampled blocks. I located the WM internal capsule including the thalamus reticulum and orientated the section relative to the ependymal wall of the third ventricle and neurons of the sub thalamic nuclei (such as the sub thalamic nucleus, the red nucleus, substantia nigra). Thalamic neuron density represented the medial, lateral, antero-ventral and lateral dorsal nuclei. Using the 'cell detection/positive cell detection' tool, the parameters were adjusted to ensure that all mature neurons within the annotated regions were included. From Figure 7, it is evident that the neurons in the thalamus are more spread out and larger compared to the

neurons detected in the cortical blocks. Therefore, the minimum cell area for the thalamus blocks was adjusted to a higher value compared to the cortical blocks to ensure the correct number of neurons were detected and to exclude other non-neuronal cells, which occasionally expressed HuC (perineuronal oligodendrocytes).

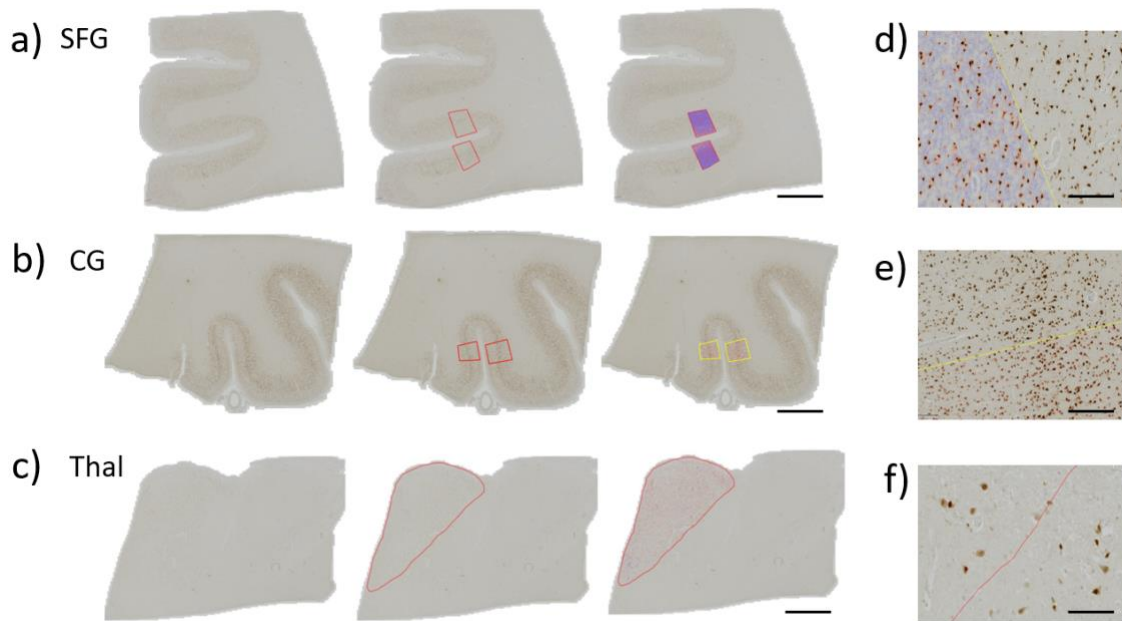


Figure 7. The annotations of regions of interest in selected brain regions to retrieve positive cell counts from control cohort. The SFG, CG and thalamic regions of the brain were annotated differently as the SFG (a), and CG (b) neuron counts were taken in two regions and the entire thalamus (c) was used for the thalamic neuron counts. The neuron sizes in the thalamus were larger than in the SFG and CG and so a lower minimum area size to capture the neurons was needed for the cortical sections. Panels d, e and f show magnified views of the SFG, CG and thalamus respectively to illustrate how neuronal cells were captured via QuPath. Scale bars: a-c = 1mm, d-e = 30µm, f = 20µm.

To minimise incorrect neuron counts an area of the image was selected to estimate red, green and blue stain vectors to ensure that the different stains and colours within the scanned image are distinguished from one another. The parameters needed to be adjusted accordingly depending on the intensity of the HuC⁺ staining and the size and staining intensity of the mature neurons. The ‘positive cell count’ command was selected, and the chosen initial parameters (see Figure 8) were used for optimisation. A

workflow script was created to run the analysis for the entire project, with the number of positive cells per mm² data measurements exported to Microsoft Excel. A quality check was performed by comparing the automated counts with a manual count (OH, BC). For certain cases these parameters did not result in a complete and accurate neuron count, thus we had to adjust. For the setup parameters, the detection image of choice was optical density sum with a requested pixel size of 0.5µm and a background radius of 0µm. The mean filter radius was adjusted between 0µm - 6µm and the sigma was between 1µm - 4µm. The maximum area captured remained consistently on 10,000 µm² for each scanned image but the minimum area was amended to be between 20µm - 30µm to ensure all mature neurons were captured on the image for quantification. The intensity parameters remained on default but the split by shape option was only selected for the thalamus sections as some of the annotations needed to be split to exclude the WM tract within the image. The 'estimate stain vectors' function attempts to account for differences in staining intensity, but it does not fully correct for these variations, so threshold values were adjusted accordingly. The intensity threshold values used for all the cases ranged between 0.05-0.35. A possible reasoning for a high positive cell count is that the split by shape command was selected which overestimates the cell count and identifies one neuron-like cell as multiple.

Positive cell detection

Setup parameters

Detection image: Optical density sum

Requested pixel size: 0.5 μm

Nucleus parameters

Background radius: 0 μm

☒ Use opening by reconstruction

Median filter radius: 0 μm

Sigma: 2.5 μm

Minimum area: 30 μm^2

Maximum area: 10000 μm^2

Intensity parameters

Threshold: 0

Max background intensity: 0

☐ Split by shape

☐ Exclude DAB (membrane staining)

Cell parameters

Cell expansion: 5 μm

☒ Include cell nucleus

General parameters

☒ Smooth boundaries

☒ Make measurements

Intensity threshold parameters

Score compartment: Nucleus: DAB OD mean

Threshold 1+: 0.1

Threshold 2+: 0.4

Threshold 3+: 0.6

☒ Single threshold

Run

Figure 8. Default parameters for positive cell detection on QuPath. The background radius, sigma, minimum and maximum area and threshold were adjusted in a case dependent manner to ensure the mature neurons were captured for each brain region. The neuron sizes in the thalamus brain region were much larger than in the SFG and CG and so a higher minimum area was used for the nucleus parameters. We wanted to exclude the oligodendrocytes in our positive cell count and so we adjusted the size parameters to ensure they did not contribute to the count, as these cells were small and easy to identify.

2.7.2 Quantifying the Density of HuC⁺ Neurons Expressing SEZ6L

The 'positive pixel count' command in QuPath was used to calculate the percentage of positive staining across the total region of interest (ROI) and to manually count the HuC⁺ neurons, generating SEZ6L expression percentages in both NGM and GML areas, which were identified using previously stained MOG sections. The 'estimate stain vectors' command was firstly applied to each image, after which the Stain 2 channel was adjusted to match the colour of the pink SEZ6L expression puncta, allowing QuPath to identify it as the positive stain. The 'detect positive staining' command was utilised using the parameters shown in Figure 9a below. This generated a positive percentage of ROI area for each image. The number of HuC⁺ cells on the same images were counted using the manual cell counter. The percentage SEZ6L expression was calculated using the following equation:

$$SEZ6L \text{ Expression } \% = \frac{\text{Average Positive Pixel Count for the Case}}{\text{Average Neuron Count for the Case}} \times 100$$

The average SEZ6L expression across the four images for each region of interest was reported at control GM, NGM and GML sites where appropriate.

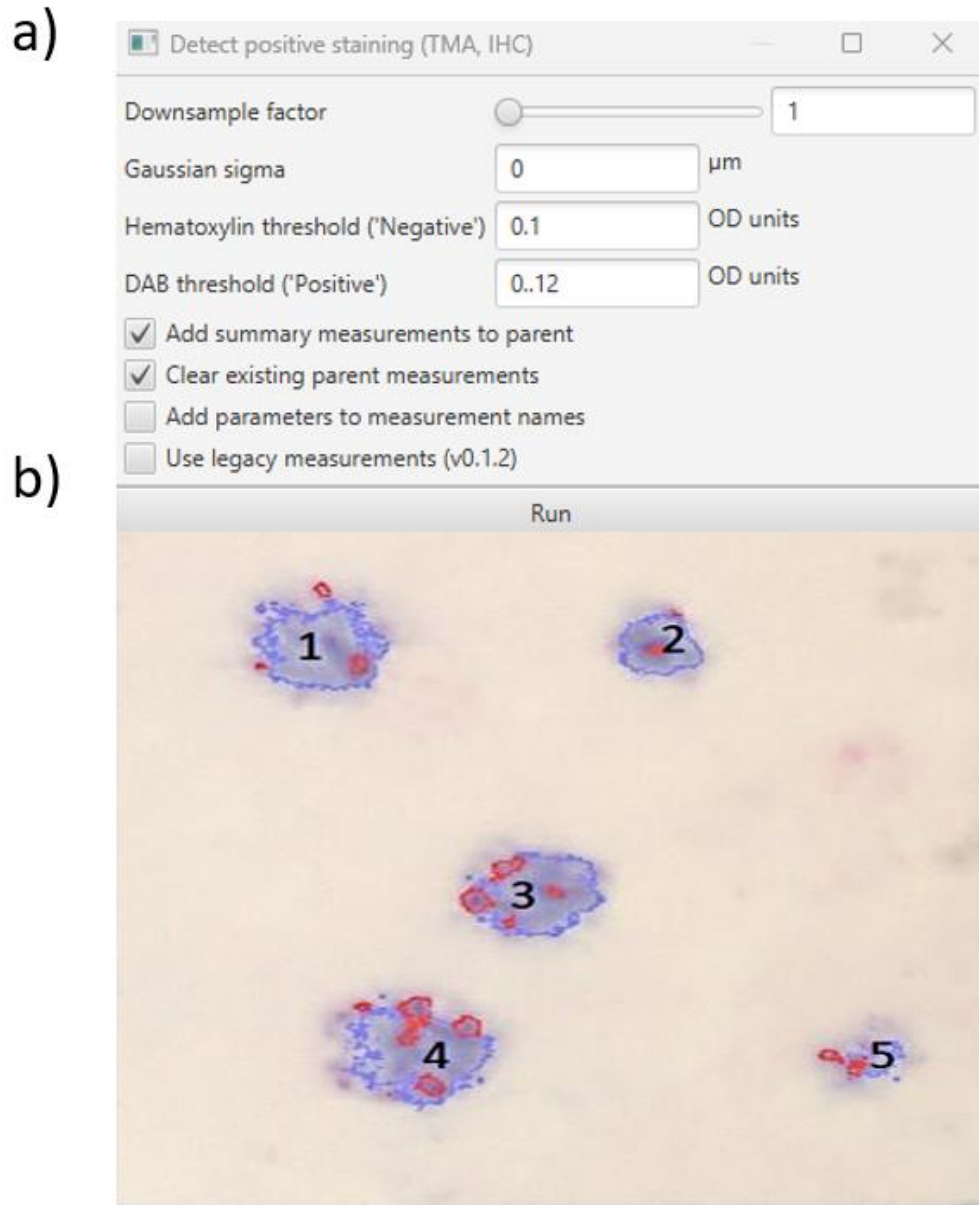


Figure 9. Comparison of QuPath approaches for SEZ6L expression analysis. a) The parameters employed for detecting the positive SEZ6L staining across the image are as shown. The applied settings ensure accurate identification of regions expressing SEZ6L staining within both NGM and GML regions. b) A visual representation of SEZ6L positive staining detected using the above parameters (shown in red). Additionally, manual counting is demonstrated by the labelled numbers indicating HuC⁺ cells which are a marker of mature neurons. The combined approach contributes to the calculation of a percentage of SEZ6L expression which can be averaged for each case in NGM and GML (where present) areas.

2.7.3 Quantifying PCSK5⁺ Cells

QuPath analysis was used to quantify PCSK5⁺ haematoxylin-stained cells in NGM and GML regions of MS cases and GM regions of control cases. To identify the areas of interest (NGM and GML), we used previously stained MOG slides for those cases in our cohort which were used to highlight lesion areas. These regions were annotated using QuPath. There were 4 annotated regions per area of interest with a combined area between 2×10^5 – $7 \times 10^5 \mu\text{m}^2$, as some of the subpial GML in the MS tissue were small, so smaller areas were used for positive cell counting. Some MS cases in our cohort did not have GML, therefore only NGM regions were annotated for these cases. The annotations were consistently placed in the cortical tissue to ensure that the positive cell counting is in the same layer for each case. An example of how the annotations were captured are shown in Figure 10.

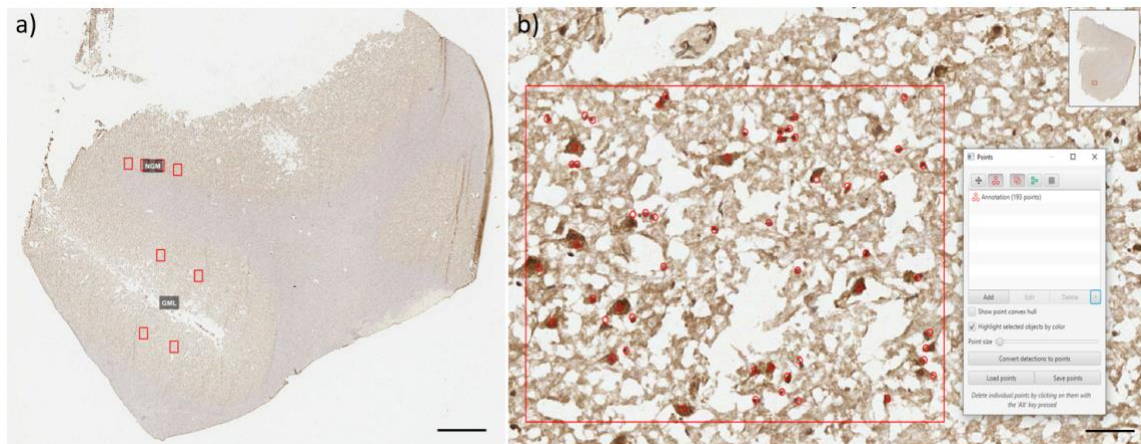


Figure 10. Quantification of PCSK5 IHC positively stained cells in MS and control cases. Previously stained MOG⁺ cases were matched with the PCSK5 IHC stained cases and used to identify distinct regions of GML of MS cases and NGM for both the MS and the control cases, which was utilised to annotate four annotations for each of these regions (a). A manual counting approach used in these selected areas to quantify relevant cells expressing PCSK5 at protein level with each dot representing the count of one cell (b). This methodology was used to calculate the number of positive cells per mm² for each region of interest per case which was statistically analysed. Scale bars: a = 2mm, b = 20 μm .

2.7.4 Quantifying the PCSK5 and COMMD10 Gene Expression in Control and MS Brain

Manual cell counting was first conducted to determine the number of PCSK5⁺ and COMMD10 puncta positive cells. The QuPath 'automated quantification' was used to report the area of positive stain. This was done by using the classifier tool (which first required the estimation of stain vectors) and setting the Stain 1 to the colour of expression of the gene of interest (pink for PCSK5 and green for COMMD10). Therefore, two different projects needed to be created to calculate values for both genes. The Stain 3 parameters were also adjusted and matched to the background of the tissue. Live classification was performed by creating a threshold for pixel classification, adjusting the resolution to very high to disable down-sampling, changing the channel to DAB and removing the prefilter. The above and below thresholds were adjusted in live time to ensure all positive staining was detected. This generated an area of positive stain per image which was divided by the image size to give the positive percentage of total ROI. As we already performed manual counts for each image, we were able to divide the positive percentage of total ROI by the number of cells detected in that image to calculate the positive percentage per positive cell. This was averaged across the 4 images per region to give an average positive percentage immunoreactivity per positive cell for the NGM and for the GML. This was repeated in the second project to obtain results for the PCSK5 and COMMD10 at NGM and GML areas for MS cases and NGM in control cases.

2.8 Statistical Analysis

Statistical analysis was performed using GraphPad Prism (Version 10). Non-parametric testing was utilised to remove assumptions of normal distribution. Statistical tests used in the project included the non-parametric t-test and Mann Whitney t-tests for 2 group analysis (for example, to compare the neuron density between the MS and control cohort in SFG, CG and thalamus and to identify differences in expression of SEZ6L or PCSK5 between MS and control cases irrespective of lesion tissue). Kruskal-Wallis with Dunn's multiple adjusted post-test was used to compare 3 or more groups, for instance, to further investigate differences in expression of SEZ6L and PCSK5 in GM control and NGM and GML of MS tissue and to analyse neuron density, demyelination and clinical differences between MS cases that carried gene variants of interest (rs10869757 and rs11144848 mapping to PCSK5, rs185263 and rs1567335 mapping to COMMD10, rs72894266 mapping to SEZ6L and rs7565433 mapping to DYSF:CYP26B1). This was also important in determining the polygenic effect of carrying more than one gene variant of interest (for example, carrying both the PCSK5 and COMMD10 gene variants to identify if this had a neuroprotective effect or a less severe MS outcome). Wilcoxon-signed ranked tests were used on paired data (for instance, MS cases with known SEZ6L gene expression or known PCSK5 positive cell density in both NGM and GML areas) to investigate differences in expression in normal tissue versus damaged tissue. The level of statistical significance for all tests was set at $p < 0.05$ (*), $p < 0.01$ (**), $p < 0.001$ (***) and $p < 0.0001$ (****).

3.0 Results

The genetic influences of MS severity are poorly understood. For this project, we focused primarily on two genes of interest, PCSK5 and COMMD10, which were identified during collaborative GWAS studies. We investigated their putative function and pattern of expression in control and MS tissue, alongside SEZ6L and DYSF, which are mapped genes described in the recent literature (Harroud et al., 2023; Jokubaitis et al., 2023; Kreft et al., 2024). In conducting this analysis, we wanted to establish a workflow to investigate novel variants and mapped genes that are associated with the pathological severity of MS to uncover important information about the genetic drivers of disease worsening.

3.1 MS is a Neurodegenerative Disease

Recent digital pathology analysis by the Howell group (Mr Ben Cooze) reported neuron density in six systematically sampled brain areas from 310 PMS cases. No control data was analysed. I therefore acquired neuron density data (HuC⁺ cells/mm²) from 28 non-neurological disease control cases in the available SFG, CG and thalamic brain regions, using the same protocols (see Figure 11). A lower neuron density in the cortical and thalamic brain regions in the MS cases in comparison to the non-neurological disease controls was apparent (see Figure 12).

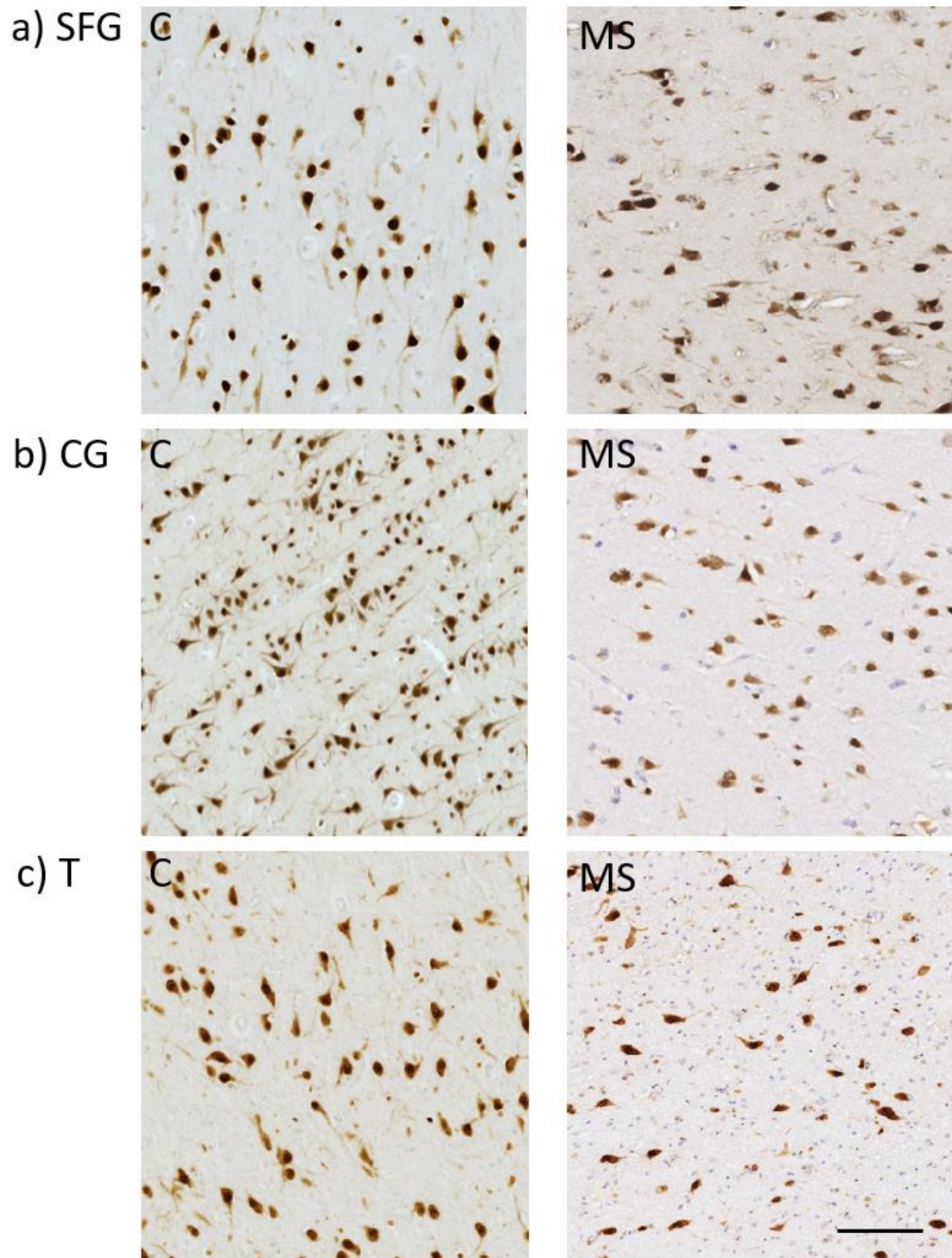


Figure 11. Immunohistochemically stained human brain tissue sections at SFG, CG and thalamic regions of MS and control. Immunostaining identified HuC⁺ mature neurons in the cortical (SFG, CG) and thalamus (T). These images reveal qualitative differences in neuron density in the different brain regions, with more noticeable differences in neuronal density in the thalamus. Scale bar: a-c = 100μm.

On comparing mean neuron density counts from these brain regions, we were able to show a 26%, 28% and a 45% average decrease in neuron density in the SFG, CG and thalamus of MS, respectively ($p < 0.05$; t-test; Figure 12a-c). A full table of control neuron density data can be found in Table 11 in supplementary. We next conducted simple Spearman analysis (see Figure 12d). This analysis showed that sex (r value = -0.289 to -0.092) and age died (r value = -0.289 to 0.312) did not correlate with neuron densities in the control cohort. Figure 12e shows that the neuron density in the MS thalamus and pons was related ($r = 0.72$; $p = 2.950e-036$; Spearman analysis; the Pons being a brain region unfortunately not available from controls). Lower thalamic and pons neuron density was also associated with poorer clinical outcomes: younger age died and shorter times from onset to death, onset to progression, onset to WC use and progression to death ($r = 0.39$ to 0.78 ; $p = 4.386e-050$ - $1.671e-007$; Spearman analysis). This observed correlation between neuron density in the thalamus and pons indicates that decreased neuron count in these regions is associated with earlier mortality and accelerated disease progression, including earlier onset of wheelchair dependence and ultimately a shortened lifespan.

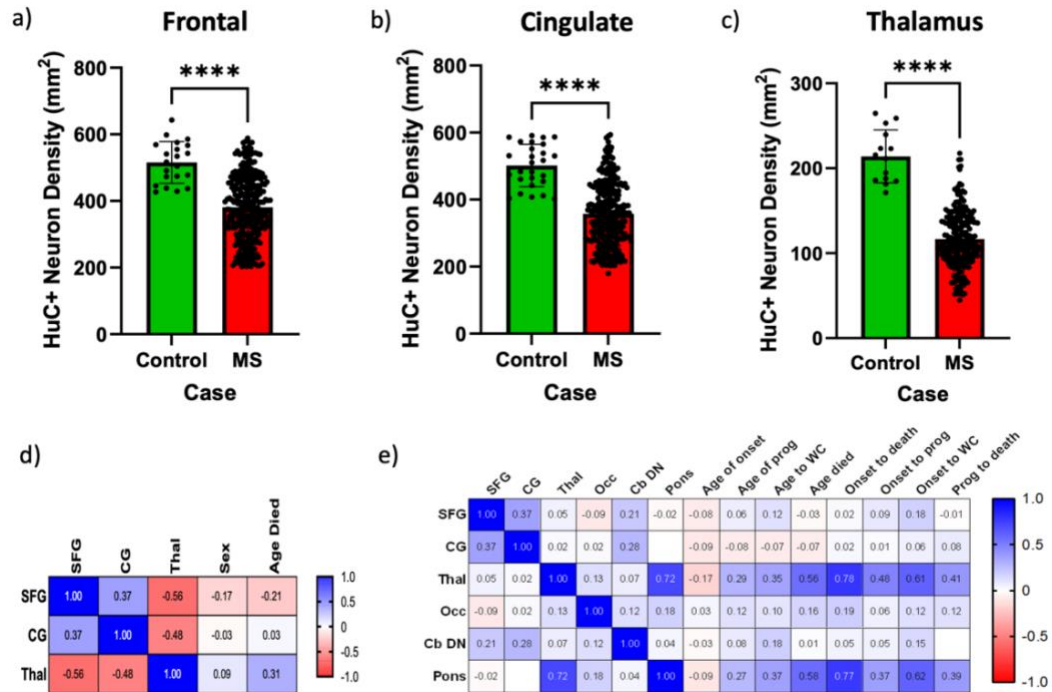


Figure 12. Neuron density in the SFG, CG and thalamus is significantly reduced in MS in comparison to controls and associated with a worse clinical outcome. a-c) Neuron density (HuC⁺/ mm²) was determined from n = 28 non-neurological disease controls and compared to MS region matched blocks. We showed a significant difference in neuron density between control and MS for all the sampled brain regions ($p < 0.05$; t-test). Each data point represents mean neuron density per analysed block per case. Bars represent group means and error bars represent standard deviations. d) Spearman correlation analysis revealed no significant correlation between the SFG, CG and thalamic neuron densities, and sex and age died of the control cohort ($p > 0.05$). e) Spearman correlation analysis revealed a significant correlation between the thalamic and pons neuron densities, and key clinical outcomes (onset to death, age died, onset to progression, onset to WC and progression to death) in MS.

3.2 DYSF is Highly Expressed at Protein Level in the Brain

We investigated the expression and localisation of DYSF, SEZ6L, PCSK5 and COMMD10 genes across multiple tissues and brain regions using various online platforms, including the Protein Atlas database, to confirm their presence. We examined relative expression levels, particularly for PCSK5 and COMMD10 and delved into their expression across cell types. Utilising both Protein Atlas and cellxgene data, we explored protein-protein interactions of these genes, assessing their neuronal associations and differences in expression between MS and control tissue, as well as between male and female cases across various cell types.

Protein Atlas data showed that DYSF has low RNA level expression in the brain but very high expression at protein level in both the brain and the respiratory system (see Figure 13a). Data from the human brain dataset revealed that the highest expression was in the WM (109.6 normalised transcripts per million; nTPM), whereas it was lowest in the choroid plexus (nTPM = 11.2). The cerebral cortex, pons and cerebellum had an expression of 55.9 nTPM, 52.5 nTPM and 26.4 nTPM respectively (see Figure 13b). The highest expression of DYSF in single cell types was detected in lymphatic endothelial cells (nTPM = 85.1) and a 60.52% lower expression was observed in excitatory neurons (nTPM = 33.6), (see Figure 13c). The protein-protein interaction map for DYSF revealed intracellular physical interactions (with medium confidence) with SNAP Associated Protein (SNAPIN) (see Figure 13d). This protein is a part of the soluble N-ethylmaleimide-sensitive factor attachment protein receptor (SNARE) complex and is essential for modulating synaptic vesicle trafficking and exocytosis. It is enriched in neurons and is also responsible for maintaining brain homeostasis, meaning that it is a valuable therapeutic target for research of brain disorders (Margiotta, 2021). The optineurin (OPTN) gene, which is also predicted to have an intracellular localisation, is physically associated (with medium confidence) with DYSF. OPTN has been implicated in immune regulation and in the maintenance of the Golgi complex, particularly in processes such as membrane trafficking and exocytosis. Mutations in this gene have been associated with motor neuron disease (Evans & Holzbaur, 2019). Immunostaining of HPA017071:Rh30 human cells demonstrated localisation of DYSF protein within the centriolar satellite and microtubules (Figure 13e).

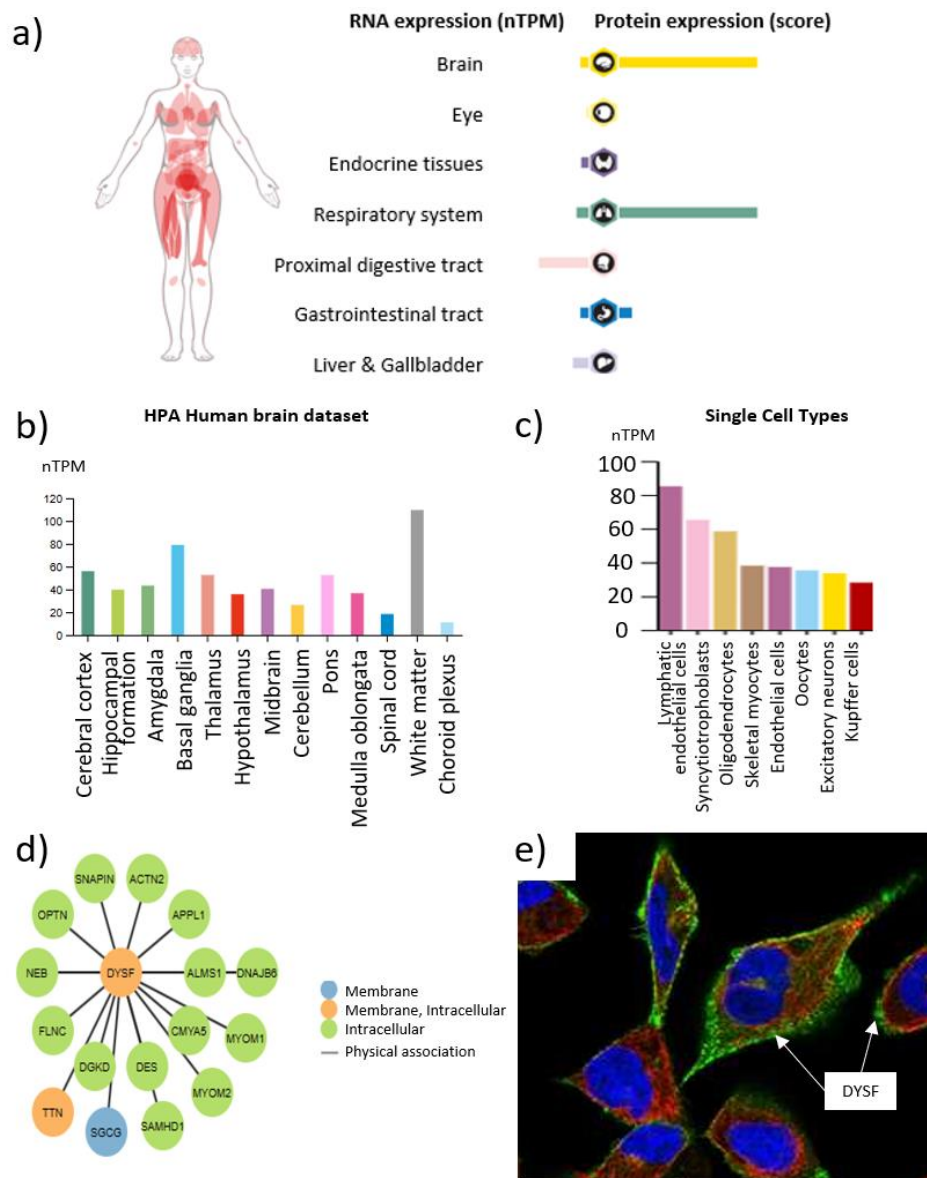


Figure 13. The DYSF protein expression is extremely high in the brain, but gene expression is considerably lower. a) Summary data from the Human Protein Atlas indicate that the DYSF gene shows low RNA expression but high protein-level expression, particularly in the brain and respiratory system. b) Further analysis of the human brain dataset reveals differential expression levels of DYSF across brain regions, with the highest expression in the WM and the lowest detected in the choroid plexus. c) DYSF expression is heterogenous across different cell types that are not exclusive to the brain. The highest expression is observed in lymphatic endothelial cells, with comparatively lower yet elevated expression levels observed in the syncytiotrophoblasts and oligodendrocytes. d) The protein-protein interaction map for DYSF indicates physical interactions with intracellular proteins such as SNAPIN, which is important for synaptic vesicle trafficking and exocytosis, and OPTN which is associated with immune regulation and regular maintenance of the Golgi apparatus. e) The subcellular localisation of DYSF is shown in HPA07071:Rh30 human cells (green) which shows that the gene is present in and around microtubules (red). Gene data available at v25.proteinatlas.org/ENSG00000135636-DYSF

3.2.1 SEZ6L is Enriched to the Brain

Protein Atlas revealed that there is a high expression of SEZ6L RNA expression in the brain. Expression is present, but low, in the eye and endocrine tissues. Despite abundant SEZ6L RNA, no SEZ6L protein expression is reported for the sampled organs, including brain (see Figure 14a). A regional analysis within the human brain revealed heterogeneous expression patterns of the SEZ6L gene, with the hippocampal formation exhibiting the highest levels of expression (nTPM = 182.7) and the lowest levels detected in the choroid plexus (nTPM = 4.6). The cerebral cortex, pons and cerebellum exhibited SEZ6L expression levels of 161.1 nTPM, 107.1 nTPM and 72.1 nTPM respectively (see Figure 14b).

Insights into the SEZ6L expression profile reveal differential abundance across distinct cell types. Data showed that oligodendrocyte precursor cells (OPCs) exhibited notably higher SEZ6L expression (nTPM = 550) and an approximately 61% decrease was observed in excitatory neurons (nTPM = 214.4). Expression levels were detected in other neuronal cells (inhibitory neurons and horizontal cells), but the levels were comparatively lower at 131.6 nTPM and 23.3 nTPM respectively (see Figure 14c).

Protein-protein interaction networks were not available for the SEZ6L gene on Protein Atlas. Human cell analysis further showed the subcellular localisation of SEZ6L, revealing its association with the perinuclear region and microtubules within the cell, as shown in Figure 14d. These findings highlight the dynamic differences in SEZ6L expression within the human, suggesting potential functional implication within neuronal and glial cell populations.

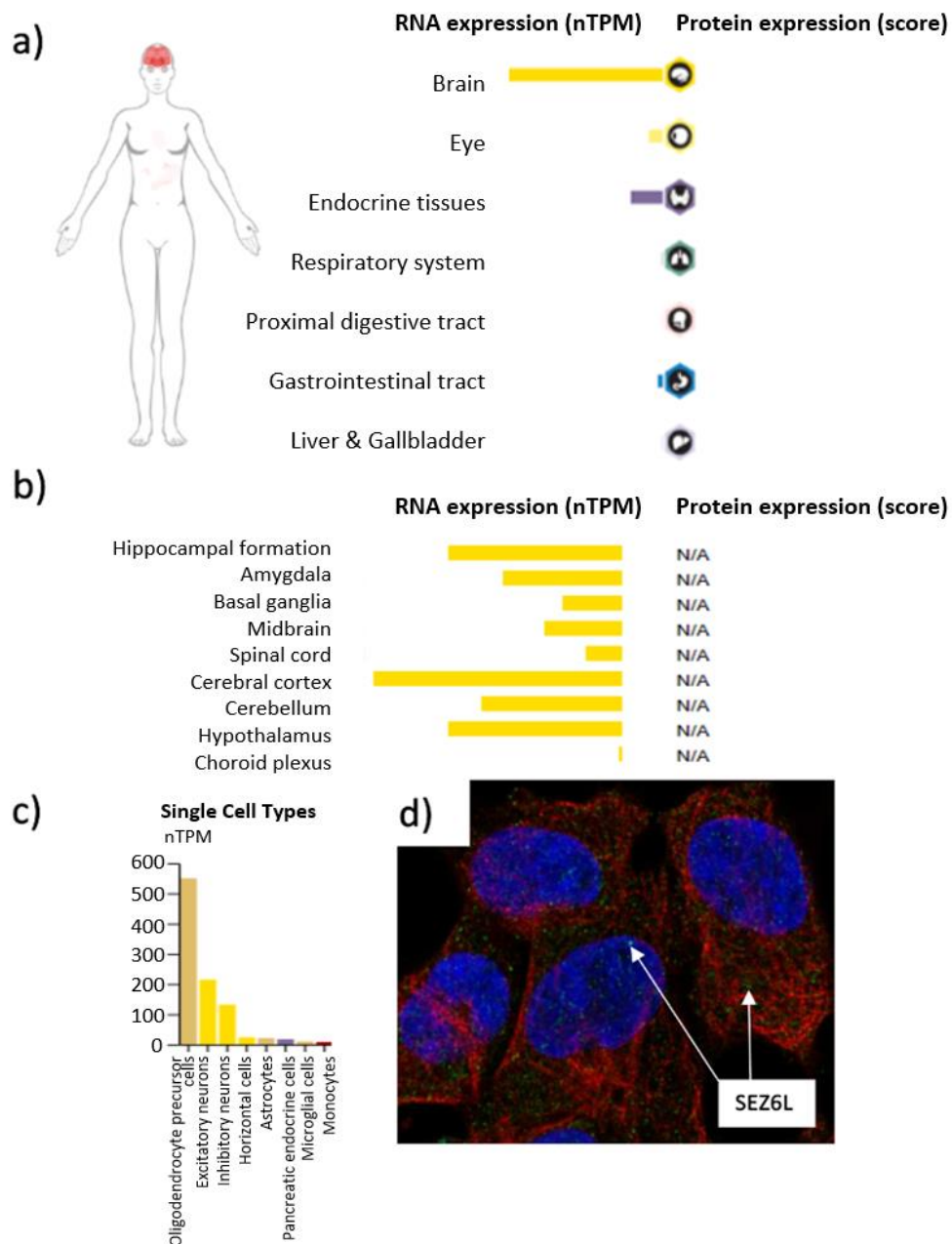


Figure 14. Differential expression and cellular location of the SEZ6L gene. a) The Human Protein Atlas revealed that there is an overall higher RNA expression of the SEZ6L gene in the brain, but no protein expression detected across any of the sampled organs. b) A heterogeneous expression of SEZ6L in the brain was detected, with the hippocampal formation having the highest RNA expression and the choroid plexus having the lowest. c) The differential expression of SEZ6L is observed across various neuronal and glial cell types, with oligodendrocyte precursor cells exhibiting the highest expression levels. SEZ6L is present in neuronal cells, including excitatory neurons and horizontal cells, albeit at lower levels of 214.4 nTPM and 131.6 nTPM respectively. d) The SEZ6L gene (green) is expressed in and around the nucleus of the cell (blue) and microtubules (red) as shown in HPA045135: SH-SY5Y human cells. Gene data available from v25.proteinatlas.org/ENSG00000100095-SEZ6L

3.2.2 The PCSK5 Gene Has Varying Levels of Expression in Different Organs

PCSK5 is highly expressed at both RNA and protein levels in the gastrointestinal tract, whereas in the brain RNA levels are low but protein levels remain high (see Figure 15a). The human brain dataset on Protein Atlas shows that PCSK5 expression is highest in the cerebral cortex (nTPM = 9) and lowest in the choroid plexus (nTPM = 3.8). The pons and cerebellum expression levels were 6.7 nTPM and 5.3 nTPM respectively (see Figure 15b). The PCSK5 gene was highly expressed in glial cells; astrocytes (nTPM = 179.8), OPCs (nTPM = 140.1) and was also expressed in inhibitory neurons and microglial cells (78 nTPM and 67.1 nTPM respectively) (see Figure 15c). The protein-protein interaction map for PCSK5 on Human Protein Atlas shows that the interactions between the genes are predicted to be intracellular (see Figure 15d). The Notch 2 N-Terminal Like A (NOTCH2NLA) gene is predicted to be secreted intracellularly and has a physical association with medium confidence with PCSK5. The NOTCH2NLA gene is unique to humans and enhances the proliferation of neural progenitor cells and can influence the quantity of neurons present in the neocortex through Notch signalling pathway modulation (Fiddes et al., 2018). Mesenchyme homeobox 2 (MEOX2) is a transcription factor that, when expressed at high levels, can cause glioma apoptosis. MEOX2 is associated with cell proliferation and survival via the Extracellular Signal-regulated Kinase/Protein Kinase B (ERK/AKT) pathway (Tachon et al., 2021). PCSK5 has been detected in the Golgi apparatus and is predicted to be secreted. PCSK5 has been shown to be expressed in HPA031072:Rh30 human cells in and around the nucleus and microtubules (see Figure 15e).

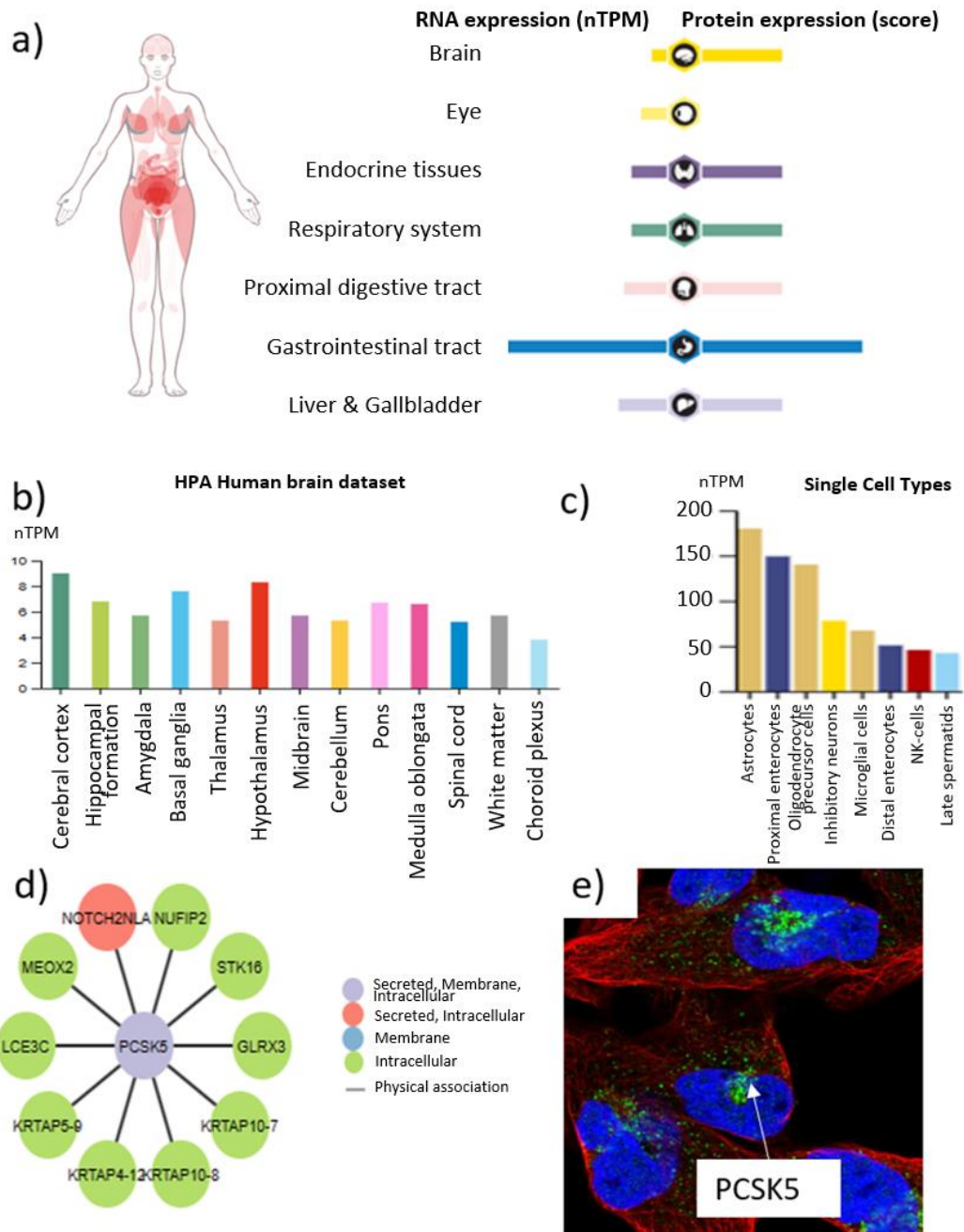


Figure 15. PCSK5 expression at RNA and protein level in various organs and cells. a) PCSK5 shows high RNA and protein expression in the gastrointestinal tract. In the brain, RNA levels are low while protein expression remains high. b) PCSK5 shows varying levels of expression across different brain regions, with highest expression observed in the cerebral cortex and lowest found in the choroid plexus. c) There is a focus on High PCSK5 expression is observed in glial cells, particularly astrocytes, OPCs and microglia, with detectable expression also present in inhibitory neurons. d) The protein-protein interaction map indicates that PCSK5 interacts intracellularly with other proteins, including NOTCH2NLA, which influences neural progenitor cell proliferation via the Notch signalling pathway. e) Immunostaining of HPA031072 human cells revealed PCSK5 localisation (green) in the Golgi apparatus and around the nucleus (blue) and microtubules (red). Gene data available from v23.proteinatlas.org/ENSG00000099139-PCSK5

3.2.3 COMMD10 Expression is Not Exclusive to the Brain

The COMMD10 gene and protein are expressed in the brain at low levels. Expression is also found in the proximal digestive tract and liver and gallbladder at much higher levels (see Figure 16a). The expression levels of COMMD10 vary slightly across different brain regions, with the lowest expression was detected in the hippocampal formation (nTPM = 11.2) and the highest in the WM (nTPM = 17). The expression levels in the cerebral cortex, pons and cerebellum were 12.3 nTPM, 14.8 nTPM and 13.6 nTPM respectively (see Figure 16b).

Single cell expression datasets revealed COMMD10 to be highest in oligodendrocytes, microglial and OPCs (nTPM = 220.3, 176.2 and 134 respectively) (See Figure 16c). COMMD10 was also expressed in inhibitory neurons and excitatory neurons at lower levels (nTPM = 86.7 and 81.9 respectively).

COMMD10 protein has 7 protein-protein interactions with other genes that are predicted to be intracellular (see Figure 16d). Interestingly, both COMMD5 and COMMD1, like COMMD10, physically interact intracellularly with COMMD10 and participate in the regulation of the NF- κ B signalling pathway and copper homeostasis through COMMD protein-protein interactions (de Bie et al., 2006). It is also evident that COMMD proteins are associated with cerebral ischemia and tumour proliferation (You et al., 2023). The COMMD10 protein also interacts with FBJ osteosarcoma oncogene (FOS). A specific gene in the FOS family, known as c-FOS, has been shown to be important for neurogenesis during cortical development in mice and its downregulation has been associated with enhanced tumour growth (Velazquez et al., 2015). These protein-protein interactions could suggest roles in modulating the inflammatory response in MS and potentially contribute to the neuroinflammatory nature of the disease. COMMD10 has been detected in the nucleoplasm and HPA054156: MCF-7 human cell staining revealed very localised expression in the nucleus with little to no expression within the microtubules (see Figure 16e).

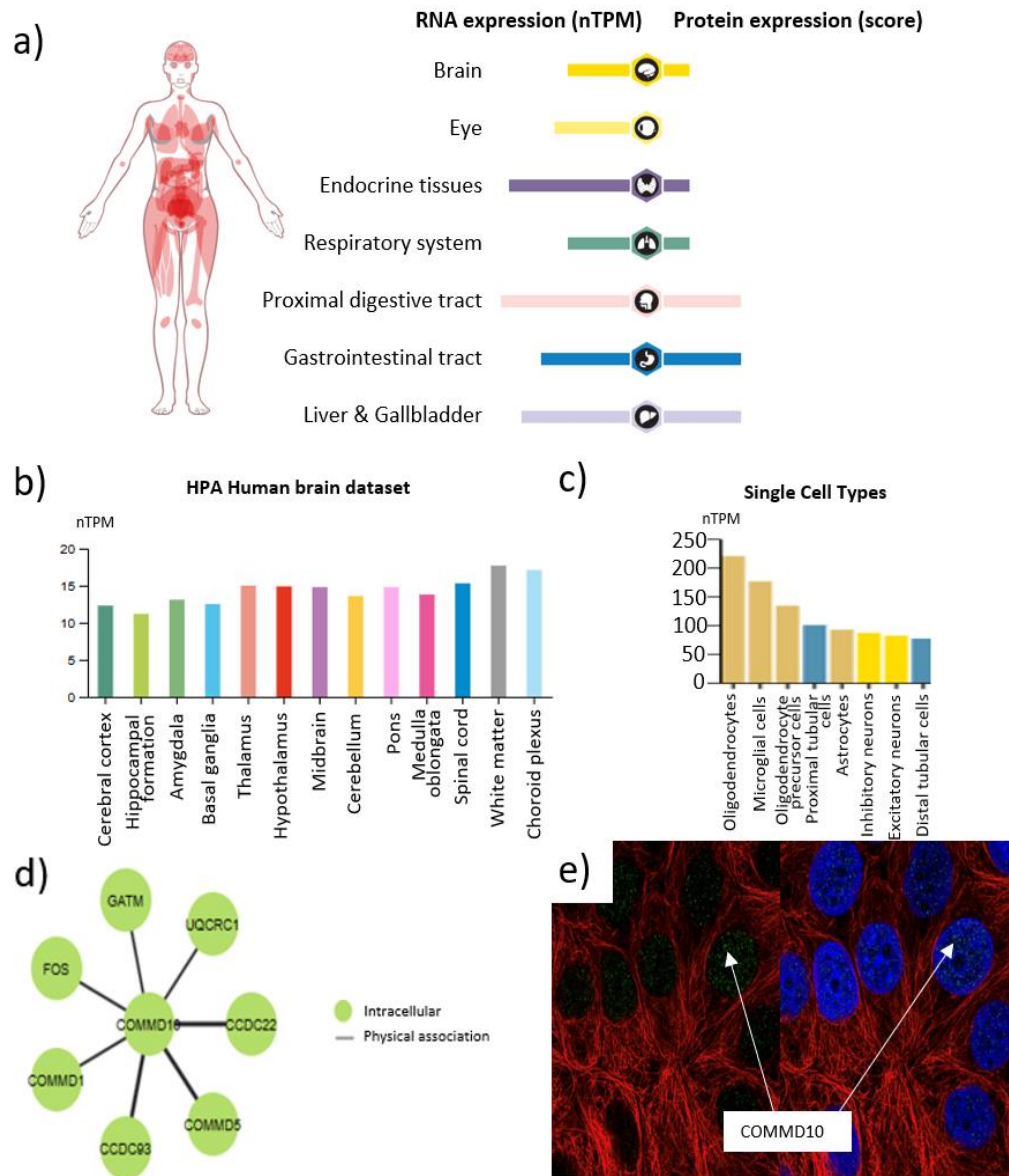


Figure 16. The COMMD10 gene is expressed in various organs and cell types. a) The COMMD10 gene has a high RNA expression in the proximal digestive tract, endocrine tissues and the liver & gallbladder. Both COMMD10 RNA and protein level expression is present in the brain but at moderately low levels. b) The expression levels of COMMD10 vary across the different brain regions, with the lowest detection observed in the hippocampal formation and the highest expression detected in the WM. c) There is high expression in neural cells such as oligodendrocytes, microglial cells and OPCs. There are also moderate levels of expression in astrocytes, inhibitory neurons and excitatory neurons. d) The interactions of COMMD10 with other proteins include COMMD5, COMMD1 and FOS proteins, which may contribute to the neuroinflammatory phenotype observed in MS patients. e) The COMMD10 gene (green) has been shown to be detected in the nucleoplasm and localised within the nucleus (blue) of the HPA054156: MCF-7 human cells. Gene data available from v23.proteinatlas.org/ENSG00000145781-COMMD10

3.2.4 An Insight into Gender Differences, Cellular Expression Profiles and Gene Expression Levels in MS and Control Cohort using Cellxgene Analysis

Using cellxgene publicly available data and in-built visualization tools, we first examined transcript expression of our genes of interest in MS and controls ($n = 12$ and $n = 9$ respectively). Expression of DYSF and COMMD10 did not differ majorly between the MS and control cohort (Figure 17a), whereas SEZ6L gene expression was highest in the control cohort (>0.75), with a greater percentage of cells expressing this gene (fraction of cells = 40% in control cohort and 30% in MS cohort). PCSK5 showed slightly higher mean expression in the MS cohort and results showed a larger fraction of cells expressing the gene compared to the control cohort. There were no major differences in the percentage of cells expressing the DYSF, PCSK5 or COMMD10 between male and females (Figure 17b). A notable difference in mean SEZ6L expression was observed between males ($n = 8$, 3 MS and 5 controls) and females ($n = 11$, 7 MS and 4 controls), with the male cohort showing a higher fraction of cells (approximately 40%) expressing the gene and a higher mean expression (>0.75). Cellxgene also allows for the visualization of gene expression in distinct cell types (Figure 17c). T cells exhibited a higher fraction of cells expressing COMMD10, with very low mean expression and percentage cells for DYSF, SEZ6L and PCSK5. Interestingly, a high percentage of OPCs displayed SEZ6L expression, while not many expressed DYSF and minimal expression of PCSK5 and COMMD10 was observed. Results showed that around 10-20% of oligodendrocytes (OLs) expressed DYSF and COMMD10, with a mean expression of 0.25-0.50, while SEZ6L and PCSK5 were expressed at lower levels. Among microglia, COMMD10 showed the highest percentage of expressing cells with a mean expression between 0.50-0.75. A small percentage of microglia expressed PCSK5, while DYSF and SEZ6L showed little expression.

In excitatory neurons (EN-L5-6, EN-L5-4 and EN-L2-3), the gene expression distribution varied. In EN-L5-6, DYSF was expressed in 10-20% of cells with a mean expression of 0.25-0.50. SEZ6L showed the highest expression among the four genes in this cell type, with approximately 40% of cells expressing the gene at a mean >0.75 . PCSK5 was

expressed in around 20-30% of cells with a mean expression of 0.50-0.75. In EN-L2-3, DYSF showed similar expression levels and mean as observed in EN-L5-4. SEZ6L was expressed in a low fraction of cells (approximately 20-30% of cells) with a mean expression of 0.50-0.75. PCSK5 was expressed in fewer than 10% of cells with a mean expression below 0.25. In EN-L2-3, DYSF showed similar expression levels as in EN-L5-4. SEZ6L exhibited high expression, with 40-50% of cells expressing the gene at a mean >0.75. PCSK5 was expressed in a minimal fraction of cells (<10%) with a mean expression below 0.25. COMMD10 expression remained relatively stable across EN-L5-6, EN-L5-4 and EN-L2-3, with approximately 20% of cells expressing the gene at a mean expression level of 0.25-0.50. Approximately 10-20% of B cells express COMMD10 at low levels (0.25-0.50), with little to no expression of DYSF, SEZ6L or PCSK5. In astrocytes, approximately 20% of cells express PCSK5 with a high mean expression 0.50-0.75, whereas approximately 10% of cells express COMMD10 at a mean expression of 0.25-0.50, DYSF and SEZ6L showed minimal expression. These findings from a publicly available dataset highlight that gene expression localisation patterns in MS versus control, gender and different cell types, revealing notable differences in expression levels and cell type-specific distributions.

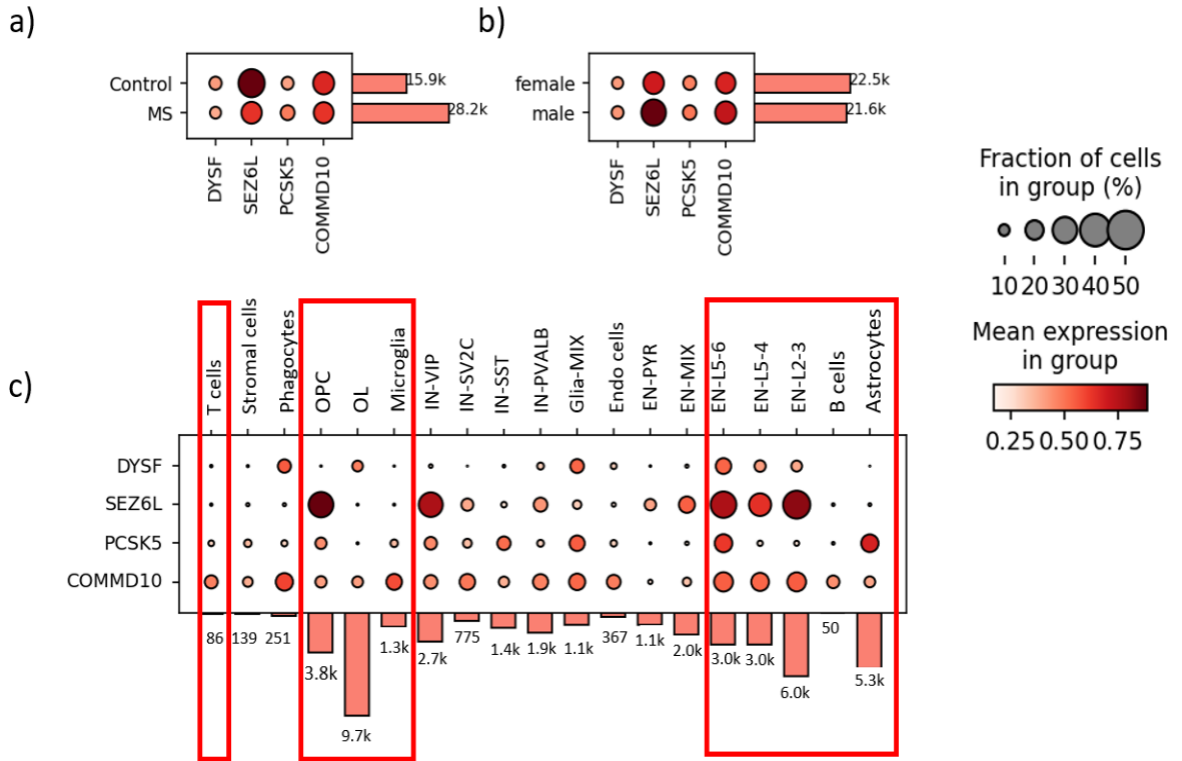


Figure 17. Gene expression patterns of DYSF, SEZ6L, PCSK5 and COMMD10 across MS and control cohorts, gender and cell types. a) SEZ6L is expressed in a higher fraction of cells and at higher levels in the control cohort compared to the MS cohort. b) Gender-specific analysis reveals no major differences in the percentage of cells expressing DYSF, PCSK5 or COMMD10 between males and females, whereas SEZ6L is expressed in a greater fraction of cells in the male cohort, with higher mean expression levels. c) Cell type-specific analysis reveals that COMMD10 has the highest gene expression, out of the genes under investigation, in T cells. OPCs, which give rise to OLs which are important for myelin production, display high SEZ6L expression levels, minimal DYSF expression and low PCSK5 and COMMD10 expression. OLs show the highest fraction of cells expressing DYSF and COMMD10, whereas SEZ6L and PCSK5 are minimally expressed. Microglia display the strongest COMMD10 expression, with a small fraction of cells expressing PCSK5 and little to no DYSF or SEZ6L detected. EN-L5-6, EN-L5-4 and EN-L2-3 refer to the different types of excitatory neurons found in the cerebral cortex, which are responsible for signal transmission and are associated with cognitive function. Among these, EN-L5-6 has the highest proportion of cells expressing DYSF, whereas EN-L2-3 had the highest SEZ6L expression. PCSK5 expression is the highest in EN-L5-6 with minimal expression in EN-L5-4 and EN-L2-3. B cells show little to no expression of DYSF, SEZ6L and PCSK5, while COMMD10 is the most expressed gene of interest. In astrocytes, a high fraction of cells expresses PCSK5 at a high mean level, while COMMD10 is expressed at lower levels and DYSF and SEZ6L show minimal expression.

3.3 DYSF:CYP26B1 rs7565433 SNP Heterozygous Alleles Are Associated with Higher Neuron Density in the Thalamus and Pons, Reduced Demyelination in the Cerebellum and a Later Onset to Progression and Age Died

The project investigated the neuropathological and clinical differences between genotypes of the DYSF, SEZ6L, PCSK5 and COMMD10 gene variants of interest. The specific novel gene variants of interest were: rs7565433 mapping to DYSF:CYP26B1, rs7289446 mapping to SEZ6L, rs10869757 and rs11144848 mapping to PCSK5 and rs185263 and rs1567335 mapping to COMMD10. The information from the 310 MS cases (see Table 1), such as (neuron density and levels of demyelination in the SFG, CG, thalamus, occipital lobe, cerebellum and pons) and relevant clinical data (age of onset, age of progression, age died, age at WC, onset to death, onset to progression, onset to WC and progression to death) were compared across the cohort for carriers of a specific gene variant (at either homozygous minor, heterozygous or homozygous major genotype). This approach was used for all our genetic variants of interest.

The DYSF-ZNF638 SNP (rs10191329; Harroud et al., 2023) was not on the genotyping chip. Our analysis has identified a second variant (rs7565433), mapping to DYSF:CYP26B1. Contrary to rs10191329, the rs7565433 is associated with clinical traits of a less severe disease, supported by the finding of a higher neuron density in the thalamus ($p = 0.0108$; Dunn's multiple comparison) (see Figure 18a) and a lower area of cerebellar demyelination (see Figure 18b).

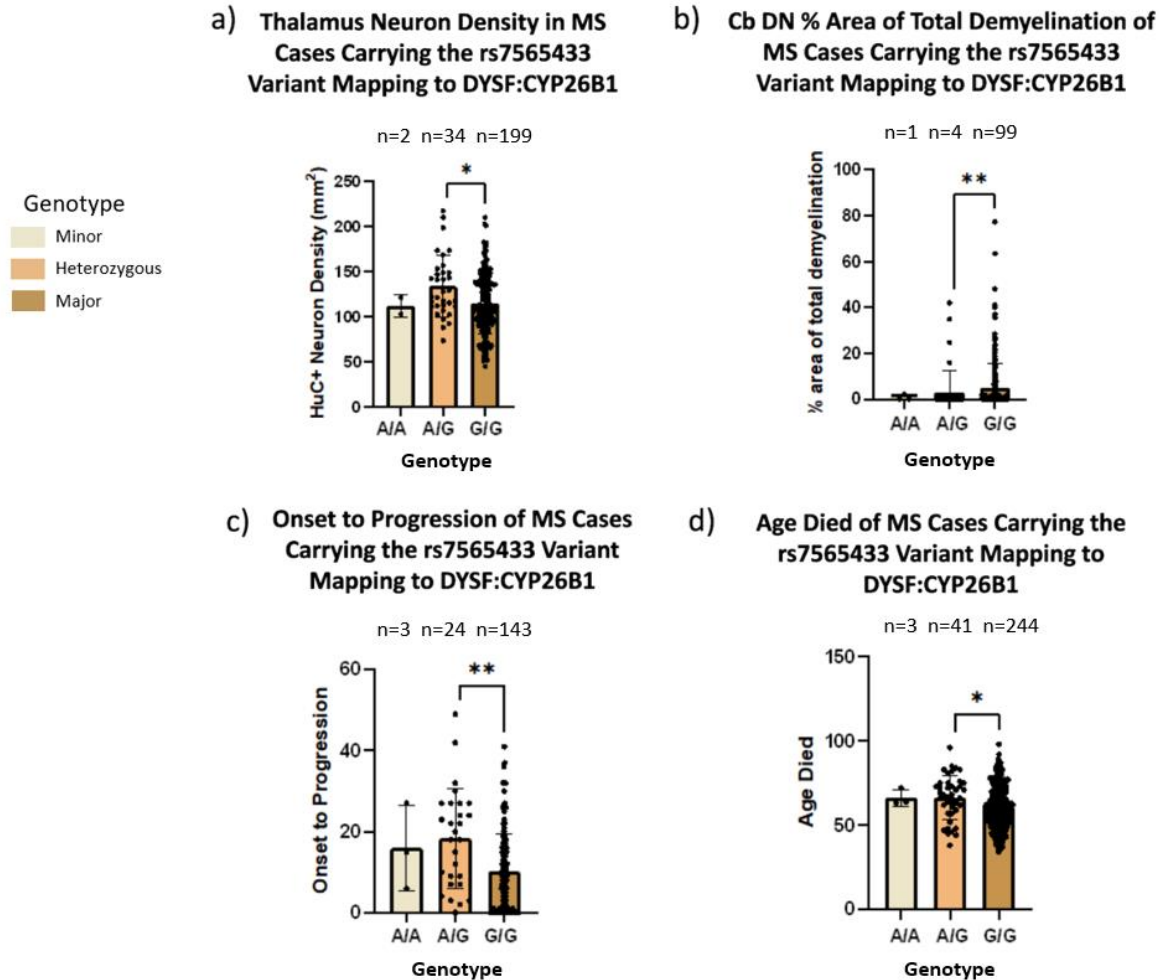


Figure 18. The heterozygous genotype A/G of rs7565433 is associated with a higher neuron density count, a lower demyelination area, a later onset to progression and a later age died. a) There is a significantly lower neuron density in the thalamus for cases with the major allele (G/G) compared to the heterozygous allele (A/G) ($p = 0.0108$; Dunn's multiple comparison). b) The percentage area of demyelination in the Cb DN increased 1.6-fold in homozygous major carriers compared with carriers of the heterozygous allele ($p = 0.0034$; Dunn's multiple comparison). c) There is a mean onset to progression difference of 8 years between heterozygous and major allele carriers ($p = 0.0013$; Dunn's multiple comparison). d) There is a mean of age died difference of 6 years between heterozygous and major alleles ($p = 0.0264$; Dunn's multiple comparison).

3.3.1 SEZ6L rs7289446 SNP Shows No Protective Features in Neuropathology and Clinical Outcomes in Our MS Cohort

The rs7289446 SNP, intronic to SEZ6L on chromosome 22, was examined in the project as it has been independently shown to be associated with a more severe MS course (Jokubaitis et al., 2023; Kreft et al., 2024). We did not observe a difference in neuron density or demyelination in any of the sampled brain regions between those carrying the rs7289446 at homozygous or heterozygous level ($p = 0.1993$ - >0.9999 ; Dunn's multiple comparison). In addition, there was also no difference in the clinical measures between the genotypes (see Table 5).

SEZ6L rs7289446	G/G and G/A	G/G and A/A	G/A and A/A
Age of onset	0.1213	0.0931	>0.9999
Age of progression	>0.9999	>0.9999	>0.9999
Age died	>0.9999	>0.9999	>0.9999
Age at WC	>0.9999	>0.9999	>0.9999
Onset to death	>0.9999	>0.9999	>0.9999
Onset to progression	0.3711	0.4217	>0.9999
Onset to WC	>0.9999	0.8013	>0.9999
Progression to death	>0.9999	>0.9999	>0.9999

Table 5. Statistical results showed no differences between the clinical data for the three rs7289446 genotypes for the SNP that is intronic to the SEZ6L gene. The p values from each Dunn's multiple comparison test across the minor (G/G), heterozygous (G/A) and major (A/A) genotype are reported. Results showed that there are no significant differences between the genotypes of the variant suggesting that carrying this variant at any genotype has no effect on neuron loss, demyelination or a worsening of MS and disability.

3.3.2 PCSK5 rs10869757 SNP Heterozygous Alleles are Associated with a Higher Neuron Density in the Thalamus and Pons

We first investigated the neuropathological and clinical differences between rs10869757 variant carriers, which was the top reported SNP in our collaborative GWAS/neuropathology study. There was a significant difference between the neuron density in both the thalamus and the pons between heterozygous and major alleles, with heterozygous carriers showing elevated neuron density compared to major carriers, but no differences in demyelination levels were observed ($p < 0.05$; Dunn's multiple comparison) (see Figure 19). The minor allele had the highest neuron density in the thalamus and pons (mean = 132 and 162 cells/mm² respectively) but this did not reach statistical significance (minor allele group size = 11 cases). Other clinically relevant information was analysed, and statistics showed no difference between the PCSK5 genotypes. A summary of these results is presented in Table 6.

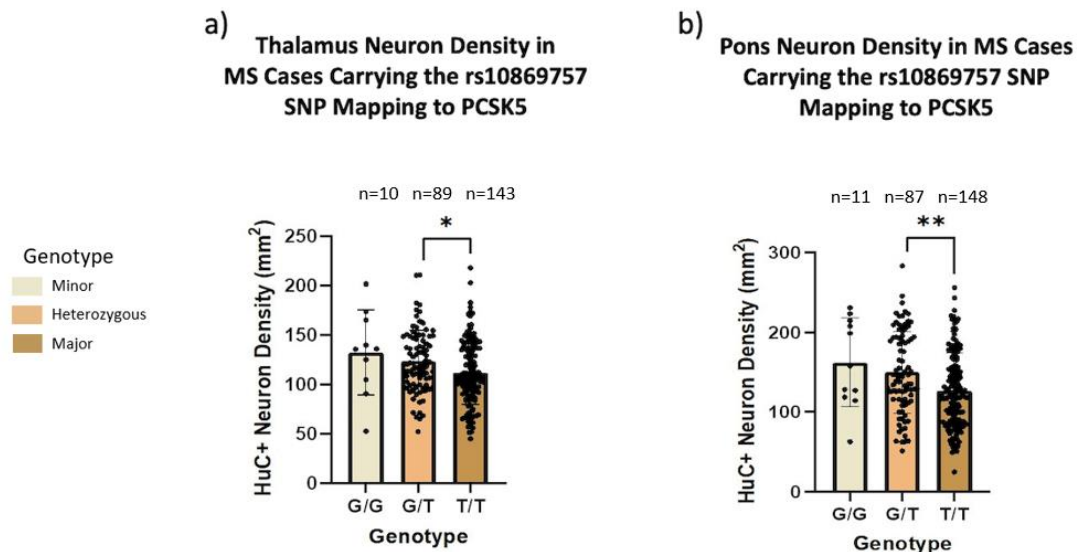


Figure 19. Individuals carrying the major rs10869757 variant exhibit lower neuron density in the thalamus and pons compared to individuals carrying the heterozygous genotype. There was a 1.1-1.2-fold decrease in the neuron density in both the thalamus and the pons in the major allele compared to the heterozygous allele (a, b). Elevated neuronal density in the thalamus and pons was observed among individuals carrying the heterozygous (G/T) allele compared to carriers of the major (T/T) allele ($p = 0.0253$ and $p = 0.0026$ respectively; Dunn's multiple comparison).

PCSK5 rs10869757	G/G and G/T	G/G and T/T	G/T and T/T
Age of onset	>0.9999	0.8785	0.5633
Age of progression	>0.9999	>0.9999	>0.9999
Age died	>0.9999	>0.9999	>0.9999
Age at WC	>0.9999	>0.9999	>0.9999
Onset to death	>0.9999	0.6201	0.3567
Onset to progression	>0.9999	>0.9999	>0.9999
Onset to WC	>0.9999	0.7224	>0.9999
Progression to death	>0.9999	0.8850	>0.9999

Table 6. Dunn's multiple comparison comparing the genotypes of the PCSK5 SNP rs10869757 and disease course. Statistical analysis shows that there are no differences in the clinical outcomes between carriers of the minor (G/G), heterozygous (G/T) and major (T/T) genotype of the rs10869757 SNP.

The same procedure was applied to a 2nd independent variant (rs11144848) mapping to PCSK5. Neuron density did not differ significantly between genotypes in any of the examined brain regions for this SNP ($p = 0.058$ to >0.9999 ; Dunn's multiple comparison). A trend toward increased neuron density in pons was observed in carriers of the minor allele compared to individuals with the heterozygous and major allele ($p = 0.0584$ and $p = 0.0590$, respectively, see Figure 20). No statistically significant differences in clinical data were observed between rs11144848 genotypes (see Table 7).

Pons Neuron Density in MS Cases Carrying the rs11144848 SNP Mapping to PCSK5

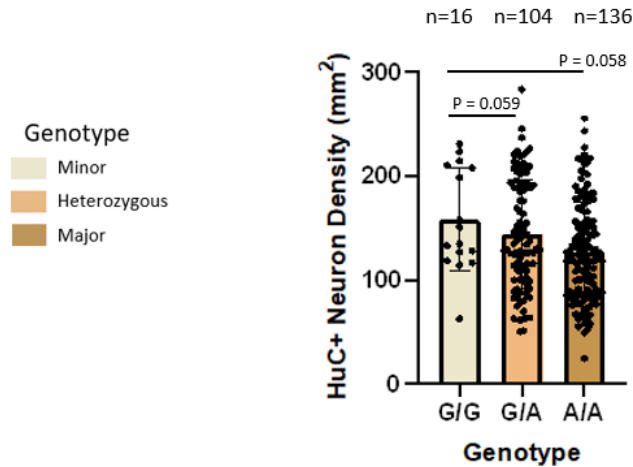


Figure 20. Comparing neuron density in the pons between the rs11144848 SNP genotypes. Neuron density in the pons did not differ significantly among individuals carrying the minor, heterozygous, or major genotypes of the SNP ($p = 0.058$ to >0.9999 ; Dunn's multiple comparison).

PCSK5 rs11144848	G/G and G/A	G/G and A/A	G/A and A/A
Age of onset	>0.9999	>0.9999	0.6857
Age of progression	>0.9999	>0.9999	>0.9999
Age died	>0.9999	>0.9999	>0.9999
Age at WC	0.8094	>0.9999	>0.9999
Onset to death	>0.9999	0.3545	0.5795
Onset to progression	>0.9999	>0.9999	>0.9999
Onset to WC	0.4321	0.2616	>0.9999
Progression to death	>0.9999	>0.9999	0.9996

Table 7. Dunn's multiple comparison comparing the genotypes of the PCSK5 SNP rs11144848 and disease course. Statistical analysis revealed no significant differences in any clinical outcomes between carriers of the minor (G/G), heterozygous (G/A), or major (A/A) allele.

3.3.3 Heterozygous and Minor Alleles of COMMD10 SNPs rs185263 and rs1567335 are Associated with Increased Neuron Density in the SFG

We report a higher neuron count in the rs185263 SNP heterozygous allele and homozygous minor allele carriers compared to major allele carriers ($p = 0.0154$ and $p = 0.0014$ respectively; Dunn's multiple comparison) (Figure 21a). When comparing the genotypes of a second variant (rs1567335) mapping to COMMD10, we also observed a higher neuron count in the SFG for heterozygous and minor allele carriers compared to major allele carriers ($p = 0.0281$ and 0.0031 respectively) (Figure 21b). Interestingly, carriers of the heterozygous allele for this variant demonstrated a 4.6-year later age of onset compared to minor allele carriers ($p = 0.0457$; Dunn's multiple comparison) (Figure 21c).

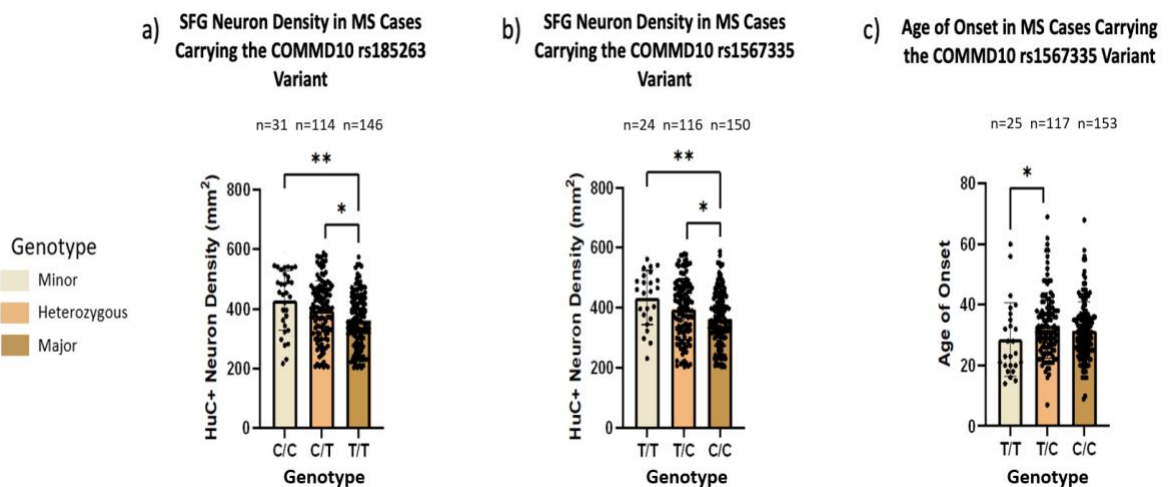


Figure 21. The neuron density in major allele carriers of the rs185263 and rs1567335 COMMD10 SNP are lowest in the SFG. Major carriers of the rs185263 and rs1567335 COMMD10 SNP had a lower neuron density in the SFG compared to minor and heterozygous SNP carriers ($p = 0.0014$ - 0.0281 ; Dunn's multiple comparison). Carriers of the rs1567335 SNP at heterozygous level had a 4.6-year higher age of onset compared to minor allele carriers ($p = 0.0457$; Dunn's multiple comparison).

3.4 The SEZ6L Gene Expression is Significantly Reduced in the MS Grey Matter Lesion

To investigate the SEZ6L expression in human brain tissue, we first performed ISH in a small cohort of MS and non-disease controls. We observed SEZ6L gene expression in

and around neuronal-like cells in MS and control and in MS GML areas, as predicted for a gene that has been shown to be enriched to CNS neurons.

We next quantified the SEZ6L gene expression, detected by ISH, between MS and control GM regions (Figure 22a). There was no significant difference in SEZ6L gene expression (number of SEZ6L⁺ puncta per cell in control and MS GM. Figure 22b, $p = 0.3202$; Mann Whitney U test). SEZ6L expression was more variable in the MS GM brain tissue samples, which represented both normal-appearing and lesional GM, in comparison to controls. We next investigated gene expression in areas of cortical demyelination by comparing SEZ6L expression in NGM and GML. There were differences observed between the control cohort when compared with the MS NGM or MS GML (see Figure 22c). However, there was a modest difference between the MS NGM and GML ($p < 0.05$; Dunn's multiple comparison). The highest SEZ6L gene expression was found in the NGM of the MS and the lowest was found in the GML. This trend of a lower SEZ6L expression in areas of demyelination is illustrated in the paired analysis for those cases with matching normal-appearing and lesion samples (Figure 22d; $p = 0.15$, $n = 6$, Wilcoxon matched paired test). A full table of SEZ6L gene expression results, calculated for each image and case, can be found in Table 12 supplementary.

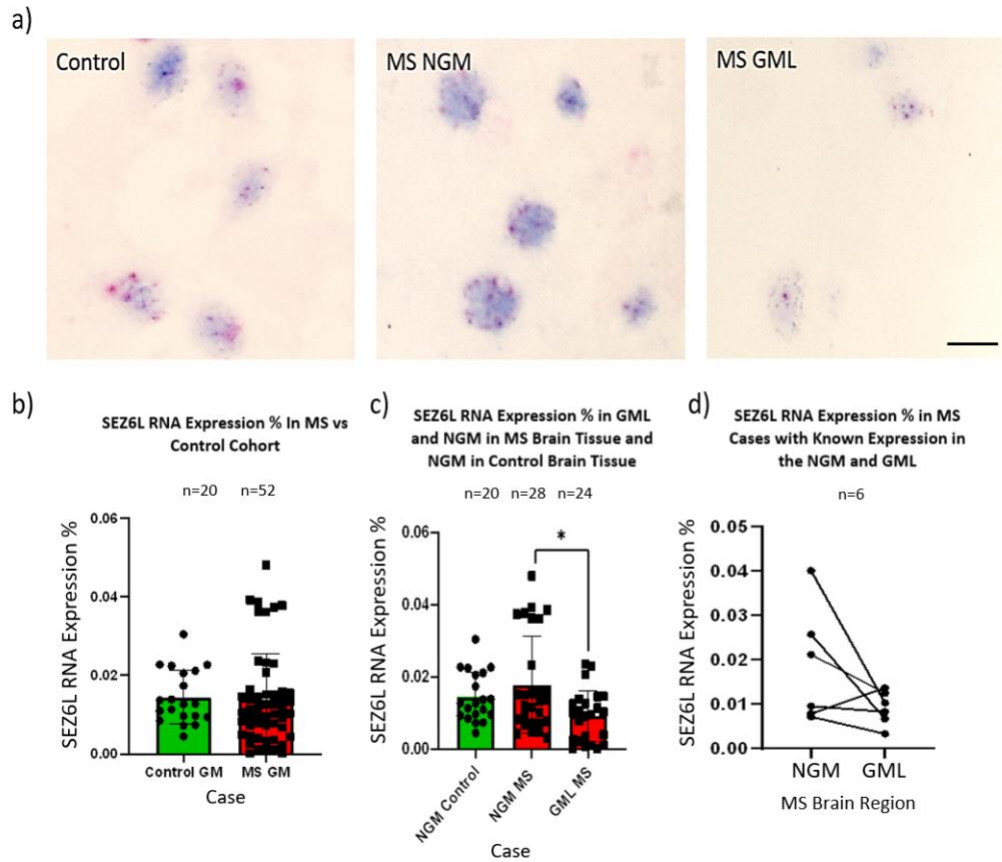


Figure 22. SEZ6L gene expression in control and MS revealed a reduced expression in MS cortical grey matter lesions. SEZ6L expression did not differ between control and MS tissue (a). When MS data were separated into NGM and GML regions, elevated SEZ6L expression in the NGM was found ($p < 0.05$; Dunn's multiple comparison) (b). Each datapoint represents SEZ6L gene expression (%) for one image (observed range = 0.000125%-0.047994%), with 4 images captured per region of interest (NGM in all cases and GML where present in MS cases). The trend for a reduced SEZ6L expression in matched areas of GML compared to NGM is illustrated in (c); (Wilcoxon paired test comparing MS NGM with GML for those cases with available samples). Abbreviations: GML, grey matter lesion; NGM, normal appearing grey matter. Scale bar: a = 30 μ m.

3.5 The PCSK5 and COMMD10 Genes are Co-Expressed in Neuronal Cells

We observed the expression of PCSK5 and COMMD10 transcripts by ISH in both the NGM and GML areas of the MS cohort and the GM of controls. Interestingly, we observed heterogeneity in the expression of the PCSK5 and COMMD10 genes within the brain tissue, as illustrated by the arrows annotated on Figure 23a. Several transcript positive cells had a neuron-like morphology and there were cells that expressed solely PCSK5 (pink) or COMMD10 (green). To further validate the expression of PCSK5 and

COMMD10 in neurons, we performed ISH combined with IHC for the neuronal antigen HuC. Our results confirmed the expression of both the PCSK5 and COMMD10 genes in and around HuC⁺ neurons (as shown in Figure 23b). Note that non-neuronal PCSK5 and COMMD10 signals were also observed.

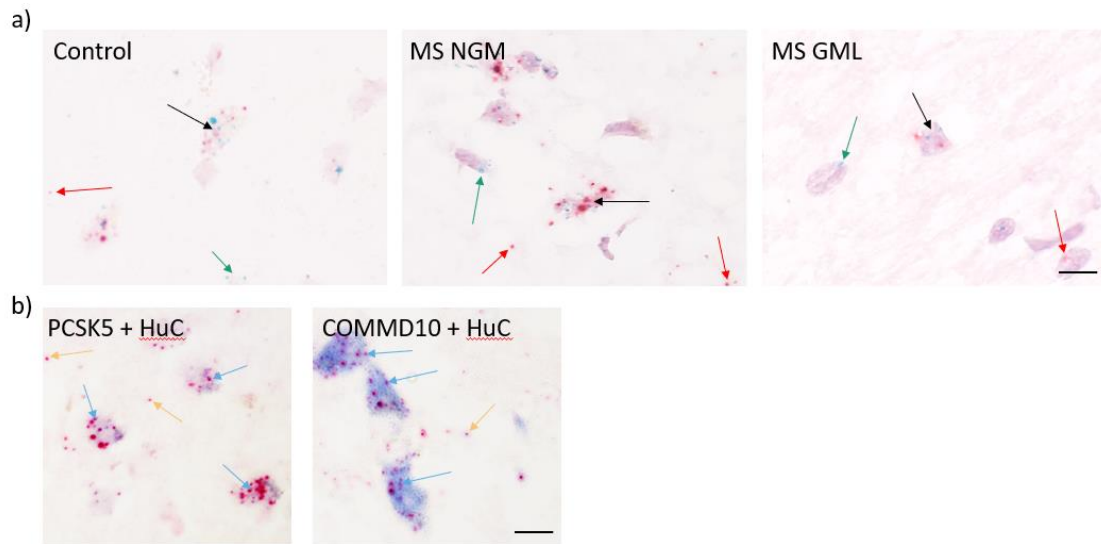


Figure 23. The co-expression of PCSK5 and COMMD10 genes were detected in and around neuronal-like cells in control and MS cohort. a) PCSK5 (pink) and COMMD10 (green), counterstained with haematoxylin, showed co-expression in large neuronal-like cells in both control and MS, as indicated by the arrows in the figure. Note the co-expression of PCSK5 and COMMD10 (black arrows), exclusive COMMD10 gene expression (green arrows) and PCSK5 expression (red arrows). b) Expression of both PCSK5 and COMMD10 in neurons (identified by anti-HuC/D; blue reaction product) and non-neuronal cells (orange arrows) was also observed. Scale bars: a = 50 μ m, b = 30 μ m.

3.5.1 PCSK5 has Elevated Expression in NGM Compared to GML of MS Cohort

The analysis of PCSK5 percentage positive puncta in MS cases compared to the control group revealed no significant differences (see Figure 24a). Dunn's multiple comparisons also revealed no significant differences between the NGM of the control cohort, the NGM of the MS cohort and GML of the MS cohort. However, a notable distinction was identified when evaluating the PCSK5 gene expression between the NGM and GML of MS cases (see Figure 24b). A pairwise correlation of MS cases with known NGM and GML values revealed a stronger association between the two GM regions (as shown in

Figure 24c). This suggests lower expression in GML areas, which could be due to fewer cells, especially HuC⁺ cells, in the lesion and damaged areas, resulting in decreased gene expression as PCSK5 is detected in neuronal-like cells.

3.5.2 COMMD10 has Elevated Expression in NGM of MS Cohort Compared to MS GML Areas and Control Cohort

COMMD10 gene expression showed a higher percentage of positive puncta in the sampled regions compared with PCSK5. Average COMMD10 expression was higher than PCSK5 across both MS NGM and GML (1.41 versus 0.442 in NGM and 0.513 versus 0.114 in GML). COMMD10 expression was higher than PCSK5 in the NGM of the control cohort, although overall levels remained low (see Figure 24a and Figure 24d). While PCSK5 expression did not differ significantly between NGM control and NGM MS, COMMD10 expression was significantly lower in the control cohort ($p = 0.0005$; Dunn's multiple comparison) (see Figure 24b and Figure 24e). The highest expression of both PCSK5 and COMMD10 in our samples is observed in the NGM of the MS cohort. The elevated expression of PCSK5 and COMMD10 may be associated with the pathological features specific to the MS cases included in the study. A significant amount of the MS cohort ($n = 11$) exhibited at least one GML and as some of the gene variants are predicted to have neuroprotective features. The cells could therefore be overexpressing these genes in the undamaged GM tissue of the MS cohort to prevent further damage and cell loss, especially in the cohort that have already presenting GM-related injury. Paired comparisons of MS cohort revealed significantly higher PCSK5⁺ puncta in NGM compared to GML ($p = 0.0098$; Wilcoxon paired test) (see Figure 24c). Similarly, COMMD10⁺ puncta were significantly elevated in MS NGM tissue compared with GML ($p = 0.0420$; Wilcoxon paired test) (See Figure 24e). A full table of these results can be found in Table 13 supplementary.

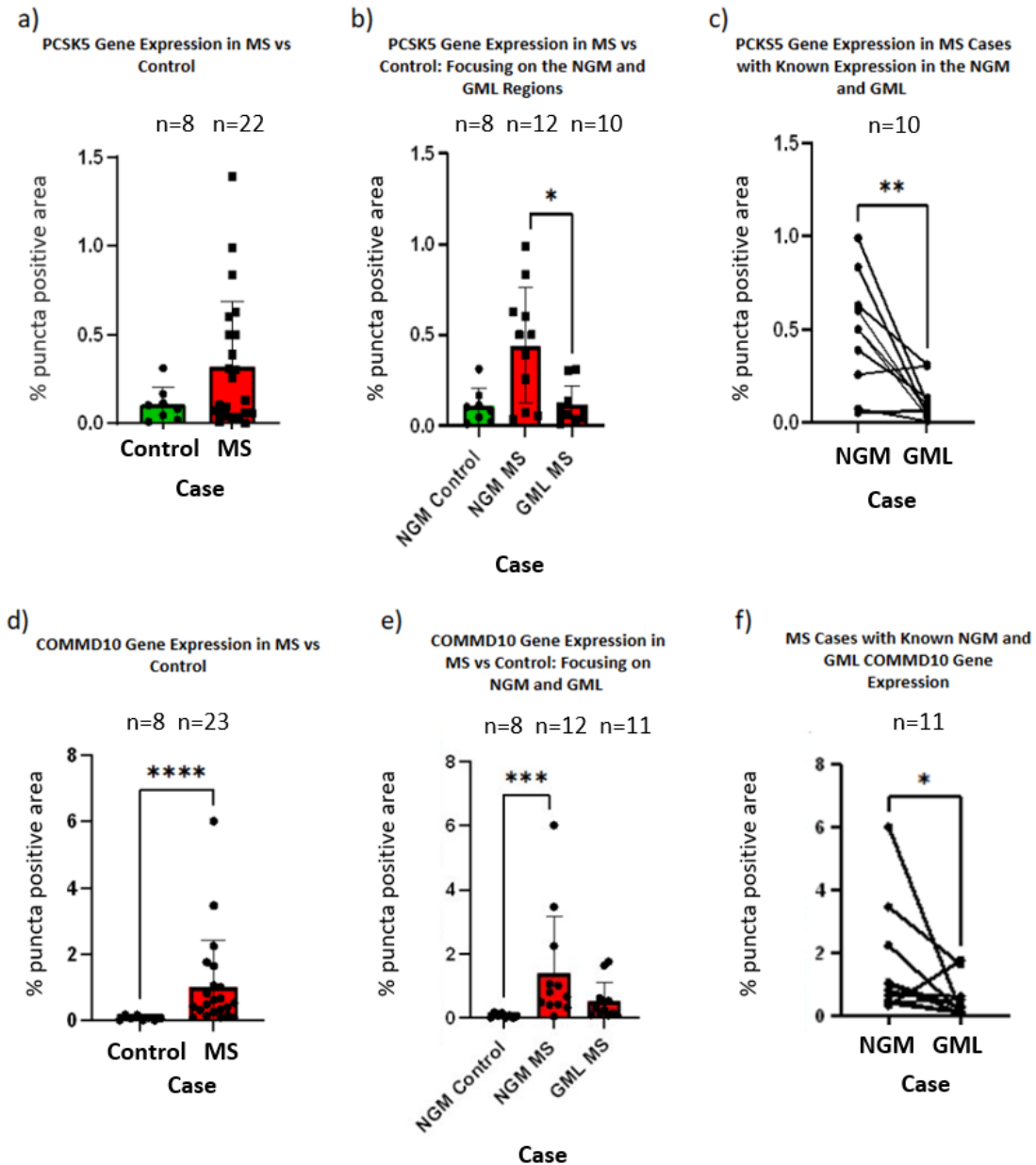


Figure 24. The highest PCSK5 and COMMD10 percentage puncta positive area was found in the MS NGM tissue. a) No significant differences in PCSK5⁺ puncta were detected between control and MS tissue ($p = 0.275$; Mann-Whitney U test). b) The PCSK5⁺ puncta percentage were significantly higher in the MS NGM compared with GML ($p = 0.0483$; Dunn's multiple comparison). c) MS Cases with known NGM and GML cortical areas revealed elevated PCSK5⁺ puncta percentages when compared to GML ($p = 0.0098$; Wilcoxon paired test). d) MS cases exhibited a notably higher percentage of COMMD10⁺ puncta compared with controls ($p < 0.0001$; Mann-Whitney U test). e) Further investigation revealed elevated COMMD10⁺ puncta in MS NGM tissue compared to control cohort ($p = 0.0005$; Dunn's multiple comparison). f) When investigating MS cases with known NGM and GML regions, elevated COMMD10⁺ puncta was observed in NGM regions ($p = 0.0420$; Wilcoxon paired test). This suggests that differences between the NGM and GML in MS cases are not uniform across the cohort and that the presence of GML regions may influence COMMD10⁺ puncta positive areas.

3.5.3 PCSK5 Protein Expression is Elevated in MS NGM

PCSK5 expression by immunostaining revealed no significant differences between the MS and control cohort, despite a higher minimum and maximum expression value (range = 0.315-0.746 and 0.215-0.660 respectively) (see Figure 25a). A trend of PCSK5⁺ cells in MS GML was observed ($p = 0.0883$ -> 0.9999 ; Dunn's multiple comparison; Figure 25b). Paired analysis revealed a reduced expression in MS GML in comparison to MS NGM (Figure 25c). A full table of results can be found in Table 14 of supplementary.

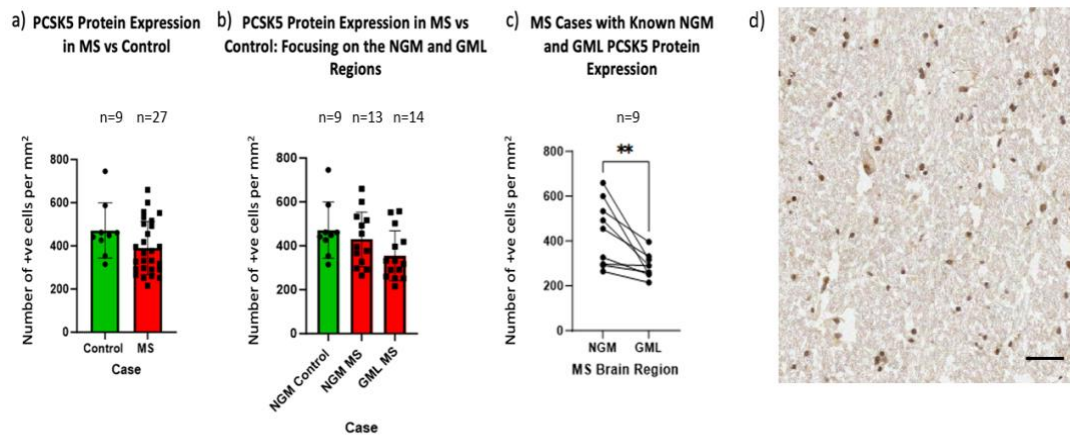


Figure 25. PCSK5⁺ cells are found widespread through normal-appearing and damaged tissue. a) No significant differences were detected when analysing MS and control PCSK5⁺ cell expression ($p = 0.1070$; Mann Whitney U test). b) Dunn's multiple comparison revealed a mean rank difference of 9.802 between the number of PCSK5⁺ cells expressed in the NGM of the control compared to the GML of MS tissue, but no significant differences were found ($p = 0.0883$; Dunn's multiple comparison). c) Using a paired test and data from MS cases that have PCSK5⁺ cell values for both sampled regions, significantly higher PCSK5⁺ cell expression is observed in MS NGM compared to GML ($p = 0.0039$; Wilcoxon paired test). d) An example of positive PCSK5 staining in our MS tissue cohort. Scale bar: d = 100μm.

3.6 Polygenic Effect of PCSK5 and COMMD10

We have shown that the PCSK5 SNPs rs10869757 and rs11144848 and the COMMD10 SNPs rs185263, rs1567335 are associated in some way with the pathological and/or clinical burden of MS and that PCSK5 and COMMD10 are frequently co-expressed by the same cells. We next investigated which MS cases in our study carried more than 1 PCSK5

or COMMD10 variants to establish whether the presence of more than one variant is associated with an additionally increased neuron density effect. It would be interesting to identify whether carrying two of those flagged gene variants at that genotype has a further consequence on neuron loss.

We filtered the data for carriers of all 4 SNPs (rs10869757, rs11144848, rs185263, rs1567335) at heterozygous level because this genotype has been shown above to have a neuroprotective effect and we therefore wanted to discover whether having these 4 SNPs at different genotypes or not makes the cases susceptible to neuron loss. A notable decrease of 24% in neuron density was identified among carriers with no variants versus carriers of heterozygous genotype of the COMMD10 SNPs only (rs185263 and rs1567335) within the SFG, where rs10869757 and rs11144848 PCSK5 SNPs were also present but not at heterozygous level for both ($p = 0.0497$; Dunn's multiple comparison) (see Figure 26a). Analysis also showed a higher neuron density in the cerebellum of carriers of all 4 SNPs at heterozygous level with a 50% lower neuron count observed in the cohort that did not carry any of the variants at any genotype ($p = 0.0343$; Dunn's multiple comparison) (Figure 26b). From both findings, it becomes evident that there exists a significant variance in neuron density between carriers of the heterozygous SNPs and those not carrying the gene variants.

Finally, I compared the clinical milestone data for the subgroups defined on carriership of two or more of the variants of interest (Table 8). Surprisingly, no significant differences in clinical outcomes between any of the subgroups were identified. The p -values obtained from Dunn's multiple comparison comparing the clinical outcomes were found to be extremely high, exceeding 0.9999.

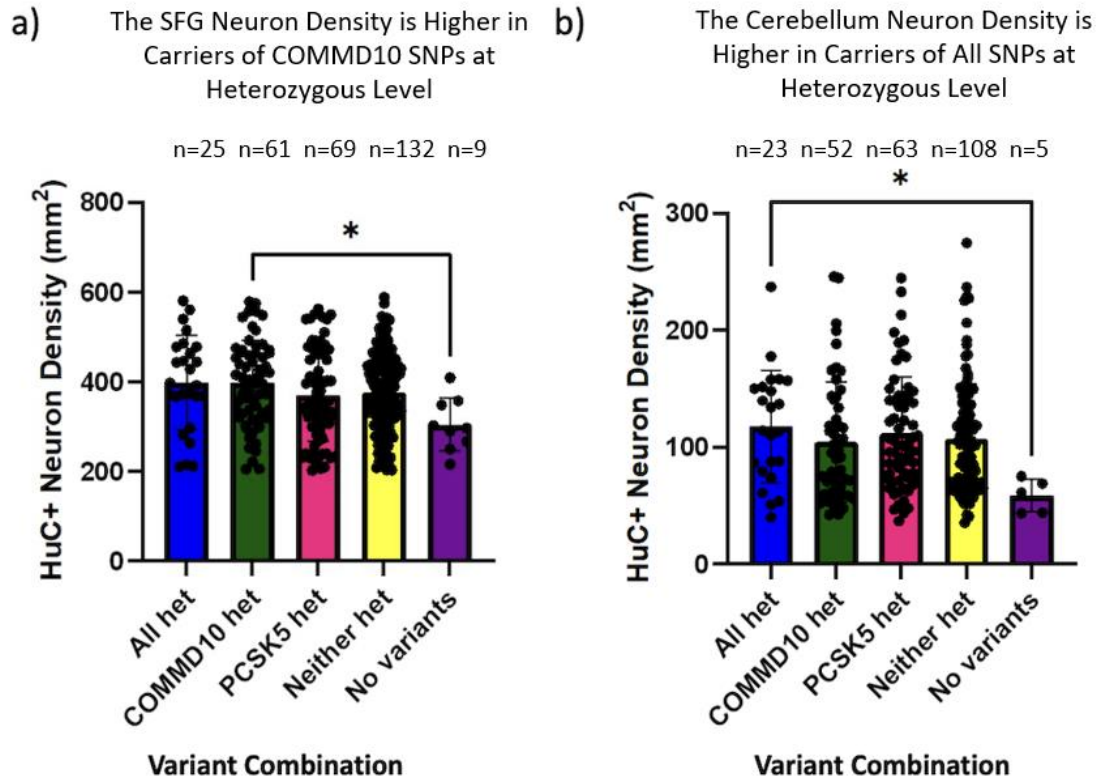


Figure 26. Neuron density is elevated in those carrying two or more variants of interest at heterozygous level. The cohort was classified into subgroups. Carriers of all four SNPs at the heterozygous level were classified as *all het*. Carriers of both SNPs mapping to COMMD10 at the heterozygous level were classified as *COMMD10 het*, while carriers of both SNPs mapping to PCSK5 at the heterozygous level were classified as *PCSK5 het*. Individuals not meeting these criteria were classified as *neither het*, nor those with none of the four SNPs at any allele level were classified as *no variants*. Analysis revealed a decrease in neuron density in individuals that did not carry the variants of interest (no variants) compared with those carrying both COMMD10 SNPs at heterozygous level in the SFG ($p = 0.0497$; Dunn's multiple comparison) and those carrying all four SNPs of interest at the heterozygous level in the cerebellum ($p = 0.0343$; Dunn's multiple comparison).

	All 4 SNPs at heterozygous level vs no variants	Both COMMD10 SNPs at heterozygous level vs no variants
Age of onset	>0.9999	>0.9999
Age of progression	N/A	N/A
Age died	>0.9999	>0.9999
Age at WC	N/A	N/A
Onset to death	>0.9999	>0.9999
Onset to progression	N/A	N/A
Onset to WC	N/A	N/A
Progression to death	N/A	N/A

Table 8. Dunn's multiple comparison reveals no significant differences in the clinical outcomes of carriers of all 4 SNPs at heterozygous level versus no variants and both COMMD10 SNPs at heterozygous level versus no variant. It is important to note that not all Dunn's multiple comparisons could be made due to incomplete dataset entries. These missing values of some of the clinical data were found in the non-variant cohort, so a direct comparison for these variables could not be made.

Discussion

This project set out to investigate the genetic contributions of DYSF, SEZ6L, PCSK5 and COMMD10 on disease severity by exploring SNPs associated with these respective genes (rs7565433 mapping to DYSF:CYP26B1, rs7289446 mapping to SEZ6L, rs10869757 and rs11144848 mapping to PCSK5 and rs185263 and rs1567335 mapping to COMMD10) in relation to quantitative measures of neuropathology and clinical disease severity. Our study focused on neuron density, as we showed neuron density to be strongly associated with disease severity. In this study, I was able to show, for the first time, that a variant mapped to DYSF:CYP26B1 is associated with more neurons and a longer disease duration; variants mapping to PCSK5 and COMMD10 were associated with elevated neuron density and that PCSK5 and COMMD10, which are often co-expressed in the same cells, are found at elevated levels in the normal appearing (non-lesion) cortical GM in MS brain tissue. To further explore these associations, PCSK5 was also characterised at protein level, as suitable assays were available. COMMD10 was assessed only at the RNA level because the antibody produced intense background staining and was unreliable when IHC was performed. The SEZ6L gene was investigated using RNAscope, but protein analysis was not possible at the time due to lack of suitable antibody. DYSF was not taken forward for ISH or protein analysis, as the SNP identified in our cohort (rs7565433) differed from the variant reported in previous studies (rs10191329) (Harroud et al., 2023), so our observation was therefore presented as a separate finding. Finally, I showed that carriership of two or more variants of interest associated with an additional neuroprotective trait. These findings warrant further investigation. We believe that the combination of genetic analysis and detailed quantitative neuropathology will reveal novel insights into the genetic and biological basis of MS progression, that could reveal new therapeutic targets and further genetic: neuropathological analysis.

Uncovering Neurodegeneration: Exploring its Impact on Clinical Measures in MS Patients

We found a significantly lower neuron count in the SFG and CG and a more substantial decrease in the thalamus MS brain. This is a noticeable amount of neuron loss and serves to reiterate how extensive neurodegeneration is in MS. Carassiti et al., (2018) conducted a study utilising oil immersion techniques and stereology to count neurons in coronal whole-hemispheric sections from 9 MS and 7 control human brains. Results showed that there was a 39% reduction in neuron count in the MS cohort, which is equivalent to a deficit of >10 billion neurons. This aligns closely with our own cortical neuron percentage decrease, which is measured using anti-HuC/D IHC and neuronal density analysis via QuPath, highlighting the large variability and reduction in neuron density compared to age-matched non-MS donors.

A decrease in neuron count was expected in the MS brain because a clinical manifestation of the disease is neurodegeneration, inflammation and demyelination (Correale et al., 2019). The further decrease in neuron counts percentage values we observed in the thalamus compared to the SFG and CG could be explained by the interconnected nature of the thalamus to other cortical, subcortical and cerebellar brain regions for sensory and motor signals (Farma & Sullivan, 2015; Hwang et al., 2017). Gratton et al., (2012) discovered that lesions found in focal regions in the brain can have a widespread and non-localised effect on the brain network. This means that damage or injury in regions, such as the cerebral cortex (SFG and CG) are relayed to the thalamus. Clinically, thalamic atrophy appears to be one of the strongest indicators of disease severity and thalamus volume is an early predictor of later disease worsening (Mahajen et al., 2020). Our observations align with the work of others and illustrate how all sampled areas are affected by neuron loss, but the extent of this neuron loss is not equal across the brain (Cifelli et al., 2002; Cooze et al., 2022).

The percentage decrease in MS neuron density for the SFG and CG when compared to the control cohort was similar. Neuron loss in the cerebral cortex could be driven by local demyelination, local activated microglia and dysfunctional astroglia, as well as

inflammatory signals arising in the perivascular and leptomeningeal spaces (Magliozzi et al., 2023). Moreover, the primary feature of MS is the focal inflammatory and demyelinating lesions that are found within the WM, optic nerve and spinal cord, which could indirectly lead to stress and damage of the connected neuron cell body. Our data agrees with many previous studies and serve to further support the understanding that the more severe progressive forms of MS manifest with significant cortical atrophy (Andravisou et al., 2019; Mey et al., 2023; Pagani et al., 2005).

Our study additionally revealed that neuron counts in the thalamus and pons of the MS brain were correlated positively ($r = 0.72$). The pons, like the thalamus, plays a role in interconnectivity which can explain why there is a correlation in neuron density between these two brain regions. The thalamus and pons neuron count also strongly correlated with certain clinical outcomes, supporting the evidence for their essential role in disease progression and their value as regional brain indicators of disease severity. We found that a lower neuron density in thalamus and pons was associated with an earlier age at death, a shorter duration from disease onset to death, a shorter time from onset to progression, a reduced interval from onset to WC and a decreased time from progression to death. Neurodegeneration and brain atrophy are key influences on pathogenesis, thus can influence the overall severity of MS and drive disability (Carassiti et al., 2018; Mey et al., 2023; Sandi et al., 2021). This was confirmed by Zivadinov et al., (2016) who conducted a 10-year follow up study of 181 patients with early onset RRMS to identify factors contributing to disease progression. Results from this study demonstrated that whole brain and cortical atrophy, together with enlargement of ventricular CSF spaces, are linked with disease progression. Therefore, a significant decline in neuron count in the thalamus and pons may accelerate disease progression, leading to more severe symptoms, increased disability and reduced lifespan. Understanding which biological and genetic factors correlate with neurodegeneration, with a particular focus on those linked to neuron density in the thalamus or pons, could reveal important new therapeutic targets or biomarkers relevant to MS progression.

It is crucial to further understand how specific genetic variations can alter the clinical course of MS, in particular its clinical manifestations and its response to treatment. It is important to investigate and consider the role of genetic variants as many gene variants have been incorrectly given a pathogenic or benign title (Charnay et al., 2021). Such misclassification could result in inappropriate treatment or missed preventative measures if a variant is incorrectly deemed as benign, which can lead to avoidable increases in disease progression or severity. A deeper understanding of the genetic variants that influence symptomatic consequences of MS, such as the neurodegeneration, could provide novel insights into underlying disease mechanisms and support the development of more personalised therapeutic approaches. It also provides an opportunity to develop new or repurposed drugs that specifically target the genetic factors influencing MS severity. It is important to understand that MS is complex with both genetic and environmental factors contributing to the disease, thus ongoing research is needed to further develop therapeutic strategies. Personalised medicine relies on genetic information so having that incorrect information could lead to more general medicine that is not targeted towards the patient.

Heterozygous rs7565433 SNP Mapping to DYSF:CYP26B1 is Suggested to be Linked to Neuroprotective Traits and Delayed Onset and Progression of MS

The DYSF protein is involved in muscle membrane repair, but mutations in the DYSF gene can cause both progressive muscular and neurological disorders (Ivanova et al., 2022; Anwar & Yokota, 2024; Spadafora et al., 2022) and have been associated with an accelerated disease course, as well as a higher frequency of cortical and brainstem lesions at autopsy (Harroud et al, 2023). We found a significantly higher neuron density count in the thalamus of carriers of the heterozygous SNP rs7565433 mapping to DYSF:CYP26B1 when compared to carriers of the major allele ($p = 0.0108$; Dunn's multiple comparison). These findings are novel and have not been previously described in the literature. This SNP represents a second variant mapping to DYSF and is independent of that recently described by the International Multiple Sclerosis Genetics

Consortium; MultipleMS Consortium (Harroud et al., 2023). This emphasises the variability of the genetic contributors from one cohort to the other. The results also show that there are differences in clinical outcomes for carriers of this SNP at heterozygous level and major level. As previously stated, the thalamus is a crucial interconnected brain region and is also important in motor and sensor signal relay and degeneration in this region is common in MS brain (Minagar et al., 2014; Torrico & Munakomi, 2023). Therefore, the increased neuron density count in the heterozygous carriers could suggest a protective effect against neuron loss, potentially delaying the onset and progression of MS. These findings align with our findings that carriers of the rs7565433 SNP at heterozygous level had a mean time to progression that was 8 years longer and mean age death 6 years higher compared to individuals with the major genotype ($p = 0.0013$ and $p = 0.0264$; Dunn's multiple comparison). The heterozygous carriers experience a delay in disease progression and tend to have a longer lifespan compared to major carriers, so this SNP could serve as a prognostic marker to predict the course of MS.

We also identified that cases carrying the major allele had a 1.6-fold increase in demyelination in comparison to heterozygous carriers, which is a considerably large amount of myelin to be lost ($p = 0.0034$; Dunn's multiple comparison). This was the only SNP that we investigated that had significant differences in percentage demyelination between the major and heterozygous genotypes. Since demyelination is another pathological hallmark of MS and leads to neuron loss, this result suggests that the major allele carriers may have increased susceptibility to a more severe disease progression. The relationship between DYSF and myelin structure could indicate a potential mechanism by which DYSF influences MS pathology through its role in membrane repair and cellular signalling in neurons. These findings relating to the SNP 7565433 suggest that the DYSF protein may have significant neurological functions that may be due to its physical interactions with SNAPIN and OPTN. The protective effects in homozygous allele carriers indicate that DYSF may influence synaptic vesicle trafficking and immune

regulations within neurons, potentially enhancing neuronal resilience and reducing demyelination.

We investigated the rs7565433 SNP as the variant we intended to study (rs10191329 mapping to DYSF:ZNF) did not appear in our GWAS study cohort. ZNF has been associated with the development of neurodegenerative diseases. The ZNF748 for example is involved in the pathogenesis of Parkinsons Disease and its overexpression causes a decrease in dopaminergic neurons in the substantia nigra (Cassandri et al., 2017). This could imply that the presence of ZNF may increase susceptibility to neurodegenerative diseases, with genetic variants potentially contributing to disease risk or progression through gene regulation. Stoney et al., (2016) identified CYP26B1 in the cerebral cortex and striatum of the rat brain, where it plays a pivotal role in retinoic acid metabolism within the brain, regulating gene transcription. The author concludes that the upregulation or downregulation of retinoic acid levels could be used as an opportunity to control cell proliferation in the sub granular zone, where neurogenesis occurs. Expression levels in the human brain were also investigated using SH-SY5Y human cell lines, revealing that colocalisation of the retinoid acid-synthesising enzyme retinaldehyde dehydrogenase (RALDH2) with catabolic enzymes are responsible for retinoid homeostasis in neurons. In particular, 9-cis retinoic acid has been shown by Huang et al., (2011) to decrease the inflammatory response within oligodendrocytes of patients with MS and encourage remyelination (Xu & Drew, 2006). These findings suggest a potential therapeutic target for modulating retinoic acid to promote neuroprotection and repair and indicate that the heterozygous allele of the SNP rs10191329 may exhibit these properties by maintaining homeostatic retinoic acid levels, thereby preventing demyelination and potentially slowing disease progression.

This SNP has been recently reported in the literature but has contradictory results. Harroud et al., (2023) reported that the minor allele of this SNP was associated with a reduced average time until requiring a walking aid by 3.7 years and an increase in brainstem and cortical anomalies, suggesting a role in greater MS severity and progression. In contrast, Gasperi et al., (2023) found that the same minor allele was

associated with increased brain atrophy, indicating a different direction of effect. Kreft et al., (2024) were unable to replicate any of these findings in their cohort and concluded that this SNP does not alter the clinical course of MS. This shows the uncertainty regarding the effects of the SNP on the severity and progression of MS. These contradictory findings reinforce the complexity of the genetic role on the clinical course of MS and that multiple genes may be responsible for the variability in MS severity and not just singular SNPs.

The SEZ6L Gene is Suggested to Have a Neuroprotective Effect in the MS Brain but Carrying the rs7289446 SNP Mapping to SEZ6L Suggests No Neuropathological or Clinical Differences

SEZ6L has been previously identified as a substrate for BACE1, a significant drug target in neurological diseases such as Alzheimer's disease (Pigoni et al., 2016). This hints at SEZ6L having an involvement in the neurodegenerative components of MS. The rs7289446 SNP, mapping to SEZ6L, has been previously investigated and demonstrated to be strongly associated with a more severe disease course in two distinct cohorts, making it a SNP of interest to explore (Jokubaitis et al., 2023; Kreft et al., 2024). However, this pattern was not replicated in our cohort, suggesting that this SNP may not be relevant to our specific patient population. This highlights the importance of considering geographical and ethnic variability in genetic studies, as these factors could influence disease characteristics. Jacobs et al., (2024) reported that individuals of Black and South Asian ethnic backgrounds in the UK experienced an earlier onset of MS compared to those of White ethnicity. Although the study did not identify significant differences in disease severity across ethnic groups, the earlier age of onset highlights the potential influence of ethnicity on MS progression. The lack of replication of the rs7289446 SNP in our cohort allows us to explore other genetic variations within SEZ6L that could have an influence on MS severity or progression.

The SEZ6L gene has also been associated with neural connectivity, but its expression levels in cortical MS and control human brain tissue have yet to be explored, making it an interesting gene to study (Nash et al., 2020). Our results indicated the presence of the SEZ6L gene in and around neuronal-like cells in both control and MS cortical brain tissue, which is supported by information that is published on Protein Atlas and cellxgene. Moreover, cellxgene also revealed high SEZ6L expression in OPCs, which is relevant given that MS is a demyelinating disease. Elevated expression of SEZ6L was observed in the NGM of the MS brain and compared to GML areas ($p < 0.05$; Dunn's multiple comparison). Inflammatory mediators such as tumour necrosis factor-alpha (TNF- α) and interferon-gamma (IFN- γ) are also elevated in MS patients, which have been widely reported in literature (Lassman et al., 2012; Palle et al., 2017). Although such studies have not directly measured SEZ6L expression, these inflammatory mediators are known to influence gene expression in OPCs (Zveik et al., 2024) and could contribute to the observed differences in SEZ6L expression between NGM and GML regions. In areas of NGM with lower inflammatory activity, SEZ6L expression may be maintained or upregulated, reflecting a neuroprotective response. In GML areas with higher inflammatory activity, SEZ6L expression may be downregulated, potentially impairing OPC functions. This suggests that high SEZ6L expression levels, particularly in OPCs, in the NGM of MS patients could represent a compensatory response to enhance myelin repair or serve as an active remyelination marker preserving regions not yet affected by lesions. This may function as a protective mechanism to delay the lesion spread or to reduce MS severity where OPCs are present to maintain myelin integrity.

It is also evident that higher SEZ6L levels were detected in the control cohort compared to GML, albeit at not significant levels but emphasises that SEZ6L is expressed in undamaged tissue. The lower expression in the GML regions indicates that neural connectivity in these regions may be impaired due to the disruption of neural networks in lesion areas. This pattern could result in less efficient information processing and neural communication between different brain regions, potentially accelerating neurodegeneration as well as cognitive and motor decline.

Further scrutiny using a Wilcoxon test, specifically comparing SEZ6L expression values in known MS cases with identified NGM and GML expression values, did not reveal statistical significance. However, a suggestive decline in SEZ6L expression is discernible. This observation hints at potential alterations in SEZ6L expression that may not achieve statistical significance in the given sample size but could still be of biological relevance. This insight prompts further exploration into the role of SEZ6L in MS pathology and warrants consideration in future studies examining larger cohorts.

Carriers of Heterozygous rs10869757 Alleles are Suggested to Have Neuroprotective Mechanisms to Delay the Onset of Neurodegeneration and Disease Progression

The PCSK5 gene is responsible for cell movement, which could play an important role in both disease progression and potential repair mechanisms in MS patients (Gong et al., 2024). The association of the heterozygous carriers of the rs10869757 SNP having a higher neuron density in the thalamus and pons could have several implications for MS patients. Firstly, a higher neuron density in these interconnected regions of the brain suggests a neuroprotective effect, which may partly contribute to the slowing down of disease progression and neurodegeneration, resulting in better long-term outcomes and less disability compared to those of minor allele carriers. A higher neuron density in the thalamus and pons could result in a better neural communication in MS patients which can delay the onset of cognitive decline and motor impairment, often seen in high severity MS cases.

The lack of statistical significance in the pons neuron density associated with the rs11144848 SNP mapping to PCSK5 suggests that this variant may have a less of an impact on neuronal preservation in MS compared to other variants mentioned. The p values comparing the minor allele and major allele genotype and the heterozygous allele with major allele ($p = 0.0584$ and $p = 0.0590$ respectively) indicate that the variant could have a small effect, but the cohort may not have been a sufficient size to be able

to confirm this. It may also be possible that the rs11144848 and rs10869757 SNPs, whilst both mapping to PCSK5, may have different functional roles within the brain. Differences between the SNPs in their location within the gene can alter gene function and regulation, which could explain why the rs10869757 SNP shows an association with neuron density in the pons and thalamus and the rs11144848 SNP does not.

Elevated PCSK5 Expression in MS NGM Suggests Neuroprotective Mechanisms

ISH combined with IHC confirmed that PCSK5 is expressed in and around neuronal-like cells (see Figure 23). This finding, along with previous knowledge of PCSK5, may suggest that this gene has an important role in neurons such as involvement in neuronal migration, which is essential for proper functioning of the CNS by ensuring that neurons reach their correct location in the brain (Hantanaka et al., 2016). In the context of our findings, PCSK5 could contribute to the repair processes by supporting mechanisms such as axonal guidance, synaptic plasticity, or remyelination support, thereby helping to preserve neuronal networks, prevent further loss and potentially slow disease progression in MS patients. The significantly elevated PCSK5 expression observed in the NGM compared to the GML in MS cases may suggest a role for PCSK5 in preserving neuronal integrity, with upregulation in less affected regions supporting neuronal function and limiting further neurodegeneration. Moreover, the lower expression within the damaged lesion tissue could be a consequence of fewer cells, especially HuC⁺ cells, in the area. Increased astrocyte and microglial activation in MS lesion sites can significantly alter gene expression profiles, potentially impacting neuronal migration and survival as PCSK5 may be affected by this altered environment. PCSK5 has also been previously associated with converting pro-MMP14 and pro-MMP2 to their active forms to facilitate microglia motility. This can have beneficial effects in lesion sites such as improved debris clearance and enhanced repair processes but can also have disadvantages such as increased inflammation depending on how these processes are regulated (Ito et al., 2021). The finding of an even higher level of significance ($p < 0.01$)

when performing a pairwise analysis of MS cases with known NGM and GML PCSK5 expression levels potentially points to a strong association between PCSK5 expression and the extent of damage or preservation in GM regions affected by MS.

The protein-protein interaction map for PCSK5, as shown in the Human Protein Atlas, indicates predicted physical associations with NOTCH2NLA and MEOX2 (Cho et al., 2022; Huttlin et al., 2021; Oughtred et al., 2021; Tu et al., 2021; Uhlén et al., 2015). In MS NGM, higher PCSK5 expression may enhance interactions with both MEOX2 and NOTCH2NLA. These predicted interactions could modulate the Notch signalling pathway, potentially promoting proliferation of neural progenitor cells, supporting neuronal maintenance and repair and influencing proper neuronal development via ERK/AKT pathway activation (Tachon et al., 2021). If interactions between PCSK5, NOTCH2NLA and MEOX2 are disrupted, neuronal survival may be compromised, potentially accelerating MS disease progression (Rai et al., 2019). Enhancing or modulating these interactions may offer valuable strategies to improve outcomes for MS patients.

Carriers of Major rs185263 and rs1567335 SNPs Mapping to COMMD10 are Suggested to Have Less Neuroprotective Mechanisms to Delay Neurodegeneration in the SFG Compared to Minor and Heterozygous Carriers

COMMD10 plays a key role in inhibiting the NF- κ B signalling pathway, which is a critical regulator of the immune response, inflammation and cell survival. This makes COMMD10 an important gene to study, as dysregulation of the NF- κ B signalling is implicated in neurodegenerative diseases via the expression of pro-inflammatory mediators (Singh & Singh, 2020). In our cohort, carriers of the major rs185263 and rs1567335 SNPs mapping to COMMD10 exhibited significantly lower neuron density in the SFG compared to heterozygous and minor allele carriers ($p = 0.0014-0.0281$; Dunn's multiple comparison), suggesting impaired neuronal survival because of reduced NF- κ B

inhibition and increased inflammatory activity. Moreover, COMMD10 is important for copper homeostasis, which is vital for cellular processes such as myelination (An et al., 2022). Major allele carriers may therefore have disrupted copper regulation, increasing the risk of oxidative stress, inflammation and contributing to the lower neuron density observed in the SFG. Dysregulated copper transport in MS has been shown to cause demyelination and oligodendrocyte loss via astrocyte-mediated mechanisms, supporting a role for altered copper homeostasis in increasing neuronal vulnerability (Colombo et al., 2021). Copper also regulates gene expression and supports neurotransmission, so disruption in copper homeostasis may exacerbate inflammatory signalling via impaired NF- κ B inhibition and elevate oxidative stress (Sheykhansari et al., 2018). These findings highlight that essential metal homeostasis is a critical factor in neuronal survival. Consequently, patients carrying the major alleles of the COMMD10 SNPs may experience a more severe MS course due to compromised copper homeostasis, which elevates free radical levels, further contributing to neuronal damage and potentially accelerating MS progression (Rossi et al., 2006). These findings suggest impaired neuronal survival in major allele carriers, potentially due to impaired NF- κ B inhibition and the associated increase in inflammatory activity. The overall lower neuron density observed in these MS major allele carriers may have important implications for disease progression.

MS Carriers of Heterozygous rs1567335 SNPs are Suggested to have a Delayed Age of Onset Which Provides Opportunity for Improved Treatment Management

Results concluded that carriers of the heterozygous rs1567335 SNP mapping to COMMD10 had a 4.6-year higher age of onset compared to minor allele carriers ($p = 0.0457$; Dunn's multiple comparison). This significant difference suggests that this SNP plays a protective role in delaying the clinical onset of MS in heterozygous carriers. A 4.6-year delay in age of onset could be beneficial for both patients and clinicians as this could mean a later disease manifestation which may result in a slower progression of

MS symptoms. For patients, this delay can result in a longer period of good quality of life before disability increase. A later disease manifestation could also translate into slower symptom progression and less accumulated disability which may allow patients more time before facing the difficult physical and neurological challenges associated with MS. For clinicians, once early signs of MS are detected, the delay in onset provides an opportunity to explore and trial different therapies that may offer greater efficacy for the patient. Given that MS is a heterogenous disease, with variability in both progression and response to treatment, this additional time allows for a more tailored and potentially more effective therapeutic approach. It is important to note that since symptoms may not appear until later in these patients, predicting the disease course of MS can still be challenging. This is particularly relevant in PMS, where the underlying pathology often manifests long before noticeable symptoms, limiting clinicians' opportunities to trial treatments or implement precautionary measures. This emphasises the importance of genetic screening of variants that may have an influence on clinical or neurological measures to identify individuals that may be at risk before symptoms arise.

Elevated COMMD10 Gene Expression in MS NGM Suggests Neuroprotective Mechanisms via Neuroinflammatory Mediation

The presence of COMMD10 in and around neuronal-like cells, along with elevated expression in the NGM of MS patients indicates that this gene may contribute to neuroprotective modulation. The significantly increased expression detected in the MS NGM may serve as a protective mechanism to inhibit NF- κ B signalling to prevent further inflammation and damage within brain tissue. However, in the GML areas where COMMD10 expression is much lower, the inflammatory responses are heightened, which can negatively impact neuronal integrity. The inhibition of the NF- κ B signalling pathway can increase the regulation of the CASP3 and CASP9 enzymes which may have a role in maintaining cellular homeostasis by removing damaged cells (Fan et al., 2020; Yang et al., 2021). The increased expression of COMMD10 in the NGM may help to

influence neuronal survival and function by promoting pathological tissue degeneration through the CASP9 and maintenance of neuronal health through the CASP3 (Asadi et al., 2022; Avrutsky & Troy, 2021).

COMMD10 also has been shown to have interactions with other COMMD family members, such as COMMD5 and COMMD1, which are also involved in NF- κ B inhibition (see Figure 16d). Due to diminished anti-inflammatory effects of COMMD10 in NGM and fewer protein-protein interactions with COMMD5 and COMMD1, patients may face increased disability due to a more rapid progression of MS. COMMD10 has also been shown to interact with FOS, which is involved in neurogenesis and cortical development, indicating that elevated COMMD10 expression may enhance the activity of c-FOS, potentially supporting cellular regeneration in the NGM. It is evident that c-FOS is used as a neuronal activity marker and is usually upregulated in response to cellular stress (Velazquez et al., 2015). This suggests that elevated c-FOS could serve as a biomarker for disease activity and disease progression in MS.

The Co-Expression of PCSK5 and COMMD10 in the MS Brain: Insights into Inflammation and Neurodegeneration

The observed perinuclear distribution of PCSK5 and COMMD10 within neuronal-like cells is particularly relevant to our project's focus on neurodegeneration, as it potentially highlights a crucial link between these genes and neuronal health, suggesting their involvement in neuroprotective mechanisms and pathways relevant to neurodegenerative processes. Understanding the role of PCSK5 and COMMD10 in neurons could offer valuable insights into the molecular mechanisms underlying neurodegeneration and may pave the way for targeted therapeutic interventions aimed at preserving neuronal integrity and function. COMMD10 is expressed at significantly higher levels than PCSK5, with peak COMMD10 expression in MS NGM being about 6 times greater than PCSK5, as indicated by Figure 24c and Figure 24f, for MS cases with known GML areas. Cellxgene revealed a higher mean expression and a greater fraction

of cells expressing COMMD10 compared to PCSK5 in both the MS and control cohort (Figure 17a). The higher expression of COMMD10 compared to PCSK5 may be a consequence for their distinct roles in cellular processes and neuroprotection. As previously stated COMMD10 is heavily involved in NF- κ B signalling pathway inhibition, this could potentially explain the high COMMD10 expression observed, particularly in the MS NGM, as a compensatory mechanism to suppress inflammation and protect neurons from further damage. In contrast, PCSK5 is involved in cell migration and may not be as involved in modulating inflammatory pathways, which could explain why elevated expression is observed but not as excessive as COMMD10 expression.

PCSK5 and COMMD10 may have biological interplay in MS, with their expression potentially reflecting response to damage in other areas of the brain, such as lesion sites. Their co-expression could serve as a neuroprotective mechanism, aiming to limit further neuroinflammatory and neurodegenerative damage. Although they are distinct genes, PCSK5 and COMMD10 may share functional overlap in regulating neuronal survival and influencing disease progression in MS.

The Presence of Grey Matter Lesions May Alter the PCSK5 Protein Availability in Multiple Sclerosis

Interestingly, we observed a higher proportion of PCSK5⁺ cells in the control cohort compared to the MS cohort. This contrasts with the PCSK5 gene expression levels, which were elevated in the NGM of MS cases relative to controls. This suggests that there may be potential post-translational modifications that affect PCSK5 protein availability. We found no significant differences between the control and MS grey matter PCSK5⁺ expression, irrespective of GML areas ($p = 0.1070$; Mann Whitney U test) and no significant differences between NGM and GML of MS tissue ($p = 0.0883$; Dunn's multiple comparison). However, a pairwise analysis of MS cases with both NGM and GML areas revealed a significantly lower expression of PCSK5⁺ in damaged lesion tissue ($p = 0.0039$; Wilcoxon paired test). These findings are robust, as expression levels for NGM and GML

areas were derived from the same brain sections, sourced from a single tissue bank with consistent practises and identical PMI values.

The significant difference in PCSK5⁺ cell expression between NGM and GML areas in MS cases suggests that the presence of lesions may alter PCSK5 protein availability. Not all MS cases exhibited GML regions and multiple factors could contribute to the reduced expression observed in these lesion areas. One such factor is the unfolded protein response (UPR), a cellular stress response activated by misfolded or unfolded proteins in the endoplasmic reticulum (ER). UPR has been reported at inflammatory lesion sites in MS and is known to trigger apoptosis (Lin & Popko, 2009; Stone & Lin, 2015). The downregulation of PCSK5⁺ cells in GML regions may therefore reflect increased ER stress, resulting in accumulation of misfolded PCSK5 protein and cell death. Previous studies using IHC have revealed the presence of UPR factors in oligodendrocytes, astrocytes, T cells, macrophages and microglia in MS lesions (Mháille et al., 2008; Cunnea et al., 2011; McMahon et al., 2012; Ní Fhlathartaigh et al., 2013). If these cell populations within the GML were positive for PCSK5 protein expression, they may be more vulnerable to UPR-induced apoptosis, thereby reducing the number of PCSK5⁺ cells and worsening disease progression. T cells and microglia/macrophage are involved in the immune response and so a decrease in these cell types can increase neuroinflammation and cause further tissue damage in the lesion. Moreover, oligodendrocytes and astrocytes play key roles in CNS myelination and homeostasis, respectively and an increase in the UPR may contribute to neuronal damage observed in the GML.

Previous studies have shown that the PCSK5 protein, encoded by the PCSK5 gene, is responsible for processing osteopontin as one of its substrates (Hoac et al., 2018). Osteopontin plays a key role in cell adhesion and migration and has been associated with MS relapses, with elevated levels observed in patients who had a shorter interval between clinical relapse and CSF withdrawal (Stampanoni et al., 2023; Wang & Denhardt, 2008). From this it could be implied that reduced PCSK5⁺ within the MS GML tissue may result in altered processing and less cleavage of osteopontin, which could

impair its role in cell survival and potentially exacerbate neuronal damage and loss in the lesion areas. The role of osteopontin in cell adhesion and migration may also influence neuronal connectivity and synaptic within CNS. Therefore, altered osteopontin processing in MS patients could disrupt these processes, contributing to neuronal dysfunction, further neurodegeneration and increased disease severity.

The lack of significant differences in PCSK5 protein expression between MS NGM and control grey matter suggests potential post-transcriptional or post-translational regulation mechanisms that are functioning correctly, enabling synthesis of PCSK5 in cells. The significantly higher expression of PCSK5⁺ cells in NGM compared to GML, specifically in MS cases with lesions implies a potential role for PCSK5 in the maintenance or protection of NGM against lesion formation or progression, preventing a disease worsening.

Finding Evidence for a Polygenic Effect on the Neuropathological and Clinical Severity of MS

Although the polygenic effect of many SNPs recently suggested to be associated with increased MS severity remain largely explored, findings from this study could highlight the significance of carrying the rs10869757 and rs11144848 SNPs (mapping to PCSK5) and rs185263 and rs1567335 (mapping to COMMD10) at heterozygous level in influencing MS progression and worsening. The main finding here was that being a heterozygous carrier of both COMMD10 SNPs has a positive influence on neuron count in the SFG and all 4 SNPs show a significant neuroprotective effect in the cerebellum. The observed differences in neuron density between carriers and non-carriers of these highlighted heterozygous SNPs suggest a protective influence against neuron loss. It appears that only the COMMD10 SNPs at the heterozygous level exert an effect on neuron loss, indicating a potentially greater neuroprotective impact associated with variants of this gene in comparison to the SNPs investigated that are mapping to PCSK5.

As the cerebellum is a very neuron dense structure containing approximately 80% of the brain's neuron count, a significant reduction in the neuron count would result in a significant decrease in the overall brain neuron density if the neurons were counted at large scale (Jimshelashvili & Dididze, 2024; Roostaei et al., 2014; Van Essen et al., 2018). We previously quantified neurons in the cerebellar dentate nucleus, a key grey matter area that projects to the neuron-rich cerebellar cortex. MS patients who enter the progressive stage show cerebellar symptoms and pyramidal cell, granule cell and dentate nucleus neuron loss is a feature of progressive MS pathology. Cerebellar atrophy can often be a predictor of disability and progression at early stages (Albert et al., 2017; Howell et al., 2015; Redono et al., 2015; Tornes et al., 2014). Most patients with progressive MS have cerebellar disease which can cause complications such as tremor and ataxia which are difficult to manage (Tornes et al., 2014; Wilkins, 2017). These findings emphasise the cerebellum as a target for preventing neurodegeneration and a site to monitor by MRI, as damage can contribute to the worsening of disability and an increase in MS progression. Carrying all 4 SNPs at the heterozygous level suggests an enhancement in neural resilience potentially leading to a better clinical outcome in comparison to MS cases that do not carry any of these SNPs. However, when comparing the clinical outcomes, it is evident that no significant differences were observed. This shows that the effects of these SNPs on neuron density are independent on the severity of the disease of these clinical parameters that are measured. It is possible that other drivers or mechanisms may be responsible for determining the clinical course of disease in this cohort, emphasising the need for further investigation to understand the relationship between genetic variants, neuron density and clinical outcomes that measure MS progression. This illustrates the complexity of the disease, suggesting that neurodegeneration may only play a minor role, while genetic and lifestyle factors could have a greater impact on patient outcomes.

Limitations of the Project

The study encountered several limitations which should be acknowledged. Firstly, neuron counts for the SFG, CG and thalamus were not available for each MS and control case due to incomplete data sets. It is important to note that 3 MS cases did not have any known HuC⁺ positive count data for the SFG, CG and thalamus and so did not contribute to the neuron density count. Additionally, during the annotation process in QuPath, it was observed that the human control tissue sections were smaller than the MS tissue sections. This led to HuC⁺ cell calculations taken from smaller regions. Incomplete datasets were also present in the 310-case cohort datasheet. Nevertheless, our cohort of 310 PMS cases represents the largest such collection on record.

Result accuracy is dependent on the quality of the histologically stained slides, the chosen staining technique and the chosen QuPath parameters and estimation stain vectors for cell and pixel counts, which can be correctly estimated with high quality images. The cohort chosen represented a wide range of MS cases with various disease durations. The QuPath software analysis generated relevant data, but the scanned images are 2-dimensional and not 3-dimensional like the brain anatomy, therefore only providing a snapshot of the cell count (reported as cells per unit area) and a thorough quantification of cells per unit volume in that region. Nevertheless, QuPath is still a valuable tool for digital pathology and analysis, and we quantified many millions of neurons in total from large regions of interest from each available donor block.

The background staining for the immunohistochemically stained PCSK5 MS and control tissue was extremely intense making it difficult for the automated counter to be used on QuPath, thus a manual counting approach had to be done to ensure there was no overestimation of PCSK5⁺ cells in the NGM and GML sampled regions. This may be due to non-specific interactions occurring within the tissue. Therefore, factors such as an increased serum concentration or using an immunohistochemical-grade bovine serum albumin within the antibody/blocking solution should be considered for future analysis to minimise background staining and enhance digital analysis.

RNAscope is highly sensitive and provides consistent results when performed correctly, making it suitable for this project, particularly given the challenges of working with human brain tissue, where mRNA is easily degraded. RNAscope recommends a method of grading the relative extent of positive puncta but we found this to be unsatisfactory. We therefore used the classifier as an automatic quantification as a more reliable approach to calculating the relative gene expression in the cells counted. When comparing clinical data across PCSK5 and COMMD10 genotypes in the MS cohort, the low frequency of minor allele carriers, combined with missing clinical information (e.g., onset to wheelchair use), prevented the use of Dunn's multiple comparison test, as at least one genotype group lacked sufficient data. In these instances, we would perform a t-test between the heterozygous and homozygous major alleles where there is data to compare. The inclusion of a cohort with enough minor allele carriers for these SNPs may have influenced the significance of the findings.

Future Work

Future work could extend the findings of the study in several ways to broaden our understanding of the genetic links underlying MS severity. Firstly, this framework we have created to analyse gene expression and further investigate novel variants of DYSF, SEZ6L, PCSK5 and COMMD10 can be applied to other gene variants of interest that have implications with MS or other neurological disorders. By exploring the gene expression in other cell types (not just neurons), such as oligodendrocytes, astrocytes and other glial cells, it may provide insights of the roles of genes in other cellular functions and mechanisms beyond the neuron. Exploring the levels of gene expression in other brain regions (such as the pons) and not just cortical blocks could provide valuable insights into the implications of the identified SNPs on regional disease heterogeneity.

It would be interesting to perform Duplex ISH staining of PCSK5 and COMMD10 in the cerebellum dentate nucleus as results in our cohort showed a 50% neuron density decline in carriers of all four heterozygous SNPs versus MS patients who did not have the variants of interest. Further investigation involves taking the genotype of the cases used for ISH and IHC protocols to quantify gene expression into consideration and staining samples from a cohort where there is equal distribution of major, heterozygous and minor genotypes for a particular SNP to analyse the influence of different genotypes on neuron density. This would be particularly interesting to determine whether carrying the heterozygous SNPs rs10869757 and rs11144848 (mapping to PCSK5) and rs185263 and rs1567335 (mapping to COMMD10), compared to minor and major alleles for that SNP holds true for MS cases experiencing less neuron loss in statistical analysis.

We can take our findings from this project and implement them into cell culturing techniques by growing induced pluripotent stem cell derived human neural progenitor cells to manipulate genes of interest in these cells, including gene knockout or investigating the transcriptome gene expression profile. The implementation of clustered regularly interspaced short palindromic repeats (CRISPR) technology, particularly CRISPR-Cas9, can be used to edit genes of interest and either express or suppress the gene without altering the gene sequence. By employing this methodology,

we can investigate these genes' role in neuronal development, maturation and differentiation (Qi et al., 2022).

Summary

Collectively, these findings suggest that genetic variants in these genes of interest may serve as important markers for predicting the course of MS and could inform therapeutic strategies aimed at preserving neuronal function and integrity while delaying disease progression. Investigating the effect of neurodegeneration on disease severity is vital, as there are currently no FDA approved drugs targeting this clinical manifestation in patients with MS. This project has highlighted genetic factors, both novel and previously described in the literature, that may influence disease severity by either having a protective effect or increasing susceptibility to neuron loss, likely worsening disease outcomes increasing disability.

This project has established a framework which can be applied to other gene variants frequently identified in GWAS studies, facilitating further investigation of the genes and their retrospective SNPs. We believe that this framework can be applied to further advance the understanding of other genes of interest by first determining their localisation patterns and establishing whether the gene is present in the tissue, such as in neuronal-like cells or key glial cells in both healthy control and diseased tissue samples. This gene expression can then be quantified to determine whether expression levels significantly vary between both cohorts. Using previously known data of clinical manifestations from the diseased cohort, differences in the disease between minor, heterozygous and major allele and whether a polygenic effect of SNPs can be explored. Whilst all these genetic contributions may not be exclusively or directly linked to neuronal functions, it is evident that some play crucial roles in these processes. Understanding the role of genetic SNPs in a MS cohort may be able to aid clinicians with predicting one's disease course which emphasises the role of genetic screening. The variability in genetic contributors and contradictory findings within the literature highlights the complexity of MS and the need for personalised approaches in targeting the disease.

Bibliography

- Abdelhak, A., Weber, M. S., & Tumani, H. (2017). Primary Progressive Multiple Sclerosis: Putting Together the Puzzle. *Frontiers in Neurology*, 8. <https://doi.org/10.3389/fneur.2017.00234>
- Adiele, R. C., & Adiele, C. A. (2019). Metabolic defects in multiple sclerosis. *Mitochondrion*, 44, 7–14. <https://doi.org/10.1016/J.MITO.2017.12.005>
- Albert, M., Barrantes-Freer, A., Lohrberg, M., Antel, J. P., Prineas, J. W., Palkovits, M., Wolff, J. R., Brück, W., & Stadelmann, C. (2017). Synaptic pathology in the cerebellar dentate nucleus in chronic multiple sclerosis. *Brain Pathology*, 27(6), 737–747. <https://doi.org/10.1111/bpa.12450>
- Allen, K. (2024). *Multiple Antigen Labelling in IHC Protocol*. Created using Biorender. Retrieved from <https://biorender.com>
- An, Y., Li, S., Huang, X., Chen, X., Shan, H., & Zhang, M. (2022). The Role of Copper Homeostasis in Brain Disease. *International Journal of Molecular Sciences*, 23(22), 13850. <https://doi.org/10.3390/ijms232213850>
- Andravizou, A., Dardiotis, E., Artemiadis, A., Sokratous, M., Siokas, V., Tsouris, Z., Aloizou, A.-M., Nikolaidis, I., Bakirtzis, C., Tsivgoulis, G., Deretzi, G., Grigoriadis, N., Bogdanos, D. P., & Hadjigeorgiou, G. M. (2019). Brain atrophy in multiple sclerosis: mechanisms, clinical relevance and treatment options. *Autoimmunity Highlights*, 10(1), 7. <https://doi.org/10.1186/s13317-019-0117-5>
- Antel, J., Antel, S., Caramanos, Z., Arnold, D. L., & Kuhlmann, T. (2012). Primary progressive multiple sclerosis: part of the MS disease spectrum or separate disease entity? *Acta Neuropathologica*, 123(5), 627–638. <https://doi.org/10.1007/s00401-012-0953-0>
- Anwar, S., & Yokota, T. (2024). The Dysferlinopathies Conundrum: Clinical Spectra, Disease Mechanism and Genetic Approaches for Treatments. *Biomolecules*, 14(3), 256. <https://doi.org/10.3390/biom14030256>
- Amin, M., & Hersh, C. M. (2023). Updates and Advances in Multiple Sclerosis Neurotherapeutics. *Neurodegenerative Disease Management*, 13(1), 47–70. <https://doi.org/10.2217/nmt-2021-0058>
- Asadi, M., Taghizadeh, S., Kaviani, E., Vakili, O., Taheri-Anganeh, M., Tahamtan, M., & Savardashtaki, A. (2022). Caspase-3: Structure, function, and biotechnological aspects. *Biotechnology and Applied Biochemistry*, 69(4), 1633–1645. <https://doi.org/10.1002/bab.2233>
- Avrutsky, M. I., & Troy, C. M. (2021). Caspase-9: A Multimodal Therapeutic Target With Diverse Cellular Expression in Human Disease. *Frontiers in Pharmacology*, 12. <https://doi.org/10.3389/fphar.2021.701301>

- Baecher-Allan, C., Kaskow, B. J., & Weiner, H. L. (2018). Multiple Sclerosis: Mechanisms and Immunotherapy. *Neuron*, 97(4), 742–768. <https://doi.org/10.1016/j.neuron.2018.01.021>
- Bankhead, P., Loughrey, M. B., Fernández, J. A., Dombrowski, Y., McArt, D. G., Dunne, P. D., McQuaid, S., Gray, R. T., Murray, L. J., Coleman, H. G., James, J. A., Salto-Tellez, M., & Hamilton, P. W. (2017). QuPath: Open source software for digital pathology image analysis. *Scientific Reports*, 7(1), 16878. <https://doi.org/10.1038/s41598-017-17204-5>
- Barrie, W., Yang, Y., Irving-Pease, E. K., Attfield, K. E., Scorrano, G., Jensen, L. T., Armen, A. P., Dimopoulos, E. A., Stern, A., Refoyo-Martinez, A., Pearson, A., Ramsøe, A., Gaunitz, C., Demeter, F., Jørkov, M. L. S., Møller, S. B., Springborg, B., Klassen, L., Hyldgård, I. M., ... Willerslev, E. (2024). Elevated genetic risk for multiple sclerosis emerged in steppe pastoralist populations. *Nature*, 625(7994), 321–328. <https://doi.org/10.1038/s41586-023-06618-z>
- Basaran, B. D., Matthews, P. M., & Bai, W. (2022). New lesion segmentation for multiple sclerosis brain images with imaging and lesion-aware augmentation. *Frontiers in Neuroscience*, 16. <https://doi.org/10.3389/fnins.2022.1007453>
- Bevan, R. J., Evans, R., Griffiths, L., Watkins, L. M., Rees, M. I., Magliozzi, R., Allen, I., McDonnell, G., Kee, R., Naughton, M., Fitzgerald, D. C., Reynolds, R., Neal, J. W., & Howell, O. W. (2018). Meningeal inflammation and cortical demyelination in acute multiple sclerosis. *Annals of Neurology*, 84(6), 829–842. <https://doi.org/10.1002/ana.25365>
- Bierhansl, L., Hartung, H.-P., Aktas, O., Ruck, T., Roden, M., & Meuth, S. G. (2022). Thinking outside the box: non-canonical targets in multiple sclerosis. *Nature Reviews Drug Discovery*, 21(8), 578–600. <https://doi.org/10.1038/s41573-022-00477-5>
- Bjornevik, K., Cortese, M., Healy, B. C., Kuhle, J., Mina, M. J., Leng, Y., Elledge, S. J., Niebuhr, D. W., Scher, A. I., Munger, K. L., & Ascherio, A. (2022). Longitudinal analysis reveals high prevalence of Epstein-Barr virus associated with multiple sclerosis. *Science*, 375(6578), 296–301. <https://doi.org/10.1126/science.abj8222>
- Braun, M., Kirsten, R., Rupp, N. J., Moch, H., Fend, F., Wernert, N., Kristiansen, G., & Perner, S. (2013). Quantification of protein expression in cells and cellular subcompartments on immunohistochemical sections using a computer supported image analysis system. *Histology and Histopathology*, 28(5), 605–610. <https://doi.org/10.14670/HH-28.605>
- Breedon, J. R., Marshall, C. R., Giovannoni, G., van Heel, D. A., Akhtar, S., Anwar, M., Arciero, E., Asgar, O., Ashraf, S., Breen, G., Chung, R., Curtis, C. J., Chaudhary, S., Chowdhury, M., Colligan, G., Deloukas, P., Durham, C., Durrani, F., Eto, F., ... Jacobs, B. M. (2023). Polygenic risk score prediction of multiple sclerosis in individuals of

South Asian ancestry. *Brain Communications*, 5(2).
<https://doi.org/10.1093/braincomms/fcad041>

Brola, W., & Steinborn, B. (2020). Pediatric multiple sclerosis – current status of epidemiology, diagnosis and treatment. *Neurologia i Neurochirurgia Polska*, 54(6), 508–517. <https://doi.org/10.5603/PJNNS.a2020.0069>

Brown, J. W. L., Coles, A., Horakova, D., Havrdova, E., Izquierdo, G., Prat, A., Girard, M., Duquette, P., Trojano, M., Lugaresi, A., Bergamaschi, R., Grammond, P., Alroughani, R., Hupperts, R., McCombe, P., Van Pesch, V., Sola, P., Ferraro, D., Grand'Maison, F., ... Robertson, N. (2019). Association of Initial Disease-Modifying Therapy With Later Conversion to Secondary Progressive Multiple Sclerosis. *JAMA*, 321(2), 175. <https://doi.org/10.1001/jama.2018.20588>

Brownlee, W. J., Tur, C., Manole, A., Eshaghi, A., Prados, F., Miszkiel, K. A., Wheeler-Kingshott, C. A. G., Houlden, H., & Ciccarelli, O. (2023). HLA-DRB1*1501 influences long-term disability progression and tissue damage on MRI in relapse-onset multiple sclerosis. *Multiple Sclerosis Journal*, 29(3), 333–342.
<https://doi.org/10.1177/13524585221130941>

Buscarinu, M. C., Reniè, R., Morena, E., Romano, C., Bellucci, G., Marrone, A., Bigi, R., Salvetti, M., & Ristori, G. (2022). Late-Onset MS: Disease Course and Safety-Efficacy of DMTs. *Frontiers in Neurology*, 13. <https://doi.org/10.3389/fneur.2022.829331>

Calabrese, M., Favaretto, A., Martini, V., & Gallo, P. (2013). Grey matter lesions in MS. *Prion*, 7(1), 20–27. <https://doi.org/10.4161/pri.22580>

Campagna, M. P., Havrdova, E. K., Horakova, D., Izquierdo, G., Matesanz, F., Eichau, S., Lechner-Scott, J., Taylor, B. V., García-Sánchez, M.-I., Alcina, A., van der Walt, A., Butzkueven, H., & Jokubaitis, V. G. (2024). No evidence for association between rs10191329 severity locus and longitudinal disease severity in 1813 relapse-onset multiple sclerosis patients from the MSBase registry. *Multiple Sclerosis Journal*.
<https://doi.org/10.1177/13524585241240406>

Carassiti, D., Altmann, D. R., Petrova, N., Pakkenberg, B., Scaravilli, F., & Schmierer, K. (2018). Neuronal loss, demyelination and volume change in the multiple sclerosis neocortex. *Neuropathology and Applied Neurobiology*, 44(4), 377–390.
<https://doi.org/10.1111/nan.12405>

Cassandri, M., Smirnov, A., Novelli, F., Pitolli, C., Agostini, M., Malewicz, M., Melino, G., & Raschellà, G. (2017). Zinc-finger proteins in health and disease. *Cell Death Discovery*, 3(1), 17071. <https://doi.org/10.1038/cddiscovery.2017.71>

Causevic, M., Dominko, K., Malnar, M., Vidatic, L., Cermak, S., Pigoni, M., Kuhn, P.-H., Colombo, A., Havas, D., Flunkert, S., McDonald, J., Gunnersen, J. M., Hutter-Paier, B., Tahirovic, S., Windisch, M., Krainc, D., Lichtenthaler, S. F., & Hecimovic, S. (2018). BACE1-cleavage of Sez6 and Sez6L is elevated in Niemann-Pick type C disease mouse brains. *PLOS ONE*, 13(7), e0200344. <https://doi.org/10.1371/journal.pone.0200344>

CELLxGENE: A performant, scalable exploration platform for high dimensional sparse matrices. (2021). In *CZI Single-Cell Biology* et al. *bioRxiv*.
<https://doi.org/10.1101/2021.04.05.438318>

CZ CELLxGENE Discover: A single-cell data platform for scalable exploration, analysis, and modeling of aggregated data. (2023). In *CZI Single-Cell Biology* et al. *bioRxiv*.
<https://doi.org/10.1101/2023.10.30.563174>

Charnay, T., Blanck, V., Cerino, M., Bartoli, M., Riccardi, F., Bonello-Palot, N., Pécheux, C., Nguyen, K., Lévy, N., Gorokhova, S., & Krahn, M. (2021). Retrospective analysis and reclassification of DYSF variants in a large French series of dysferlinopathy patients. *Genetics in Medicine*, 23(8), 1574–1577.
<https://doi.org/10.1038/s41436-021-01164-3>

Chen, Y.-C., Liu, Y.-L., Tsai, S.-J., Kuo, P.-H., Huang, S.-S., & Lee, Y.-S. (2019). LRRTM4 and PCSK5 Genetic Polymorphisms as Markers for Cognitive Impairment in A Hypotensive Aging Population: A Genome-Wide Association Study in Taiwan. *Journal of Clinical Medicine*, 8(8), 1124. <https://doi.org/10.3390/jcm8081124>

Cho, N. H., Cheveralls, K. C., Brunner, A.-D., Kim, K., Michaelis, A. C., Raghavan, P., Kobayashi, H., Savy, L., Li, J. Y., Canaj, H., Kim, J. Y. S., Stewart, E. M., Gnann, C., McCarthy, F., Cabrera, J. P., Brunetti, R. M., Chhun, B. B., Dingle, G., Hein, M. Y., ... Leonetti, M. D.(2022). OpenCell: Endogenous tagging for the cartography of human cellular organization. *Science*, 375(6585). <https://doi.org/10.1126/science.abi6983>

Chu, T., Shields, LisaB. E., Zeng, W., Zhang, Y., Wang, Y., Barnes, G., Shields, C., & Cai, J. (2021). Dynamic glial response and crosstalk in demyelination-remyelination and neurodegeneration processes. *Neural Regeneration Research*, 16(7), 1359.
<https://doi.org/10.4103/1673-5374.300975>

Cifelli, A., Arridge, M., Jezard, P., Esiri, M. M., Palace, J., & Matthews, P. M. (2002). Thalamic neurodegeneration in multiple sclerosis. *Annals of Neurology*, 52(5), 650–653. <https://doi.org/10.1002/ana.10326>

Cobo-Calvo, A., Tur, C., Otero-Romero, S., Carbonell-Mirabent, P., Ruiz, M., Pappolla, A., Villaciers Alvarez, J., Vidal-Jordana, A., Arrambide, G., Castilló, J., Galan, I., Rodríguez Barranco, M., Midaglia, L. S., Nos, C., Rodríguez Acevedo, B., Zabalza de Torres, A., Mongay, N., Rio, J., Comabella, M., ... Montalban, X. (2023). Association of Very Early Treatment Initiation With the Risk of Long-term Disability in Patients With a First Demyelinating Event. *Neurology*, 101(13).
<https://doi.org/10.1212/WNL.0000000000207664>

Cohan, S. L., Benedict, R. H. B., Cree, B. A. C., DeLuca, J., Hua, L. H., & Chun, J. (2022). The Two Sides of Siponimod: Evidence for Brain and Immune Mechanisms in Multiple Sclerosis. *CNS Drugs*, 36(7), 703–719. <https://doi.org/10.1007/s40263-022-00927-z>

- Colombo, E., Triolo, D., Bassani, C., Bedogni, F., Di Dario, M., Dina, G., Fredrickx, E., Fermo, I., Martinelli, V., Newcombe, J., Taveggia, C., Quattrini, A., Comi, G., & Farina, C. (2021). Dysregulated copper transport in multiple sclerosis may cause demyelination via astrocytes. *Proceedings of the National Academy of Sciences*, 118(27). <https://doi.org/10.1073/pnas.2025804118>
- Cooze, B. J., Dickerson, M., Loganathan, R., Watkins, L. M., Grounds, E., Pearson, B. R., Bevan, R. J., Morgan, B. P., Magliozzi, R., Reynolds, R., Neal, J. W., & Howell, O. W. (2022). The association between neurodegeneration and local complement activation in the thalamus to progressive multiple sclerosis outcome. *Brain Pathology*, 32(5). <https://doi.org/10.1111/bpa.13054>
- Cooze, B., Neal, J., Vineed, A., Oliveira, J. C., Griffiths, L., Allen, K. H., Hawkins, K., Yadanar, H., Gerhards, K., Farkas, I., Reynolds, R., & Howell, O. (2024). Digital Pathology Identifies Associations between Tissue Inflammatory Biomarkers and Multiple Sclerosis Outcomes. *Cells*, 13(12), 1020. <https://doi.org/10.3390/cells13121020>
- Correale, J., Gaitán, M. I., Ysraelit, M. C., & Fiol, M. P. (2016). Progressive multiple sclerosis: from pathogenic mechanisms to treatment. *Brain*, aww258. <https://doi.org/10.1093/brain/aww258>
- Correale, J., Marrodan, M., & Ysraelit, M. C. (2019). Mechanisms of Neurodegeneration and Axonal Dysfunction in Progressive Multiple Sclerosis. *Biomedicines*, 7(1), 14. <https://doi.org/10.3390/biomedicines7010014>
- Cotsapas, C., & Mitrovic, M. (2018). Genome-wide association studies of multiple sclerosis. *Clinical & Translational Immunology*, 7(6). <https://doi.org/10.1002/cti2.1018>
- Cree, B. A. C., Arnold, D. L., Chataway, J., Chitnis, T., Fox, R. J., Pozo Ramajo, A., Murphy, N., & Lassmann, H. (2021). Secondary Progressive Multiple Sclerosis. *Neurology*, 97(8), 378–388. <https://doi.org/10.1212/WNL.00000000000012323>
- Crowe, A., & Yue, W. (2019). Semi-quantitative Determination of Protein Expression Using Immunohistochemistry Staining and Analysis: An Integrated Protocol. *BIO-PROTOCOL*, 9(24). <https://doi.org/10.21769/BioProtoc.3465>
- Cunnea, P., Mháille, A. N., McQuaid, S., Farrell, M., McMahon, J., & FitzGerald, U. (2011). Expression profiles of endoplasmic reticulum stress-related molecules in demyelinating lesions and multiple sclerosis. *Multiple Sclerosis Journal*, 17(7), 808–818. <https://doi.org/10.1177/1352458511399114>
- de Bie, P., van de Sluis, B., Burstein, E., Duran, K. J., Berger, R., Duckett, C. S., Wijmenga, C., & Klomp, L. W. J. (2006). Characterization of COMMD protein–protein interactions in NF-κB signalling. *Biochemical Journal*, 398(1), 63–71. <https://doi.org/10.1042/BJ20051664>

DeLuca, G. C., Alterman, R., Martin, J. L., Mittal, A., Blundell, S., Bird, S., Beale, H., Hong, L. S., & Esiri, M. M. (2013). Casting light on multiple sclerosis heterogeneity: the role of HLA-DRB1 on spinal cord pathology. *Brain*, 136(4), 1025–1034. <https://doi.org/10.1093/brain/awt031>

Dimitriou, N. G., Meuth, S. G., Martinez-Lapiscina, E. H., Albrecht, P., & Menge, T. (2023). Treatment of Patients with Multiple Sclerosis Transitioning Between Relapsing and Progressive Disease. *CNS Drugs*, 37(1), 69–92. <https://doi.org/10.1007/s40263-022-00977-3>

Doshi, A., & Chataway, J. (2016). Multiple sclerosis, a treatable disease. *Clinical Medicine (London, England)*, 16(Suppl 6), s53–s59. <https://doi.org/10.7861/clinmedicine.16-6-s53>

Duncan, G. J., Simkins, T. J., & Emery, B. (2021). Neuron-Oligodendrocyte Interactions in the Structure and Integrity of Axons. *Frontiers in Cell and Developmental Biology*, 9. <https://doi.org/10.3389/fcell.2021.653101>

Evans, C. S., & Holzbaur, E. L. F. (2019). Autophagy and mitophagy in ALS. *Neurobiology of Disease*, 122, 35–40. <https://doi.org/10.1016/j.nbd.2018.07.005>

Faissner, S., & Gold, R. (2019). Progressive multiple sclerosis: latest therapeutic developments and future directions. *Therapeutic Advances in Neurological Disorders*, 12, 175628641987832. <https://doi.org/10.1177/1756286419878323>

Fama, R., & Sullivan, E. V. (2015). Thalamic structures and associated cognitive functions: Relations with age and aging. *Neuroscience & Biobehavioral Reviews*, 54, 29–37. <https://doi.org/10.1016/j.neubiorev.2015.03.008>

Fan, Y., Zhang, L., Sun, Y., Yang, M., Wang, X., Wu, X., Huang, W., Chen, L., Pan, S., & Guan, J. (2020). Expression profile and bioinformatics analysis of COMMD10 in BALB/C mice and human. *Cancer Gene Therapy*, 27(3–4), 216–225. <https://doi.org/10.1038/s41417-019-0087-9>

Favorova, O. O., Bashinskaia, V. V., Kulakova, O. G., Favorov, A. V., & Boiko, A. N. (2014). Genome-wide association study as a method for genetic architecture analysis in polygenic diseases (by the example of multiple sclerosis). *Molekuliarnaia Biologiya*, 48(4), 573–586. <https://pubmed.ncbi.nlm.nih.gov/25842843/>

Fiddes, I. T., Lodewijk, G. A., Mooring, M., Bosworth, C. M., Ewing, A. D., Mantalas, G. L., Novak, A. M., van den Bout, A., Bishara, A., Rosenkrantz, J. L., Lorig-Roach, R., Field, A. R., Haeussler, M., Russo, L., Bhaduri, A., Nowakowski, T. J., Pollen, A. A., Dougherty, M. L., Nettle, X., ... Haussler, D. (2018). Human-Specific NOTCH2NL Genes Affect Notch Signaling and Cortical Neurogenesis. *Cell*, 173(6), 1356–1369.e22. <https://doi.org/10.1016/j.cell.2018.03.051>

Filippi, M., Preziosa, P., Banwell, B. L., Barkhof, F., Ciccarelli, O., De Stefano, N., Geurts, J. J. G., Paul, F., Reich, D. S., Toosy, A. T., Traboulsee, A., Wattjes, M. P.,

- Yousry, T. A., Gass, A., Lubetzki, C., Weinshenker, B. G., & Rocca, M. A. (2019). Assessment of lesions on magnetic resonance imaging in multiple sclerosis: practical guidelines. *Brain*, 142(7), 1858–1875. <https://doi.org/10.1093/brain/awz144>
- Filippi, M., Preziosa, P., Barkhof, F., Chard, D. T., De Stefano, N., Fox, R. J., Gasperini, C., Kappos, L., Montalban, X., Moraal, B., Reich, D. S., Rovira, À., Toosy, A. T., Traboulsee, A., Weinshenker, B. G., Zeydan, B., Banwell, B. L., & Rocca, M. A. (2021). Diagnosis of Progressive Multiple Sclerosis From the Imaging Perspective. *JAMA Neurology*, 78(3), 351. <https://doi.org/10.1001/jamaneurol.2020.4689>
- Filippi, M., & Rocca, M. A. (2019). Classifying silent progression in relapsing–remitting MS. *Nature Reviews Neurology*, 15(6), 315–316. <https://doi.org/10.1038/s41582-019-0199-8>
- Fitzgerald, K. C., Kim, K., Smith, M. D., Aston, S. A., Fioravante, N., Rothman, A. M., Krieger, S., Cofield, S. S., Kimbrough, D. J., Bhargava, P., Saidha, S., Whartenby, K. A., Green, A. J., Mowry, E. M., Cutter, G. R., Lublin, F. D., Baranzini, S. E., De Jager, P. L., & Calabresi, P. A. (2019). Early complement genes are associated with visual system degeneration in multiple sclerosis. *Brain*, 142(9), 2722–2736. <https://doi.org/10.1093/brain/awz188>
- Ford, H. (2020). Clinical presentation and diagnosis of multiple sclerosis. *Clinical Medicine*, 20(4), 380–383. <https://doi.org/10.7861/clinmed.2020-0292>
- Gasperi, C., Wiltgen, T., McGinnis, J., Cerri, S., Moridi, T., Ouellette, R., Pukaj, A., Voon, C., Bafligil, C., Lauerer, M., Andlauer, T. F. M., Held, F., Aly, L., Shchetynsky, K., Stridh, P., Harroud, A., Wiestler, B., Kirschke, J. S., Zimmer, C., ... Mühlau, M. (2023). A Genetic Risk Variant for Multiple Sclerosis Severity is Associated with Brain Atrophy. *Annals of Neurology*, 94(6), 1080–1085. <https://doi.org/10.1002/ana.26807>
- Ghasemi, N., Razavi, S., & Nikzad, E. (2017). Multiple Sclerosis: Pathogenesis, Symptoms, Diagnoses and Cell-Based Therapy. *Cell Journal*, 19(1), 1–10. <https://doi.org/10.22074/cellj.2016.4867>
- Gong, H., Yang, X., An, L., Zhang, W., Liu, X., Shu, L., & Yang, L. (2024). PCSK5 downregulation promotes the inhibitory effect of andrographolide on glioblastoma through regulating STAT3. *Molecular and Cellular Biochemistry*. <https://doi.org/10.1007/s11010-024-04977-3>
- Goris, A., Vandebergh, M., McCauley, J. L., Saarela, J., & Cotsapas, C. (2022). Genetics of multiple sclerosis: lessons from polygenicity. *The Lancet Neurology*, 21(9), 830–842. [https://doi.org/10.1016/S1474-4422\(22\)00255-1](https://doi.org/10.1016/S1474-4422(22)00255-1)
- Gourraud, P., Harbo, H. F., Hauser, S. L., & Baranzini, S. E. (2012). The genetics of multiple sclerosis: an up-to-date review. *Immunological Reviews*, 248(1), 87–103. <https://doi.org/10.1111/j.1600-065X.2012.01134.x>

Gozzo, L., Romano, G. L., Brancati, S., Longo, L., Vitale, D. C., & Drago, F. (2023). The therapeutic value of treatment for multiple sclerosis: analysis of health technology assessments of three European countries. *Frontiers in Pharmacology*, 14. <https://doi.org/10.3389/fphar.2023.1169400>

Gratton, C., Nomura, E. M., Pérez, F., & D'Esposito, M. (2012). Focal Brain Lesions to Critical Locations Cause Widespread Disruption of the Modular Organization of the Brain. *Journal of Cognitive Neuroscience*, 24(6), 1275–1285. https://doi.org/10.1162/jocn_a_00222

Gray, E., Amjad, A., Robertson, J., Beveridge, J., Scott, S., Peryer, G., Braisher, M., Pugh, C., Peres, S., Marrie, R. A., Sormani, M. P., & Chataway, J. (2023). Enhancing involvement of people with multiple sclerosis in clinical trial design. *Multiple Sclerosis Journal*, 29(9), 1162–1173. <https://doi.org/10.1177/13524585231189678>

Griffiths, L., Reynolds, R., Evans, R., Bevan, R. J., Rees, M. I., Gveric, D., Neal, J. W., & Howell, O. W. (2020). Substantial subpial cortical demyelination in progressive multiple sclerosis: have we underestimated the extent of cortical pathology? *Neuroimmunology and Neuroinflammation*. <https://doi.org/10.20517/2347-8659.2019.21>

Harroud, A., Stridh, P., McCauley, J. L., Saarela, J., van den Bosch, A. M. R., Engelenburg, H. J., Beecham, A. H., Alfredsson, L., Alikhani, K., Amezcua, L., Andlauer, T. F. M., Ban, M., Barcellos, L. F., Barizzzone, N., Berge, T., Berthele, A., Bittner, S., Bos, S. D., Briggs, F. B. S., ... Stefánsson, K. (2023). Locus for severity implicates CNS resilience in progression of multiple sclerosis. *Nature*, 619(7969), 323–331. <https://doi.org/10.1038/s41586-023-06250-x>

Hatanaka, Y., Zhu, Y., Torigoe, M., Kits, Y., & Murakami, F. (2016). From migration to settlement: the pathways, migration modes and dynamics of neurons in the developing brain. *Proceedings of the Japan Academy, Series B*, 92(1), 1–19. <https://doi.org/10.2183/pjab.92.1>

Hauser, S. L., & Cree, B. A. C. (2020). Treatment of Multiple Sclerosis: A Review. *The American Journal of Medicine*, 133(12), 1380-1390.e2. <https://doi.org/10.1016/j.amjmed.2020.05.049>

Hawkes, C. H., Giovannoni, G., Lechner-Scott, J., & Levy, M. (2020). Is the incidence of multiple sclerosis really increasing? *Multiple Sclerosis and Related Disorders*, 45, 102527. <https://doi.org/10.1016/j.msard.2020.102527>

Hoac, B., Susan-Resiga, D., Essalmani, R., Marcinkiewicz, E., Seidah, N. G., & McKee, M. D. (2018). Osteopontin as a novel substrate for the proprotein convertase 5/6 (PCSK5) in bone. *Bone*, 107, 45–55. <https://doi.org/10.1016/j.bone.2017.11.002>

Hornsey, M. A., Laval, S. H., Barresi, R., Lochmüller, H., & Bushby, K. (2013). Muscular dystrophy in dysferlin-deficient mouse models. *Neuromuscular Disorders*, 23(5), 377–387. <https://doi.org/10.1016/j.nmd.2013.02.004>

Howell, O. W., Schulz-Trieglaff, E. K., Carassiti, D., Gentleman, S. M., Nicholas, R., Roncaroli, F., & Reynolds, R. (2015). Extensive grey matter pathology in the cerebellum in multiple sclerosis is linked to inflammation in the subarachnoid space. *Neuropathology and Applied Neurobiology*, 41(6), 798–813. <https://doi.org/10.1111/nan.12199>

Huang, J. K., Jarjour, A. A., Nait Oumesmar, B., Kerninon, C., Williams, A., Krezel, W., Kagechika, H., Bauer, J., Zhao, C., Baron-Van Evercooren, A., Chambon, P., Ffrench-Constant, C., & Franklin, R. J. M. (2011). Retinoid X receptor gamma signaling accelerates CNS remyelination. *Nature Neuroscience*, 14(1), 45–53. <https://doi.org/10.1038/nn.2702>

Huang, W.-J., Chen, W.-W., & Zhang, X. (2017). Multiple sclerosis: Pathology, diagnosis and treatments. *Experimental and Therapeutic Medicine*, 13(6), 3163–3166. <https://doi.org/10.3892/etm.2017.4410>

Huisman, E., Papadimitropoulou, K., Jarrett, J., Bending, M., Firth, Z., Allen, F., & Adlard, N. (2017). Systematic literature review and network meta-analysis in highly active relapsing–remitting multiple sclerosis and rapidly evolving severe multiple sclerosis. *BMJ Open*, 7(3), e013430. <https://doi.org/10.1136/bmjopen-2016-013430>

Huttlin, E. L., Bruckner, R. J., Navarrete-Perea, J., Cannon, J. R., Baltier, K., Gebreab, F., Gygi, M. P., Thornock, A., Zarraga, G., Tam, S., Szpyt, J., Gassaway, B. M., Panov, A., Parzen, H., Fu, S., Golbazi, A., Maenpaa, E., Stricker, K., Guha Thakurta, S., ... Gygi, S. P. (2021). Dual proteome-scale networks reveal cell-specific remodeling of the human interactome. *Cell*, 184(11), 3022–3040.e28. <https://doi.org/10.1016/j.cell.2021.04.011>

Hwang, K., Bertolero, M. A., Liu, W. B., & D’Esposito, M. (2017). The Human Thalamus Is an Integrative Hub for Functional Brain Networks. *The Journal of Neuroscience*, 37(23), 5594–5607. <https://doi.org/10.1523/JNEUROSCI.0067-17.2017>

Inojosa, H., Proschmann, U., Akgün, K., & Ziemssen, T. (2021). A focus on secondary progressive multiple sclerosis (SPMS): challenges in diagnosis and definition. *Journal of Neurology*, 268(4), 1210–1221. <https://doi.org/10.1007/s00415-019-09489-5>

Ito, H., Nozaki, K., Sakimura, K., Abe, M., Yamawaki, S., & Aizawa, H. (2021). Activation of proprotein convertase in the mouse habenula causes depressive-like behaviors through remodeling of extracellular matrix. *Neuropsychopharmacology*, 46(2), 442–454. <https://doi.org/10.1038/s41386-020-00843-0>

Ivanova, A., Smirnikhina, S., & Lavrov, A. (2022). Dysferlinopathies: Clinical and genetic variability. *Clinical Genetics*, 102(6), 465–473. <https://doi.org/10.1111/cge.14216>

Jacobs, B. M., Schalk, L., Tregaskis-Daniels, E., Tank, P., Hoque, S., Peter, M., Tuite-Dalton, K., Witts, J., Bove, R., & Dobson, R. (2024). The relationship between

ethnicity and multiple sclerosis characteristics in the United Kingdom: A UK MS Register study. *Multiple Sclerosis Journal*, 30(11–12), 1544–1555.
<https://doi.org/10.1177/13524585241277018>

Jakimovski, D., Bittner, S., Zivadinov, R., Morrow, S. A., Benedict, R. H., Zipp, F., & Weinstock-Guttman, B. (2024). Multiple sclerosis. In *The Lancet* (Vol. 403, pp. 183–202). [https://doi.org/10.1016/S0140-6736\(23\)01473-3](https://doi.org/10.1016/S0140-6736(23)01473-3)

Jakimovski, D., Guan, Y., Ramanathan, M., Weinstock-Guttman, B., & Zivadinov, R. (2019). Lifestyle-based Modifiable Risk Factors in Multiple Sclerosis: Review of Experimental and Clinical Findings. *Neurodegenerative Disease Management*, 9(3), 149–172. <https://doi.org/10.2217/nmt-2018-0046>

Jimshelishvili, S., & Dididze, M. (2024). *Neuroanatomy, Cerebellum*. In *Statpearls*. Retrieved from <https://www.ncbi.nlm.nih.gov/pubmed/30844194>

Jokubaitis, V. G., & Butzkueven, H. (2023). A genetic basis for the severity of multiple sclerosis. *The Lancet Neurology*, 22(10), 879–881. [https://doi.org/10.1016/S1474-4422\(23\)00319-8](https://doi.org/10.1016/S1474-4422(23)00319-8)

Jokubaitis, V. G., Campagna, M. P., Ibrahim, O., Stankovich, J., Kleinova, P., Matesanz, F., Hui, D., Eichau, S., Slee, M., Lechner-Scott, J., Lea, R., Kilpatrick, T. J., Kalincik, T., De Jager, P. L., Beecham, A., McCauley, J. L., Taylor, B. V, Vucic, S., Laverick, L., ... Butzkueven, H. (2023). Not all roads lead to the immune system: the genetic basis of multiple sclerosis severity. *Brain*, 146(6), 2316–2331.
<https://doi.org/10.1093/brain/awac449>

Jokubaitis, V. G., Pia Campagna, M., Ibrahim, O., Stankovich, J., Matesanz, F., Hui, D., Eichau, S., Slee, M., Lechner, J., Lea, R., Kilpatrick, T. J., Kalincik, T., De Jager, P. L., Beecham, A., McCauley, J. L., Taylor, B. V, Vucic, S., Vodehnalova, K., García-Sánchez, M.-I., ... Butzkueven, H. (2022). Not all roads lead to the immune system: the genetic basis of multiple sclerosis severity. *Brain*, 2316–2331.
<https://doi.org/10.1093/brain/awac449/6854441>

Jonkman, L. E., Soriano, A. L., Amor, S., Barkhof, F., van der Valk, P., Vrenken, H., & Geurts, J. J. G. (2015). Can MS lesion stages be distinguished with MRI? A postmortem MRI and histopathology study. *Journal of Neurology*, 262(4), 1074–1080. <https://doi.org/10.1007/s00415-015-7689-4>

Kalafatakis, I., & Karagogeos, D. (2021). Oligodendrocytes and Microglia: Key Players in Myelin Development, Damage and Repair. *Biomolecules*, 11(7), 1058.
<https://doi.org/10.3390/biom11071058>

Kalincik, T. (2015). Multiple Sclerosis Relapses: Epidemiology, Outcomes and Management. A Systematic Review. *Neuroepidemiology*, 44(4), 199–214.
<https://doi.org/10.1159/000382130>

- Kalincik, T., Buzzard, K., Jokubaitis, V., Trojano, M., Duquette, P., Izquierdo, G., Girard, M., Lugaresi, A., Grammond, P., Grand'Maison, F., Oreja-Guevara, C., Boz, C., Hupperts, R., Petersen, T., Giuliani, G., Iuliano, G., Lechner-Scott, J., Barnett, M., Bergamaschi, R., ... Butzkueven, H. (2014). Risk of relapse phenotype recurrence in multiple sclerosis. *Multiple Sclerosis Journal*, 20(11), 1511–1522. <https://doi.org/10.1177/1352458514528762>
- Kappos, L., Bar-Or, A., Cree, B. A. C., Fox, R. J., Giovannoni, G., Gold, R., Vermersch, P., Arnold, D. L., Arnould, S., Scherz, T., Wolf, C., Wallström, E., Dahlke, F., Achiron, A., Achtnichts, L., Agan, K., Akman-Demir, G., Allen, A. B., Antel, J. P., ... Ziemssen, T. (2018). Siponimod versus placebo in secondary progressive multiple sclerosis (EXPAND): a double-blind, randomised, phase 3 study. *The Lancet*, 391(10127), 1263–1273. [https://doi.org/10.1016/S0140-6736\(18\)30475-6](https://doi.org/10.1016/S0140-6736(18)30475-6)
- Karlsson, M., Zhang, C., Méar, L., Zhong, W., Digre, A., Katona, B., Sjöstedt, E., Butler, L., Odeberg, J., Dusart, P., Edfors, F., Oksvold, P., von Feilitzen, K., Zwahlen, M., Arif, M., Altay, O., Li, X., Ozcan, M., Mardinoglu, A., ... Lindskog, C. (2021). A single-cell type transcriptomics map of human tissues. *Science Advances*, 7(31). <https://doi.org/10.1126/sciadv.abh2169>
- Kee, R., Naughton, M., McDonnell, G. V., Howell, O. W., & Fitzgerald, D. C. (2022). A Review of Compartmentalised Inflammation and Tertiary Lymphoid Structures in the Pathophysiology of Multiple Sclerosis. *Biomedicines*, 10(10), 2604. <https://doi.org/10.3390/biomedicines10102604>
- Klaver, R., De Vries, H. E., Schenk, G. J., & Geurts, J. J. G. (2013). Grey matter damage in multiple sclerosis. *Prion*, 7(1), 66–75. <https://doi.org/10.4161/pri.23499>
- Klineova, S., & Lublin, F. D. (2018). Clinical Course of Multiple Sclerosis. *Cold Spring Harbor Perspectives in Medicine*, 8(9), a028928. <https://doi.org/10.1101/cshperspect.a028928>
- Knowles, S., Middleton, R., Cooze, B., Farkas, I., Leung, Y. Y., Allen, K., Winslade, M., Owen, D. R. J., Magliozzi, R., Reynolds, R., Neal, J. W., Pearson, O., Nicholas, R., Pickrell, W. O., & Howell, O. W. (2024). Comparing the Pathology, Clinical, and Demographic Characteristics of Younger and Older-Onset Multiple Sclerosis. *Annals of Neurology*, 95(3), 471–486. <https://doi.org/10.1002/ana.26843>
- Kreft, K. L., Uzochukwu, E., Loveless, S., Willis, M., Wynford-Thomas, R., Harding, K. E., Holmans, P., Lawton, M., Tallantyre, E. C., & Robertson, N. P. (2024). Relevance of Multiple Sclerosis Severity Genotype in Predicting Disease Course: A Real-World Cohort. *Annals of Neurology*, 95(3), 459–470. <https://doi.org/10.1002/ana.26831>
- Krieger, S. C., Antoine, A., & Sumowski, J. F. (2022). EDSS 0 is not normal: Multiple sclerosis disease burden below the clinical threshold. *Multiple Sclerosis Journal*, 28(14), 2299–2303. <https://doi.org/10.1177/13524585221108297>

- Kuhlmann, T., Moccia, M., Coetzee, T., Cohen, J. A., Correale, J., Graves, J., Marrie, R. A., Montalban, X., Yong, V. W., Thompson, A. J., Reich, D. S., Amato, M. P., Banwell, B., Barkhof, F., Chataway, J., Chitnis, T., Comi, G., Derfuss, T., Finlayson, M., ... Waubant, E. (2023). Multiple sclerosis progression: time for a new mechanism-driven framework. *The Lancet Neurology*, 22(1), 78–88. [https://doi.org/10.1016/S1474-4422\(22\)00289-7](https://doi.org/10.1016/S1474-4422(22)00289-7)
- Kutzelnigg, A., Lucchinetti, C. F., Stadelmann, C., Brück, W., Rauschka, H., Bergmann, M., Schmidbauer, M., Parisi, J. E., & Lassmann, H. (2005). Cortical demyelination and diffuse white matter injury in multiple sclerosis. *Brain*, 128(11), 2705–2712. <https://doi.org/10.1093/brain/awh641>
- Lassmann, H. (2014). Mechanisms of white matter damage in multiple sclerosis. *Glia*, 62(11), 1816–1830. <https://doi.org/10.1002/glia.22597>
- Lassmann, H. (2018). Multiple Sclerosis Pathology. *Cold Spring Harbor Perspectives in Medicine*, 8(3), a028936. <https://doi.org/10.1101/cshperspect.a028936>
- Lassmann, H., van Horssen, J., & Mahad, D. (2012). Progressive multiple sclerosis: pathology and pathogenesis. *Nature Reviews Neurology*, 8(11), 647–656. <https://doi.org/10.1038/nrneurol.2012.168>
- Lebrun-Frénay, C., Okuda, D. T., Siva, A., Landes-Chateau, C., Azevedo, C. J., Mondot, L., Carra-Dallière, C., Zephir, H., Louapre, C., Durand-Dubief, F., Le Page, E., Bensa, C., Ruet, A., Ciron, J., Laplaud, D. A., Casez, O., Mathey, G., de Seze, J., Zeydan, B., ... Kantarci, O. H. (2023). The radiologically isolated syndrome: revised diagnostic criteria. *Brain*, 146(8), 3431–3443. <https://doi.org/10.1093/brain/awad073>
- Lennon, N. J., Kottyan, L. C., Kachulis, C., Abul-Husn, N. S., Arias, J., Belbin, G., Below, J. E., Berndt, S. I., Chung, W. K., Cimino, J. J., Clayton, E. W., Connolly, J. J., Crosslin, D. R., Dikilitas, O., Velez Edwards, D. R., Feng, Q., Fisher, M., Freimuth, R. R., Ge, T., ... Kenny, E. E. (2024). Selection, optimization and validation of ten chronic disease polygenic risk scores for clinical implementation in diverse US populations. *Nature Medicine*, 30(2), 480–487. <https://doi.org/10.1038/s41591-024-02796-z>
- Lewis, C. M., & Vassos, E. (2020). Polygenic risk scores: from research tools to clinical instruments. *Genome Medicine*, 12(1), 44. <https://doi.org/10.1186/s13073-020-00742-5>
- Lin, W., & Popko, B. (2009). Endoplasmic reticulum stress in disorders of myelinating cells. *Nature Neuroscience*, 12(4), 379–385. <https://doi.org/10.1038/nn.2273>
- Lu, T., Zhou, S., Wu, H., Forgetta, V., Greenwood, C. M. T., & Richards, J. B. (2021). Individuals with common diseases but with a low polygenic risk score could be prioritized for rare variant screening. *Genetics in Medicine*, 23(3), 508–515. <https://doi.org/10.1038/s41436-020-01007-7>

Lublin, F. D. (2014). New Multiple Sclerosis Phenotypic Classification. *European Neurology*, 72(Suppl. 1), 1–5. <https://doi.org/10.1159/000367614>

Lublin, F. D., Häring, D. A., Ganjgahi, H., Ocampo, A., Hatami, F., Čuklina, J., Aarden, P., Dahlke, F., Arnold, D. L., Wiendl, H., Chitnis, T., Nichols, T. E., Kieseier, B. C., & Bermel, R. A. (2022). How patients with multiple sclerosis acquire disability. *Brain*, 145(9), 3147–3161. <https://doi.org/10.1093/brain/awac016>

Lublin, F. D., Reingold, S. C., Cohen, J. A., Cutter, G. R., Sørensen, P. S., Thompson, A. J., Wolinsky, J. S., Balcer, L. J., Banwell, B., Barkhof, F., Bebo, B., Calabresi, P. A., Clanet, M., Comi, G., Fox, R. J., Freedman, M. S., Goodman, A. D., Inglese, M., Kappos, L., ... Polman, C. H. (2014). Defining the clinical course of multiple sclerosis. *Neurology*, 83(3), 278–286. <https://doi.org/10.1212/WNL.0000000000000560>

Lucchinetti, C. F., Popescu, B. F. G., Bunyan, R. F., Moll, N. M., Roemer, S. F., Lassmann, H., Brück, W., Parisi, J. E., Scheithauer, B. W., Giannini, C., Weigand, S. D., Mandrekar, J., & Ransohoff, R. M. (2011). Inflammatory Cortical Demyelination in Early Multiple Sclerosis. *New England Journal of Medicine*, 365(23), 2188–2197. <https://doi.org/10.1056/NEJMoa1100648>

Luchetti, S., Fransen, N. L., van Eden, C. G., Ramaglia, V., Mason, M., & Huitinga, I. (2018). Progressive multiple sclerosis patients show substantial lesion activity that correlates with clinical disease severity and sex: a retrospective autopsy cohort analysis. *Acta Neuropathologica*, 135(4), 511–528. <https://doi.org/10.1007/s00401-018-1818-y>

Lunde, H. M. B., Assmus, J., Myhr, K.-M., Bø, L., & Grytten, N. (2017). Survival and cause of death in multiple sclerosis: a 60-year longitudinal population study. *Journal of Neurology, Neurosurgery & Psychiatry*, 88(8), 621–625. <https://doi.org/10.1136/jnnp-2016-315238>

Ma, Q., Shams, H., Didonna, A., Baranzini, S. E., Cree, B. A. C., Hauser, S. L., Henry, R. G., & Oksenberg, J. R. (2023). Integration of epigenetic and genetic profiles identifies multiple sclerosis disease-critical cell types and genes. *Communications Biology*, 6(1), 342. <https://doi.org/10.1038/s42003-023-04713-5>

Macaron, G., & Ontaneda, D. (2019). Diagnosis and Management of Progressive Multiple Sclerosis. *Biomedicines*, 7(3), 56. <https://doi.org/10.3390/biomedicines7030056>

Madireddy, L., Patsopoulos, N. A., Cotsapas, C., Bos, S. D., Beecham, A., McCauley, J., Kim, K., Jia, X., Santaniello, A., Caillier, S. J., Andlauer, T. F. M., Barcellos, L. F., Berge, T., Bernardinelli, L., Martinelli-Boneschi, F., Booth, D. R., Briggs, F., Celius, E. G., Comabella, M., ... Baranzini, S. E. (2019). A systems biology approach uncovers cell-specific gene regulatory effects of genetic associations in multiple sclerosis. *Nature Communications*, 10(1). <https://doi.org/10.1038/s41467-019-09773-y>

- Magaki, S., Hojat, S. A., Wei, B., So, A., & Yong, W. H. (2019). An Introduction to the Performance of Immunohistochemistry. *Methods in Molecular Biology (Clifton, N.J.)*, 1897, 289–298. https://doi.org/10.1007/978-1-4939-8935-5_25
- Magliozzi, R., Howell, O. W., Calabrese, M., & Reynolds, R. (2023). Meningeal inflammation as a driver of cortical grey matter pathology and clinical progression in multiple sclerosis. *Nature Reviews Neurology*, 19(8), 461–476. <https://doi.org/10.1038/s41582-023-00838-7>
- Magliozzi, R., Howell, O. W., Reeves, C., Roncaroli, F., Nicholas, R., Serafini, B., Aloisi, F., & Reynolds, R. (2010). A Gradient of neuronal loss and meningeal inflammation in multiple sclerosis. *Annals of Neurology*, 68(4), 477–493. <https://doi.org/10.1002/ana.22230>
- Magliozzi, R., Reynolds, R., & Calabrese, M. (2018). MRI of cortical lesions and its use in studying their role in MS pathogenesis and disease course. *Brain Pathology*, 28(5), 735–742. <https://doi.org/10.1111/bpa.12642>
- Magyari, M., & Sorensen, P. S. (2020). Comorbidity in Multiple Sclerosis. *Frontiers in Neurology*, 11. <https://doi.org/10.3389/fneur.2020.00851>
- Mahad, D. H., Trapp, B. D., & Lassmann, H. (2015). Pathological mechanisms in progressive multiple sclerosis. *The Lancet Neurology*, 14(2), 183–193. [https://doi.org/10.1016/S1474-4422\(14\)70256-X](https://doi.org/10.1016/S1474-4422(14)70256-X)
- Mahajan, K. R., Nakamura, K., Cohen, J. A., Trapp, B. D., & Ontaneda, D. (2020). Intrinsic and Extrinsic Mechanisms of Thalamic Pathology in Multiple Sclerosis. *Annals of Neurology*, 88(1), 81–92. <https://doi.org/10.1002/ana.25743>
- Manouchehri, N., Shirani, A., Salinas, V. H., Tardo, L., Hussain, R. Z., Pitt, D., & Stuve, O. (2022). Clinical trials in multiple sclerosis: past, present, and future. *Neurologia i Neurochirurgia Polska*, 56(3), 228–235. <https://doi.org/10.5603/PJNNS.a2022.0041>
- Margiotta, A. (2021). Role of SNAREs in Neurodegenerative Diseases. *Cells*, 10(5), 991. <https://doi.org/10.3390/cells10050991>
- Martin, J. E., Raffel, J., & Nicholas, R. (2016). Progressive Dwindling in Multiple Sclerosis: An Opportunity to Improve Care. *PLOS ONE*, 11(7), e0159210. <https://doi.org/10.1371/journal.pone.0159210>
- McMahon, J., McQuaid, S., Reynolds, R., & FitzGerald, U. (2012). Increased expression of ER stress- and hypoxia-associated molecules in grey matter lesions in multiple sclerosis. *Multiple Sclerosis Journal*, 18(10), 1437–1447. <https://doi.org/10.1177/1352458512438455>
- Mey, G. M., Mahajan, K. R., & DeSilva, T. M. (2023). Neurodegeneration in multiple sclerosis. *WIREs Mechanisms of Disease*, 15(1). <https://doi.org/10.1002/wsbm.1583>

Mháille, A. N., McQuaid, S., Windebank, A., Cunnea, P., McMahon, J., Samali, A., & FitzGerald, U. (2008). Increased Expression of Endoplasmic Reticulum Stress-Related Signaling Pathway Molecules in Multiple Sclerosis Lesions. *Journal of Neuropathology & Experimental Neurology*, 67(3), 200–211. <https://doi.org/10.1097/NEN.0b013e318165b239>

Milo, R., & Miller, A. (2014). Revised diagnostic criteria of multiple sclerosis. *Autoimmunity Reviews*, 13(4–5), 518–524. <https://doi.org/10.1016/j.autrev.2014.01.012>

Minagar, A., Barnett, M. H., Benedict, R. H. B., Pelletier, D., Pirko, I., Sahraian, M. A., Frohman, E., & Zivadinov, R. (2013). The thalamus and multiple sclerosis. *Neurology*, 80(2), 210–219. <https://doi.org/10.1212/WNL.0b013e31827b910b>

MS Society. (2020). *MS in the UK*. MS Prevalence Report. Retrieved September 22, 2024, from <https://www.mssociety.org.uk/what-we-do/our-work/our-evidence/ms-in-the-uk>

MS Society. (2022, February 7). *Disease Modifying Therapies*. MS Society. <https://www.mssociety.org.uk/living-with-ms/treatments-and-therapies/disease-modifying-therapies>

Müller, S. A., Shmueli, M. D., Feng, X., Tüshaus, J., Schumacher, N., Clark, R., Smith, B. E., Chi, A., Rose-John, S., Kennedy, M. E., & Lichtenthaler, S. F. (2023). The Alzheimer's disease-linked protease BACE1 modulates neuronal IL-6 signaling through shedding of the receptor gp130. *Molecular Neurodegeneration*, 18(1), 13. <https://doi.org/10.1186/s13024-023-00596-6>

Mycko, M. P., & Baranzini, S. E. (2020). microRNA and exosome profiling in multiple sclerosis. *Multiple Sclerosis Journal*, 26(5), 599–604. <https://doi.org/10.1177/1352458519879303>

Nash, A., Aumann, T. D., Pigoni, M., Lichtenthaler, S. F., Takeshima, H., Munro, K. M., & Gunnarsen, J. M. (2020). Lack of Sez6 Family Proteins Impairs Motor Functions, Short-Term Memory, and Cognitive Flexibility and Alters Dendritic Spine Properties. *Cerebral Cortex*, 30(4), 2167–2184. <https://doi.org/10.1093/cercor/bhz230>

National Center for Biotechnology Information (NCBI). (1988). *NCBI*. Bethesda, MD: National Library of Medicine (US). Retrieved August 13th, 2024, from <https://www.ncbi.nlm.nih.gov/>

National Institute for Health and Care Excellence. (2019). *Ocrelizumab for treating primary progressive multiple sclerosis*. <https://www.nice.org.uk/guidance/ta585>

National Institute of Health and Care Excellence. (2022). *Multiple sclerosis in adults: management*. <https://www.nice.org.uk/guidance/ng220>

Ní Fhlathartaigh, M., McMahon, J., Reynolds, R., Connolly, D., Higgins, E., Counihan, T., & FitzGerald, U. (2013). Calreticulin and other components of endoplasmic

reticulum stress in rat and human inflammatory demyelination. *Acta Neuropathologica Communications*, 1(1), 37. <https://doi.org/10.1186/2051-5960-1-37>

Nishanth, K., Tariq, E., Nzvere, F. P., Miqdad, M., & Cancarevic, I. (2020). Role of Smoking in the Pathogenesis of Multiple Sclerosis: A Review Article. *Cureus*. <https://doi.org/10.7759/cureus.9564>

O’Gorman, C., Lucas, R., & Taylor, B. (2012). Environmental Risk Factors for Multiple Sclerosis: A Review with a Focus on Molecular Mechanisms. *International Journal of Molecular Sciences*, 13(9), 11718–11752. <https://doi.org/10.3390/ijms130911718>

Okuda, D. T., Kantarci, O., Lebrun-Frénay, C., Sormani, M. P., Azevedo, C. J., Bovis, F., Hua, L. H., Amezcua, L., Mowry, E. M., Hotermans, C., Mendoza, J., Walsh, J. S., von Hehn, C., Vargas, W. S., Donlon, S., Naismith, R. T., Okai, A., Pardo, G., Repovic, P., ... Pelletier, D. (2023). Dimethyl Fumarate Delays Multiple Sclerosis in Radiologically Isolated Syndrome. *Annals of Neurology*, 93(3), 604–614. <https://doi.org/10.1002/ana.26555>

Olsson, T., Barcellos, L. F., & Alfredsson, L. (2017). Interactions between genetic, lifestyle and environmental risk factors for multiple sclerosis. *Nature Reviews Neurology*, 13(1), 25–36. <https://doi.org/10.1038/nrneurol.2016.187>

Ong-Pålsson, E., Njavro, J. R., Wilson, Y., Pighi, M., Schmidt, A., Müller, S. A., Meyer, M., Hartmann, J., Busche, M. A., Gunnersen, J. M., Munro, K. M., & Lichtenthaler, S. F. (2022). The β -Secretase Substrate Seizure 6-Like Protein (SEZ6L) Controls Motor Functions in Mice. *Molecular Neurobiology*, 59(2), 1183–1198. <https://doi.org/10.1007/s12035-021-02660-y>

Oughtred, R., Rust, J., Chang, C., Breitkreutz, B., Stark, C., Willems, A., Boucher, L., Leung, G., Kolas, N., Zhang, F., Dolma, S., Coulombe-Huntington, J., Chatr-aryamontri, A., Dolinski, K., & Tyers, M. (2021). The BioGRID database: A comprehensive biomedical resource of curated protein, genetic, and chemical interactions. *Protein Science*, 30(1), 187–200. <https://doi.org/10.1002/pro.3978>

Pagani, E., Rocca, M. A., Gallo, A., Rovaris, M., Martinelli, V., Comi, G., & Filippi, M. (2005). Regional brain atrophy evolves differently in patients with multiple sclerosis according to clinical phenotype. *AJNR. American Journal of Neuroradiology*, 26(2), 341–346.

Palle, P., Monaghan, K. L., Milne, S. M., & Wan, E. C. K. (2017). Cytokine Signaling in Multiple Sclerosis and Its Therapeutic Applications. *Medical Sciences*, 5(4), 23. <https://doi.org/10.3390/medsci5040023>

Pan, G., Simpson, S., van der Mei, I., Charlesworth, J. C., Lucas, R., Ponsonby, A.-L., Zhou, Y., Wu, F., & Taylor, B. V. (2016). Role of genetic susceptibility variants in predicting clinical course in multiple sclerosis: a cohort study. *Journal of Neurology*,

Neurosurgery & Psychiatry, 87(11), 1204–1211. <https://doi.org/10.1136/jnnp-2016-313722>

Parvaz, N., & Jalali, Z. (2021). Molecular evolution of PCSK family: Analysis of natural selection rate and gene loss. *PLOS ONE*, 16(10), e0259085. <https://doi.org/10.1371/journal.pone.0259085>

Phan, K. P., Pelargos, P., Tsytsykova, A. V., Tsitsikov, E. N., Wiley, G., Li, C., Bebak, M., & Dunn, I. F. (2023). COMMD10 Is Essential for Neural Plate Development during Embryogenesis. *Journal of Developmental Biology*, 11(1), 13. <https://doi.org/10.3390/jdb11010013>

Pigoni, M., Wanngren, J., Kuhn, P.-H., Munro, K. M., Gunnersen, J. M., Takeshima, H., Feederle, R., Voytyuk, I., De Strooper, B., Levasseur, M. D., Hrupka, B. J., Müller, S. A., & Lichtenthaler, S. F. (2016). Seizure protein 6 and its homolog seizure 6-like protein are physiological substrates of BACE1 in neurons. *Molecular Neurodegeneration*, 11(1), 67. <https://doi.org/10.1186/s13024-016-0134-z>

Popescu, B. F. Gh., Pirko, I., & Lucchinetti, C. F. (2013). Pathology of Multiple Sclerosis. *CONTINUUM: Lifelong Learning in Neurology*, 19, 901–921. <https://doi.org/10.1212/01.CON.0000433291.23091.65>

Pozzilli, C., Pugliatti, M., Vermersch, P., Grigoriadis, N., Alkhawajah, M., Airas, L., & Oreja-Guevara, C. (2023). Diagnosis and treatment of progressive multiple sclerosis: A position paper. *European Journal of Neurology*, 30(1), 9–21. <https://doi.org/10.1111/ene.15593>

Prins, M., Schul, E., Geurts, J., van der Valk, P., Drukarch, B., & van Dam, A. (2015). Pathological differences between white and grey matter multiple sclerosis lesions. *Annals of the New York Academy of Sciences*, 1351(1), 99–113. <https://doi.org/10.1111/nyas.12841>

Qi, S., Sivakumar, S., & Yu, H. (2022). CRISPR-Cas9 screen in human embryonic stem cells to identify genes required for neural differentiation. *STAR Protocols*, 3(4), 101682. <https://doi.org/10.1016/j.xpro.2022.101682>

Rai, S. N., Dilmashin, H., Birla, H., Singh, S. Sen, Zahra, W., Rathore, A. S., Singh, B. K., Singh, S. P. (2019). The Role of PI3K/Akt and ERK in Neurodegenerative Disorders. *Neurotoxicity Research*, 35(3), 775–795. <https://doi.org/10.1007/s12640-019-0003-y>

Reay, W. R., & Cairns, M. J. (2021). Advancing the use of genome-wide association studies for drug repurposing. *Nature Reviews Genetics*, 22(10), 658–671. <https://doi.org/10.1038/s41576-021-00387-z>

Redondo, J., Kemp, K., Hares, K., Rice, C., Scolding, N., & Wilkins, A. (2015). Purkinje Cell Pathology and Loss in Multiple Sclerosis Cerebellum. *Brain Pathology*, 25(6), 692–700. <https://doi.org/10.1111/bpa.12230>

- Reich, D. S., Lucchinetti, C. F., & Calabresi, P. A. (2018). Multiple Sclerosis. *New England Journal of Medicine*, 378(2), 169–180. <https://doi.org/10.1056/NEJMr1401483>
- Reynders, T., D’haeseleer, M., De Keyser, J., Nagels, G., & D’hooghe, M. B. (2017). Definition, prevalence and predictive factors of benign multiple sclerosis. *ENeurologicalSci*, 7, 37–43. <https://doi.org/10.1016/j.ensci.2017.05.002>
- Rodgers, J., Friede, T., Vonberg, F. W., Constantinescu, C. S., Coles, A., Chataway, J., Duddy, M., Emsley, H., Ford, H., Fisniku, L., Galea, I., Harrower, T., Hobart, J., Huseyin, H., Kipps, C. M., Marta, M., McDonnell, G. V, McLean, B., Pearson, O. R., ... Nicholas, R. (2022). The impact of smoking cessation on multiple sclerosis disease progression. *Brain*, 145(4), 1368–1378. <https://doi.org/10.1093/brain/awab385>
- Rodríguez Murúa, S., Farez, M. F., & Quintana, F. J. (2022). The Immune Response in Multiple Sclerosis. *Annual Review of Pathology: Mechanisms of Disease*, 17(1), 121–139. <https://doi.org/10.1146/annurev-pathol-052920-040318>
- Roostaei, T., Nazeri, A., Sahraian, M. A., & Minagar, A. (2014). The Human Cerebellum. *Neurologic Clinics*, 32(4), 859–869. <https://doi.org/10.1016/j.ncl.2014.07.013>
- Rossi, L., Arciello, M., Capo, C., & Rotilio, G. (2006). Copper imbalance and oxidative stress in neurodegeneration. *The Italian Journal of Biochemistry*, 55(3–4), 212–221.
- Saleem, S., Anwar, A., Fayyaz, M., Anwer, F., & Anwar, F. (2019). An Overview of Therapeutic Options in Relapsing-remitting Multiple Sclerosis. *Cureus*. <https://doi.org/10.7759/cureus.5246>
- Sandi, D., Friczka-Nagy, Z., Bencsik, K., & Vécsei, L. (2021). Neurodegeneration in Multiple Sclerosis: Symptoms of Silent Progression, Biomarkers and Neuroprotective Therapy—Kynurenines Are Important Players. *Molecules*, 26(11), 3423. <https://doi.org/10.3390/molecules26113423>
- Sartori, A., Abdoli, M., & Freedman, M. S. (2017). Can we predict benign multiple sclerosis? Results of a 20-year long-term follow-up study. *Journal of Neurology*, 264(6), 1068–1075. <https://doi.org/10.1007/s00415-017-8487-y>
- Sayers, E. W., Bolton, E. E., Brister, J. R., Canese, K., Chan, J., Comeau, D. C., Connor, R., Funk, K., Kelly, C., Kim, S., Madej, T., Marchler-Bauer, A., Lanczycki, C., Lathrop, S., Lu, Z., Thibaud-Nissen, F., Murphy, T., Phan, L., Skripchenko, Y., ... Sherry, S. T. (2022). Database resources of the national center for biotechnology information. *Nucleic Acids Research*, 50(D1), D20–D26. <https://doi.org/10.1093/nar/gkab1112>
- Schirmer, L., Velmeshev, D., Holmqvist, S., Kaufmann, M., Werneburg, S., Jung, D., Vistnes, S., Stockley, J. H., Young, A., Steindel, M., Tung, B., Goyal, N., Bhaduri, A., Mayer, S., Engler, J. B., Bayraktar, O. A., Franklin, R. J. M., Haeussler, M., Reynolds, R., ... Rowitch, D. H. (2019). Neuronal vulnerability and multilineage diversity in

multiple sclerosis. *Nature*, 573(7772), 75–82. <https://doi.org/10.1038/s41586-019-1404-z>

Shams, H., Shao, X., Santaniello, A., Kirkish, G., Harroud, A., Ma, Q., Isobe, N., Schaefer, C. A., Mccauley, J. L., Cree, B. A. C., Didonna, A., Baranzini, S. E., Patsopoulos, N. A., Hauser, S. L., Barcellos, L. F., Henry, R. G., & Oksenberg, J. R. (2023). Polygenic risk score association with multiple sclerosis susceptibility and phenotype in Europeans. *Brain*, 146(2), 645–656. <https://doi.org/10.1093/brain/awac092>

Sheykhansari, S., Kozielski, K., Bill, J., Sitti, M., Gemmati, D., Zamboni, P., & Singh, A. V. (2018). Redox metals homeostasis in multiple sclerosis and amyotrophic lateral sclerosis: a review. *Cell Death & Disease*, 9(3), 348. <https://doi.org/10.1038/s41419-018-0379-2>

Shih, R.-H., Wang, C.-Y., & Yang, C.-M. (2015). NF-kappaB Signaling Pathways in Neurological Inflammation: A Mini Review. *Frontiers in Molecular Neuroscience*, 8. <https://doi.org/10.3389/fnmol.2015.00077>

Simkins, T. J., Duncan, G. J., & Bourdette, D. (2021). Chronic Demyelination and Axonal Degeneration in Multiple Sclerosis: Pathogenesis and Therapeutic Implications. *Current Neurology and Neuroscience Reports*, 21(6), 26. <https://doi.org/10.1007/s11910-021-01110-5>

Singh, S., & Singh, T. G. (2020). Role of Nuclear Factor Kappa B (NF-κB) Signalling in Neurodegenerative Diseases: A Mechanistic Approach. *Current Neuropharmacology*, 18(10), 918–935. <https://doi.org/10.2174/1570159X18666200207120949>

Sintzel, M. B., Rametta, M., & Reder, A. T. (2018). Vitamin D and Multiple Sclerosis: A Comprehensive Review. *Neurology and Therapy*, 7(1), 59–85. <https://doi.org/10.1007/s40120-017-0086-4>

Sjöstedt, E., Zhong, W., Fagerberg, L., Karlsson, M., Mitsios, N., Adori, C., Oksvold, P., Edfors, F., Limiszewska, A., Hikmet, F., Huang, J., Du, Y., Lin, L., Dong, Z., Yang, L., Liu, X., Jiang, H., Xu, X., Wang, J., ... Mulder, J. (2020). An atlas of the protein-coding genes in the human, pig, and mouse brain. *Science*, 367(6482). <https://doi.org/10.1126/science.aay5947>

Sorensen, P. S., Fox, R. J., & Comi, G. (2020). The window of opportunity for treatment of progressive multiple sclerosis. *Current Opinion in Neurology*, 33(3), 262–270. <https://doi.org/10.1097/WCO.0000000000000811>

Spadafora, P., Qualtieri, A., Cavalcanti, F., Di Palma, G., Gallo, O., De Benedittis, S., Cerantonio, A., & Citrigno, L. (2022). A Novel Homozygous Variant in DYSF Gene Is Associated with Autosomal Recessive Limb Girdle Muscular Dystrophy R2/2B. *International Journal of Molecular Sciences*, 23(16). <https://doi.org/10.3390/ijms23168932>

Stampanoni Bassi, M., Buttari, F., Gilio, L., Iezzi, E., Galifi, G., Carbone, F., Micillo, T., Dolcetti, E., Azzolini, F., Bruno, A., Borrelli, A., Mandolesi, G., Rovella, V., Storto, M., Finardi, A., Furlan, R., Centonze, D., & Matarese, G. (2023). Osteopontin Is Associated with Multiple Sclerosis Relapses. *Biomedicines*, 11(1), 178.

<https://doi.org/10.3390/biomedicines11010178>

Steinman, L. (2014). Immunology of Relapse and Remission in Multiple Sclerosis. *Annual Review of Immunology*, 32(1), 257–281. <https://doi.org/10.1146/annurev-immunol-032713-120227>

Stone, S., & Lin, W. (2015). The unfolded protein response in multiple sclerosis. *Frontiers in Neuroscience*, 9. <https://doi.org/10.3389/fnins.2015.00264>

Stoney, P. N., Fragoso, Y. D., Saeed, R. B., Ashton, A., Goodman, T., Simons, C., Gomaa, M. S., Sementilli, A., Sementilli, L., Ross, A. W., Morgan, P. J., & McCaffery, P. J. (2016). Expression of the retinoic acid catabolic enzyme CYP26B1 in the human brain to maintain signaling homeostasis. *Brain Structure and Function*, 221(6), 3315–3326. <https://doi.org/10.1007/s00429-015-1102-z>

Szumaska, D., Cioroch, M., Keeling, A., Prat, A., Seidah, N. G., & Bhattacharya, S. (2017). Pcsk5 is required in the early cranio-cardiac mesoderm for heart development. *BMC Developmental Biology*, 17(1), 6. <https://doi.org/10.1186/s12861-017-0148-y>

Tachon, G., Masliantsev, K., Rivet, P., Desette, A., Milin, S., Gueret, E., Wager, M., Karayan-Tapon, L., & Guichet, P.-O. (2021). MEOX2 Transcription Factor Is Involved in Survival and Adhesion of Glioma Stem-like Cells. *Cancers*, 13(23), 5943. <https://doi.org/10.3390/cancers13235943>

Tafti, D., Ehsan, M., & Xixis, K. L. (2024). *Multiple Sclerosis*. In *StatPearls*. Retrieved from <https://www.ncbi.nlm.nih.gov/pubmed/29763024>

Tallantyre, E. C., Major, P. C., Atherton, M. J., Davies, W. A., Joseph, F., Tomassini, V., Pickersgill, T. P., Harding, K. E., Willis, M. D., Winter, M., & Robertson, N. P. (2019). How common is truly benign MS in a UK population? *Journal of Neurology, Neurosurgery & Psychiatry*, 90(5), 522–528. <https://doi.org/10.1136/jnnp-2018-318802>

Thul, P. J., Åkesson, L., Wiking, M., Mahdessian, D., Geladaki, A., Ait Blal, H., Alm, T., Asplund, A., Björk, L., Breckels, L. M., Bäckström, A., Danielsson, F., Fagerberg, L., Fall, J., Gatto, L., Gnann, C., Hober, S., Hjelmare, M., Johansson, F., ... Lundberg, E. (2017). A subcellular map of the human proteome. *Science*, 356(6340). <https://doi.org/10.1126/science.aal3321>

Tornes, L., Conway, B., & Sheremata, W. (2014). Multiple Sclerosis and the Cerebellum. *Neurologic Clinics*, 32(4), 957–977. <https://doi.org/10.1016/j.ncl.2014.08.001>

Torricco, T. J., & Munakomi, S. (2023). *Neuroanatomy, Thalamus*. In StatPearls. Retrieved from <https://www.ncbi.nlm.nih.gov/pubmed/31194341>

Tu, Y. X. (Iris), Sydor, A. M., Coyaoud, E., Laurent, E. M. N., Dyer, D., Mellouk, N., St-Germain, J., Vernon, R. M., Forman-Kay, J. D., Li, T., Hua, R., Zhao, K., Ridgway, N. D., Kim, P. K., Raught, B., & Brumell, J. H. (2022). Global Proximity Interactome of the Human Macroautophagy Pathway. *Autophagy*, 18(5), 1174–1186. <https://doi.org/10.1080/15548627.2021.1965711>

Tur, C., Carbonell-Mirabent, P., Cobo-Calvo, Á., Otero-Romero, S., Arrambide, G., Midaglia, L., Castelló, J., Vidal-Jordana, Á., Rodríguez-Acevedo, B., Zabalza, A., Galán, I., Nos, C., Salerno, A., Auger, C., Pareto, D., Comabella, M., Río, J., Sastre-Garriga, J., Rovira, À., ... Montalban, X. (2023). Association of Early Progression Independent of Relapse Activity With Long-term Disability After a First Demyelinating Event in Multiple Sclerosis. *JAMA Neurology*, 80(2), 151. <https://doi.org/10.1001/jamaneurol.2022.4655>

Tur, C., & Rocca, M. A. (2024). Progression Independent of Relapse Activity in Multiple Sclerosis. *Neurology*, 102(1). <https://doi.org/10.1212/WNL.0000000000207936>

Uhlén, M., Fagerberg, L., Hallström, B. M., Lindskog, C., Oksvold, P., Mardinoglu, A., Sivertsson, Å., Kampf, C., Sjöstedt, E., Asplund, A., Olsson, I., Edlund, K., Lundberg, E., Navani, S., Szgyarto, C. A.-K., Odeberg, J., Djureinovic, D., Takanen, J. O., Hober, S., ... Pontén, F. (2015). Tissue-based map of the human proteome. *Science*, 347(6220). <https://doi.org/10.1126/science.1260419>

Umeton, R., Bellucci, G., Bigi, R., Romano, S., Buscarinu, M. C., Reniè, R., Rinaldi, V., Pizzolato Umeton, R., Morena, E., Romano, C., Mechelli, R., Salvetti, M., & Ristori, G. (2022). Multiple sclerosis genetic and non-genetic factors interact through the transient transcriptome. *Scientific Reports*, 12(1), 7536. <https://doi.org/10.1038/s41598-022-11444-w>

Van Essen, D. C., Donahue, C. J., & Glasser, M. F. (2018). Development and Evolution of Cerebral and Cerebellar Cortex. *Brain, Behavior and Evolution*, 91(3), 158–169. <https://doi.org/10.1159/000489943>

Velazquez, F. N., Caputto, B. L., & Boussin, F. D. (2015). c-Fos importance for brain development. *Aging*, 7(12), 1028–1029. <https://doi.org/10.18632/aging.100862>

Voskuhl, R. R., Patel, K., Paul, F., Gold, S. M., Scheel, M., Kuchling, J., Cooper, G., Asseger, S., Chien, C., Brandt, A. U., Meyer, C. E., & MacKenzie-Graham, A. (2020). Sex differences in brain atrophy in multiple sclerosis. *Biology of Sex Differences*, 11(1), 49. <https://doi.org/10.1186/s13293-020-00326-3>

Walton, C., King, R., Rechtman, L., Kaye, W., Leray, E., Marrie, R. A., Robertson, N., La Rocca, N., Uitdehaag, B., van der Mei, I., Wallin, M., Helme, A., Angood Napier, C., Rijke, N., & Baneke, P. (2020). Rising prevalence of multiple sclerosis worldwide:

- Insights from the Atlas of MS, third edition. *Multiple Sclerosis Journal*, 26(14), 1816–1821. <https://doi.org/10.1177/1352458520970841>
- Wang, C., Ruiz, A., & Mao-Draayer, Y. (2018). Assessment and Treatment Strategies for a Multiple Sclerosis Relapse. *Journal of Immunology and Clinical Research*, 5(1).
- Wang, F., Flanagan, J., Su, N., Wang, L.-C., Bui, S., Nielson, A., Wu, X., Vo, H.-T., Ma, X.-J., & Luo, Y. (2012). RNAscope. The Journal of Molecular Diagnostics, 14(1), 22–29. <https://doi.org/10.1016/j.jmoldx.2011.08.002>
- Wang, K. X., & Denhardt, D. T. (2008). Osteopontin: Role in immune regulation and stress responses. *Cytokine & Growth Factor Reviews*, 19(5–6), 333–345. <https://doi.org/10.1016/j.cytogfr.2008.08.001>
- Waubant, E., Lucas, R., Mowry, E., Graves, J., Olsson, T., Alfredsson, L., & Langer-Gould, A. (2019). Environmental and genetic risk factors for MS: an integrated review. *Annals of Clinical and Translational Neurology*, 6(9), 1905–1922. <https://doi.org/10.1002/acn3.50862>
- Wilkins, A. (2017). Cerebellar Dysfunction in Multiple Sclerosis. *Frontiers in Neurology*, 8. <https://doi.org/10.3389/fneur.2017.00312>
- Wingerchuk, D. M. (2012). Smoking: effects on multiple sclerosis susceptibility and disease progression. *Therapeutic Advances in Neurological Disorders*, 5(1), 13–22. <https://doi.org/10.1177/1756285611425694>
- Xu, J., & Drew, P. D. (2006). 9-Cis-retinoic acid suppresses inflammatory responses of microglia and astrocytes. *Journal of Neuroimmunology*, 171(1–2), 135–144. <https://doi.org/10.1016/j.jneuroim.2005.10.004>
- Yamout, B., & Al Khawajah, M. (2017). Radiologically isolated syndrome and multiple sclerosis. *Multiple Sclerosis and Related Disorders*, 17, 234–237. <https://doi.org/10.1016/j.msard.2017.08.016>
- Yamout, B., & Alroughani, R. (2018). Multiple Sclerosis. *Seminars in Neurology*, 38(02), 212–225. <https://doi.org/10.1055/s-0038-1649502>
- Yang, M., Wu, X., Li, L., Li, S., Li, N., Mao, M., Pan, S., Du, R., Wang, X., Chen, M., Xiao, N., Zhu, X., He, G., Zhang, L., Huang, W., Pan, H., Deng, L., Chen, L., Liang, L., & Guan, J. (2021). COMMD10 inhibits tumor progression and induces apoptosis by blocking NF-κB signal and values up BCLC staging in predicting overall survival in hepatocellular carcinoma. *Clinical and Translational Medicine*, 11(5). <https://doi.org/10.1002/ctm2.403>
- You, G., Zhou, C., Wang, L., Liu, Z., Fang, H., Yao, X., & Zhang, X. (2023). COMMD proteins function and their regulating roles in tumors. *Frontiers in Oncology*, 13. <https://doi.org/10.3389/fonc.2023.1067234>

Zeydan, B., & Kantarci, O. H. (2020). Impact of Age on Multiple Sclerosis Disease Activity and Progression. *Current Neurology and Neuroscience Reports*, 20(7), 24. <https://doi.org/10.1007/s11910-020-01046-2>

Zhu, W., & Xia, Z. (2024). Treatment discontinuation in older people with multiple sclerosis. *Current Opinion in Neurology*, 37(3), 220–227. <https://doi.org/10.1097/WCO.0000000000001272>

Ziemssen, T., Derfuss, T., de Stefano, N., Giovannoni, G., Palavra, F., Tomic, D., Vollmer, T., & Schippling, S. (2016). Optimizing treatment success in multiple sclerosis. *Journal of Neurology*, 263(6), 1053–1065. <https://doi.org/10.1007/s00415-015-7986-y>

Zivadinov, R., Uher, T., Hagemeyer, J., Vaneckova, M., Ramasamy, D. P., Tyblova, M., Bergsland, N., Seidl, Z., Dwyer, M. G., Krasensky, J., Havrdova, E., & Horakova, D. (2016). A serial 10-year follow-up study of brain atrophy and disability progression in RRMS patients. *Multiple Sclerosis Journal*, 22(13), 1709–1718. <https://doi.org/10.1177/1352458516629769>

Zveik, O., Rechtman, A., Brill, L., & Vaknin-Dembinsky, A. (2024). Anti- and pro-inflammatory milieu differentially regulate differentiation and immune functions of oligodendrocyte progenitor cells. *Immunology*, 171(4), 618–633. <https://doi.org/10.1111/imm.13757>

Supplementary Tables

Case	Sex	Relapse onset (Y/N)	Age of onset (years)	Age died (years)
MS077	female	Y	23	57
MS079	female	Y	25	49
MS080	female	Y	36	71
MS081	male	Y	24	72
MS082	female	Y	21	49
MS083	male	Y	38	54
MS086	female	Y	51	81
MS088	female	Y	33	54
MS090	male	Y	34	62
MS091	male	Y	36	81
MS092	female	Y	21	38
MS093	female	Y	31	57
MS094	female	Y	36	42
MS097	male	Y	33	55
MS098	male	Y	44	58
MS099	female	Y	40	81
MS100	male	Y	37	46
MS102	male	Y	20	73
MS103	female	Y	55	77
MS104	male	Y	41	53
MS105	male	Y	27	73
MS106	female	Y	18	39
MS107	male	Y	22	38
MS109	female	Y	35	60
MS111	male	Y	38	92
MS114	female	Y	37	52
MS120	female	Y	37	72
MS121	female	Y	36	49
MS125	female	Y	45	76
MS126	male	Y	43	75
MS127	male	Y	28	52
MS128	female	Y	28	78
MS129	female	-	42	66
MS130	female	Y	27	57
MS133	male	Y	35	63
MS136	male	Y	28	40

MS139	female	Y	40	62
MS141	male	Y	29	66
MS143	female	Y	43	62
MS146	female	Y	31	63
MS149	female	Y	36	82
MS151	female	Y	27	60
MS153	female	Y	18	50
MS154	female	Y	23	34
MS155	female	Y	43	80
MS157	female	Y	17	39
MS159	female	Y	30	55
MS160	female	Y	29	44
MS162	female	Y	36	58
MS163	female	Y	39	45
MS165	female	Y	38	59
MS166	female	Y	16	52
MS168	female	Y	58	88
MS170	male	-	26	56
MS176	male	Y	10	37
MS179	female	Y	44	70
MS180	female	Y	26	44
MS181	female	Y	39	71
MS182	female	Y	23	56
MS184	-	-	-	-
MS187	female	Y	27	57
MS191	female	Y	16	48
MS192	female	Y	31	78
MS197	female	Y	24	51
MS198	female	Y	36	63
MS199	-	-	-	-
MS200	male	Y	25	44
MS203	female	Y	26	53
MS207	female	Y	22	46
MS216	female	Y	48	58
MS218	female	Y	30	56
MS222	male	Y	31	70
MS229	male	Y	37	53
MS230	female	Y	22	42
MS231	female	Y	32	59
MS234	female	Y	23	39
MS235	male	Y	19	53

MS236	female	-	-	-
MS237	male	Y	37	77
MS241	female	Y	43	83
MS242	female	Y	38	57
MS245	male	Y	37	63
MS247	female	Y	60	67
MS248	female	Y	42	58
MS249	female	Y	7	59
MS255	male	Y	20	45
MS256	female	Y	29	53
MS261	male	Y	39	68
MS263	female	Y	35	73
MS264	female	Y	32	68
MS265	female	Y	22	74
MS269	male	Y	31	72
MS272	female	Y	26	64
MS273	male	Y	29	61
MS274	male	Y	24	56
MS275	female	Y	29	63
MS280	female	Y	30	47
MS286	male	Y	29	45
MS288	female	Y	56	83
MS289	male	Y	27	45
MS292	-	-	-	-
MS294	-	-	-	-
MS296	male	-	19	59
MS297	female	Y	44	58
MS298	male	Y	29	72
MS300	female	Y	21	56
MS301	female	Y	42	62
MS302	male	Y	33	59
MS303	female	Y	37	63
MS304	male	Y	29	52
MS306	male	Y	35	78
MS307	male	Y	35	55
MS311	female	Y	28	45
MS312	female	Y	45	68
MS313	male	Y	37	66
MS317	female	Y	18	48
MS318	female	Y	25	59
MS319	female	Y	52	63

MS325	male	Y	48	51
MS326	male	Y	29	62
MS330	female	Y	19	59
MS331	male	Y	32	57
MS335	male	Y	24	62
MS338	female	Y	37	50
MS340	female	Y	33	53
MS341	female	Y	30	52
MS342	female	Y	29	35
MS347	male	Y	22	50
MS348	female	Y	20	46
MS352	male	Y	24	43
MS356	female	Y	28	45
MS363	male	Y	15	42
MS364	female	Y	22	56
MS371	male	Y	23	40
MS372	female	Y	36	82
MS374	female	Y	33	71
MS376	female	Y	38	58
MS377	female	-	27	50
MS378	male	Y	41	53
MS379	female	Y	32	49
MS381	female	Y	43	80
MS383	male	Y	34	42
MS387	female	Y	32	43
MS389	female	Y	27	55
MS398	female	Y	30	58
MS402	male	Y	25	46
MS403	female	Y	27	54
MS404	female	Y	20	55
MS405	male	Y	36	62
MS406	male	Y	14	62
MS407	female	Y	25	44
MS408	male	Y	28	39
MS409	-	-	-	-
MS410	female	Y	33	47
MS411	male	Y	31	61
MS412	male	Y	47	74
MS413	male	Y	34	61
MS419	-	-	-	-
MS422	male	-	35	58

MS423	female	Y	24	54
MS425	female	Y	26	47
MS426	female	Y	18	48
MS430	female	Y	20	61
MS432	male	Y	16	48
MS438	female	-	35	53
MS439	female	Y	25	62
MS444	male	Y	28	49
MS445	female	Y	30	62
MS448	female	Y	32	37
MS450	male	Y	29	54
MS458	-	-	-	-
MS461	male	Y	23	43
MS462	male	Y	33	66
MS466	female	Y	29	65
MS470	female	Y	29	64
MS473	female	Y	26	40
MS474	female	Y	18	57
MS478	female	Y	24	63
MS483	female	Y	41	49
MS485	female	Y	27	57
MS489	female	Y	39	76
MS491	female	Y	36	64
MS492	female	Y	34	66
MS494	female	Y	31	65
MS496	male	Y	37	77
MS497	female	Y	29	60
MS499	female	-	25	72
MS500	male	Y	21	50
MS506	female	Y	9	61
MS510	female	Y	16	38
MS513	male	Y	33	51
MS517	female	Y	24	48
MS520	male	Y	31	74
MS523	female	Y	31	63
MS527	male	Y	21	46
MS528	female	-	20	45
MS529	male	-	56	80
MS530	male	Y	21	42
MS532	male	Y	29	68
MS535	female	Y	24	65

MS536	female	Y	26	47
MS538	male	-	28	-
MS541	female	Y	18	68
MS542	female	Y	38	76
MS543	female	Y	26	66
MS544	female	Y	48	73
MS545	male	-	23	55
MS547	female	-	32	69
MS549	male	Y	20	50
MS555	female	Y	35	59
MS558	female	Y	23	62
MS562	female	Y	22	62
MS567	female	Y	29	45
MS573	female	Y	23	71
MS575	female	Y	26	54
MS576	male	Y	44	75
MS578	female	Y	20	68
MS579	female	Y	31	66
MS581	female	Y	34	71
MS583	female	-	69	87
MS584	female	Y	30	42
MS585	female	Y	24	53
MS586	female	Y	21	57
MS587	female	-	38	58
MS588	male	Y	19	57
MS589	female	-	35	64
MS594	female	-	25	83
MS595	female	-	47	77
MS596	female	-	38	77
MS598	female	-	16	71
MS600	female	-	32	63
MS601	male	Y	34	70
MS602	-	-	-	-
MS603	female	Y	37	75
MS604	male	Y	28	61
MS605	female	-	-	90
MS606	male	Y	21	50
MS607	female	N	49	63
MS608	female	-	16	70
MS609	male	Y	40	64
MS613	male	Y	33	65

MS618	female	Y	33	56
MS619	male	-	32	66
MS620	female	Y	27	89
MS621	female	-	35	85
MS622	female	-	47	87
MS623	male	Y	35	53
MS624	female	Y	22	69
MS625	female	Y	30	60
MS626	female	Y	26	67
MS630	female	-	41	74
MS633	male	-	21	42
MS635	male	Y	68	75
MS636	male	Y	56	62
MS637	female	Y	60	74
MS639	female	Y	43	81
MS640	female	-	29	69
MS641	female	Y	45	69
MS643	female	Y	30	96
MS644	female	-	48	69
MS645	female	-	54	83
MS646	female	Y	25	46
MS648	male	-	37	66
MS652	male	-	58	76
MS653	female	-	21	46
MS654	female	-	50	75
MS657	female	N	43	77
MS661	female	-	32	50
MS662	female	-	43	70
MS664	male	-	29	63
MS665	female	-	24	74
MS668	female	-	55	82
MS669	female	-	25	84
MS671	male	-	31	76
MS674	male	-	41	65
MS676	female	-	22	67
MS678	female	-	30	63
MS679	female	-	43	69
MS680	female	N	62	98
MS681	female	N	58	86
MS682	female	-	28	83
MS683	female	-	44	67

MS684	female	Y	36	85
MS685	female	-	30	73
MS686	male	-	50	75
MS687	male	-	37	76
MS688	female	-	36	73
MS689	male	-	31	71
MS690	female	-	40	77
MS691	female	-	39	65
MS693	female	-	32	69
MS694	female	-	43	64
MS695	female	-	35	57
MS698	female	-	33	70
MS699	-	-	-	-
MS703	male	-	24	44
MS710	-	-	-	-
MS713	female	-	28	59
MS714	female	Y	33	82
MS715	male	Y	35	78
MS716	male	N	24	47
MS719	male	Y	42	72
MS721	male	N	43	55
MS722	female	Y	25	53
MS732	-	-	-	-
MS738	female	N	22	60
MS739	female	N	28	77
MS740	female	N	31	75
MS742	male	N	32	84
MS743	male	N	20	58

Table 9. Full clinical data of the MS cases used in the project. Tissue sections and immunostained slides were available from the UK MS Tissue bank for n = 310 cases (199 females, 31 years of age at onset, 59 years of age at death, 227 with a relapse-onset). Each row represents an individual MS case identified by a unique case ID. The table includes sex (male, female or unknown), whether one or more relapses were reported in the first 2 years following disease onset (yes, no or not known), age of onset (years) and age died (years).

	DYSF:CYP26B1			SEZ6L		
SNP	rs7565433			rs7289446		
Genotype	Minor	Heterozygous	Major	Minor	Heterozygous	Major
Number of MS Cases	3	41	255	30	122	147
	PCSK5					
SNP	rs10869757			rs11144848		
Genotype	Minor	Heterozygous	Major	Minor	Heterozygous	Major
Number of MS Cases	11	107	179	17	119	162
	COMMD10					
SNP	rs185263			rs1567335		
Genotype	Minor	Heterozygous	Major	Minor	Heterozygous	Major
Number of MS Cases	32	117	149	26	118	154

Table 10. Number of MS cases for each SNP of interest across the cohort. This table presents the number of cases, from the MS cohort (n = 310), carrying each genotype (homozygous minor, heterozygous and homozygous major, for all SNPs included in the genetic analysis. Genotyping was performed using the Illumina Infinium Omni 2.5 Exome BeadChip array.

Case	SFG	CG	Thalamus
C026	427.22	411.75	239.55
C032	428.67	528.51	187.78
C045	504.4	-	223.33
C036	-	402.17	194.53
C037	-	565.9	-
C039	534.46	572.8	-
C048	-	461.21	211.44
NP011 13	438.01	572.3	-
NP012 13	569.33	586.31	-
NP023 12	472.79	474.22	253.11
NP039 13	555.19	407.79	-
NP046 12	-	417.17	258.76
NP052 12	436.67	471.34	184.99
NP073 11	567.18	530.77	171.26
NP073 13	-	530.26	-
NP088 12	517.17	585.37	223.19
NP093 11	-	403.57	264.66
NP103 13	477.87	510.27	-
NP109 13	540.8	551.42	-
NP122 11	542.69	538.36	215.70
NP126 13	445.99	465.26	-
NP127 13	575.43	590.84	-
NP128 13	491.33	483.03	-
NP132 12	598.61	483.74	185.78
NP141 13	-	454.23	-
NP161 13	474.47	517.32	-
NP172 13	585.67	442.25	-
R1 1231 93	643.28	587.22	181.37

Table 11. Control neuron counts for the SFG, CG and thalamic areas of interest. The neuron density (number of positive cells per mm²) was calculated using QuPath and compared with MS neuron counts from the same regions.

Case and Image Number	Positive % of total ROI area	Number of HuC ⁺ cells	SEZ6L % Expression (Positive % of total ROI/Number of HuC ⁺ cells)
NP 13 39 NGM 1	0.3861	17	0.022711765
NP 13 39 NGM 2	0.1929	20	0.009645
NP 13 39 NGM 3	0.4928	24	0.020533333
NP 13 39 NGM 4	0.3651	12	0.030425
NP 13 161 NGM 1	0.1103	13	0.008484615
NP 13 161 NGM 2	0.152	12	0.012666667
NP 13 161 NGM 3	0.0884	12	0.007366667
NP 13 161 NGM 4	0.1083	15	0.00722
NP 13 172 NGM 1	0.2718	12	0.02265
NP 13 172 NGM 2	0.191	11	0.017363636
NP 13 172 NGM 3	0.0581	13	0.004469231
NP 13 172 NGM 4	0.1151	9	0.012788889
NP 073 NGM 1	0.1207	11	0.010972727
NP 073 NGM 2	0.4654	22	0.021154545
NP 073 NGM 3	0.2496	18	0.013866667
NP 073 NGM 4	0.2604	23	0.011321739
NP13 011 NGM 1	0.2337	25	0.009348
NP13 011 NGM 2	0.2598	19	0.013673684
NP13 011 NGM 3	0.3817	17	0.022452941
NP13 011 NGM 4	0.2519	26	0.009688462
MS 425 NGM 1	0.1697	22	0.007713636
MS 425 NGM 2	0.2614	16	0.0163375
MS 425 NGM 3	0.0737	17	0.004335294
MS 425 NGM 4	0.0688	22	0.003127273
MS 425 GML 1	0.0621	3	0.0207
MS 425 GML 2	0.0583	4	0.014575
MS 425 GML 3	0.0799	8	0.0099875
MS 425 GML 4	0.0765	8	0.0095625
MS 438 GML 1	0.0158	2	0.0079
MS 438 GML 2	0.004	1	0.004
MS 438 GML 3	0.0146	1	0.0146
MS 438 GML 4	0.0236	1	0.0236
MS 438 NGM 1	0.1852	12	0.015433333
MS 438 NGM 2	0.3249	9	0.0361
MS 438 NGM 3	0.2328	10	0.02328
MS 438 NGM 4	0.1115	11	0.010136364
MS 457 GML 1	0.0114	5	0.00228
MS 457 GML 2	0.092	4	0.023
MS 457 GML 3	0.1011	8	0.0126375
MS 457 GML 4	0.0213	6	0.00355
MS 457 NGM 1	0.471	13	0.036230769
MS 457 NGM 2	0.5785	15	0.038566667

MS 457 NGM 3	0.8159	17	0.047994118
MS 457 NGM 4	0.3018	8	0.037725
MS 473 GML 1	0.0633	6	0.01055
MS 473 GML 2	0.0032	3	0.001066667
MS 473 GML 3	0.0732	8	0.00915
MS 473 GML 4	0.075	6	0.0125
MS 473 NGM 1	0.1661	11	0.0151
MS 473 NGM 2	0.1678	14	0.011985714
MS 473 NGM 3	0.0605	13	0.004653846
MS 473 NGM 4	0.1014	15	0.00676
MS 513 GML 1	0.0016	8	0.0002
MS 513 GML 2	0.0123	12	0.001025
MS 513 GML 3	0.0077	9	0.000855556
MS 513 GML 4	0.0569	5	0.01138
MS 513 NGM 1	0.1223	25	0.004892
MS 513 NGM 2	0.1862	20	0.00931
MS 513 NGM 3	0.159	22	0.007227273
MS 513 NGM 4	0.1598	22	0.007263636
MS 523 NGM 1	0.2001	15	0.01334
MS 523 NGM 2	0.1276	8	0.01595
MS 523 NGM 3	0.075	9	0.008333333
MS 523 NGM 4	0.1497	11	0.013609091
MS 530 GML 1	0.0556	4	0.0139
MS 530 GML 2	0.0005	4	0.000125
MS 530 GML 3	0.0616	6	0.010266667
MS 530 GML 4	0.0286	11	0.0026
MS 530 NGM 1	0.1618	14	0.011557143
MS 530 NGM 2	0.4483	12	0.037358333
MS 530 NGM 3	0.1052	7	0.015028571
MS 530 NGM 4	0.431	11	0.039181818

Table 12. SEZ6L percentage expression calculations for MS and non-neurological disease control cohort.

To calculate the percentage SEZ6L expression, images were captured for each region of interest per case (4 images captured for NGM per MS and control cases and an additional 4 images captured for the GML regions in MS cases where present). When comparing the MS cases with known NGM and GML SEZ6L expression values, a Wilcoxon paired test was conducted where the mean SEZ6L percentage expression across the 4 images for each case at either a NGM or GML area was used.

Case	PCSK5		COMMD10	
	NGM	GML	NGM	GML
NP011	0.046951	-	0.166698	-
NP126	0.082063	-	0.005451	-
NP127	0.167129	-	0.06602	-
NP128	0.010579	-	0.07831	-
NP139	0.311885	-	0.013109	-
NP161	0.102797	-	0.04746	-
NP172	0.020378	-	0.154513	-
NP073	0.114065	-	0.005976	-
MS408	0.387979	0.133274	1.007765	0.073454
MS423	0.600417	0.058275	6.018038	0.149214
MS425	0.834253	0.039851	0.664806	0.614931
MS438	0.500903	0.032333	3.47156	1.639637
MS473	0.073253	0.007892	0.321394	1.756407
MS485	0.053388	0.062093	1.05836	0.25868
MS492	0.034793	-	0.813056	0.306748
MS497	0.990068	0.102717	2.240241	0.139895
MS510	0.629641	0.310383	0.394835	0.088118
MS523	0.501217	0.09339	0.481692	0.090314
MS527	0.256632	0.30397	0.41876	0.530779
MS538	1.39158	-	0.039881	-

Table 13. PCSK5 and COMMD10 Duplex positive cell counts from MS cortical areas of interest in lesion and non-lesion areas. The Duplex positive cell counts for PCSK5 and COMMD10 were calculated by manually identifying and counting cells that co-expressed both markers within NGM and GML (where present) regions in MS cases and NGM regions in non-neurological disease control cases. QuPath was used to quantify PCSK5 and COMMD10 expression in MS and control samples by reporting the area of positive stain per image, normalised to the total ROI and further divided by the number of positive cells to calculate the average positive percentage immunoreactivity in NGM and GML regions per case.

Case	NGM	GML
MS402	516.379012	-
MS407	-	557.4366704
MS422	600.0734696	251.0833728
MS423	454.7925243	331.619549
MS425	-	418.472288
MS438	-	331.619549
MS461	296.8784534	290.474536
MS473	292.1410312	260.5582171
MS485	265.2956392	215.2067153
MS491	326.8821269	251.0833728
MS492	377.4146296	-
MS497	366.3606446	-
MS510	-	502.1667456
MS513	-	552.2833891
MS523	394.7406609	-
MS527	492.4859673	291.3562021
MS530	659.7613334	317.8850061
MS543	533.8397509	396.6203783
NP13 011	314.8753561	-
NP13 012	587.1499287	-
NP13 126	353.7722762	-
NP13 127	461.8154562	-
NP13 128	441.4037233	-
NP13 139	426.0949237	-
NP13 161	745.9314329	-
NP13 172	449.0581232	-
NP073	460.7761237	-

Table 14. PCSK5 IHC positive cell counts from MS and non-neurological disease control cortical areas of interest and lesion and non-lesion areas. PCSK5 expression was quantified across four annotated regions of interest per case within NGM and GML (where present) regions in MS cases and NGM regions in non-neurological disease control cases. Manual counts of PCSK5⁺ cells were performed within each region using QuPath, and the density of PCSK5⁺ cells was calculated as the number of positive cells per mm² in NGM and GML regions per case.